The Use of Laboratory and Agent-based Models to Evaluate the Role of Natural Transformation in Biofilms in the Formation and Spread of Antibiotic Resistant Bacteria in Water Systems

by

Laxmi Annapurna Modali

A dissertation submitted in partial fulfillment
of the requirements for the degree of
Doctor of Philosophy
(Epidemiology)
in the University of Michigan
2014

Doctoral Committee:

Associate Professor Chuanwu Xi, Chair
Professor Betsy Foxman
Associate Professor Carl F. Marrs
Research Professor Rick Riolo
Professor Carl P. Simon

2014

Dedicated to Sridhar, Shyla & Siya

Acknowledgements

I would like to acknowledge the following individuals, without whom I would not have been able to complete this dissertation.

First and foremost, I am especially thankful to my advisor Chuanwu Xi. You provided encouragement, understanding and constructive criticism when needed. In addition, you created a wonderful and collaborative lab environment. I truly appreciate all the time you have spent helping me - whether it was troubleshooting in the lab or revising chapter drafts. I have also learned a lot from you in terms of navigating the professional setting and I hope to take these skills with me during my career development.

I am also grateful to Betsy Foxman for bringing me into the IPID program and for being a wonderful mentor. It was because of the IPID program that I came to appreciate the utility and necessity of interdisciplinary work. I have no doubt that my time at Michigan was enriched from being in this program. Your words of encouragement over the years and your advice are highly valued. I am grateful for all your guidance.

I would also like to thank Carl Marrs for his help on all the laboratory work and for helping me focus my model work. I have always appreciated your positive spirit and your attention to detail. Thank you for all the time you have spent on my work and for your suggestions.

I am equally grateful to my other committee members: Carl Simon and Rick Riolo. You both made the idea of modeling less daunting and introduced me to a whole new

Aditya, I can't imagine two better nephews and role models for my daughters. And to my husband, Sridhar – you are my best friend and my biggest cheerleader. Thank you for being on my side, always. You displayed a lot of patience during this long process, especially towards the end. You never faltered in your confidence that I would finish, even when I did. This degree is as much yours as it is mine. I admire the pride you take in your work and your strong work ethic. It's not a coincidence that you garner so much respect from your colleagues and have such a loyal professional network. I hope I can achieve a modicum of that level of respect and confidence from my peers as I progress in my postgraduate career. Most importantly to my two daughters Siya and Shyla – thank you for the joy you both bring to us. You are and always will be my greatest accomplishment.

Finally, I would like to acknowledge the final support for this thesis work from the IPID training grant, the University of Michigan Rackham Graduate School and the Xi research group.

Table of Contents

List of Figures

List of Tables

Abstract

Biofilms are aggregates of bacterial cells enclosed in an extracellular matrix. When encased in a biofilm, bacteria function differently. In particular, there is a hypothesis that frequency of gene transfer in biofilms is higher than that in corresponding planktonic counterparts, in part due to increased competence. When the acquired genes increase virulence or ability to treat bacteria, as is the case with antibiotic resistance gene, the potential downstream impacts on human health can be substantial. Biofilms, along with trace levels of antibiotics and antibiotic resistance determinants, are a common occurrence in water treatment and distribution systems. This dissertation assesses the role of natural transformation in biofilms in the formation and dissemination of antibiotic resistant bacteria in water networks using laboratory and agent-based models. In an initial set of laboratory experiments, we demonstrated detectable transformation frequencies in *Acinetobacter baylyi* strain AC811 biofilms exposed to varying genomic and donor DNA encoding antibiotic resistance in a once-through flow system replicating environmental conditions in water system pipes. An additional set of experiments compared transformation frequencies of AC811 biofilm and planktonic cells incubated with donor plasmid DNA. The microtiter experiment data showed that the transformation frequencies of suspended cells were at least 10-fold higher than that of the biofilm cells. Similarly, the

flow system experiment data indicated that transformation frequencies of the planktonic samples were approximately 10-fold higher than frequencies of corresponding biofilm samples. qPCR was used to quantify *comP* gene expression in AC811. Comparison *comP* gene expression trends in biofilm and planktonic cells suggests that the observed frequency differences are due to a variation in competence state between biofilm and free-floating cells. These results suggest that the assumption of increased competence of biofilm cells as compared to planktonic cells may not be generalizable across all bacterial species. Development of an agent-based model allowed us to study additional factors that may affect transformation frequency and in a setting that allows visualization of the biofilm structure. We developed an extension to the iDynoMiCs agent-based model and used this extended model to assess the effect of resistance gene burden value on the persistence of resistant bacteria in a biofilm exposed to donor DNA and varying antimicrobial concentrations. Several trends are apparent in simulations results. Bacteria harboring no cost and low cost fitness genes will persist in the absence of selective pressure and increasing antimicrobial concentration in the influent promotes increased resistance expansion within the single-species biofilm. Results suggest that influent antimicrobial concentration can substantially affect the type and frequency of resistance genes circulating in the environment. This model can be a tool to test hypotheses that are difficult to conduct in the laboratory setting and can be used to drive future laboratory studies.

Chapter 1

Introduction

1.1 Background

Biofilms are microbial communities formed by sessile aggregates of bacteria attached to organic or inert surfaces.[1-3] They are encased within an extracellular matrix and exhibit distinct properties from their planktonic counterparts.[2, 4, 5] A general assumption is that frequency of gene transfer in biofilms is greater than among planktonic cells due to advantages afforded by the matrix, close spatial orientation of the cells and increased genetic competence.[6-9] Biofilms, along with trace levels of antibiotics and antibiotic resistance determinants, are a common occurrence in water treatment and distribution systems.[10-12] Antibiotic selective pressure and horizontal gene transfer of antibiotic resistance genes may contribute to emergence of antibiotic resistant bacteria from water systems.[13-15] It is unknown if exposure to antibiotic resistant bacteria in the water is associated with increased risk of bacterial infection in the general population.[11] But, there is increasing evidence that clinically important resistance genes have emerged from environmental sources.[10] And in fact, water systems can serve as a reservoir for the spread of antibiotic resistance to opportunistic pathogens.[11] This dissertation research investigates

various factors that influence natural transformation and/or persistence of resistance genes in *Acineotbacter baylyi* strain BD413 biofilms such as exposure to donor DNA, competence gene expression, resistance gene metabolic burden and antimicrobial inhibition using laboratory and agent-based models.

This thesis contains five chapters. The second chapter is a review of the various components that contribute to natural transformation in biofilms in water systems. This review of literature also includes a discussion of the physiologic properties and natural transformation of the model organism, *Acinetobacter baylyi* strain BD413. The third chapter describes a series of laboratory studies using *Acinetobacter baylyi* strain BD413. In the first set of experiments, *Acinetobacter* sp. strain BD413 biofilms developed in flow systems were exposed to varying donor genomic and plasmid DNA encoding antibiotic resistance. The next set of experiments tested the hypothesis that growth in a biofilm increases competence. Transformation frequencies of biofilms developed in static and dynamic flow systems were compared with their respective planktonic counterparts. Expression patterns of *comP*, a competence gene in the BD413 competence pathway, were also compared between the two growth modes. The fourth chapter describes the development of an agent-based model that simulates DNA uptake, genetic transformation, resistance gene expression and antimicrobial inhibition in a single species biofilm. This extended agent-based model was also used to assess the effect of resistance gene burden value on the persistence of resistant bacteria in a biofilm exposed to donor DNA and varying antimicrobial concentration. The fifth and final chapter provides a summary of the

study conclusions and suggestions for future work. Findings from this work contribute to the larger study of the spread of antibiotic resistant bacteria in water distribution systems.

1.2 References

1. Dunne, W.M., *Bacterial adhesion: seen any good biofilms lately?*, in *Clin. Microbiol. Rev.* 2002. p. 155-166.
2. Singh, R., D. Paul, and R.K. Jain, *Biofilms: implications in bioremediation.*, in *Trends in Microbiology*. 2006. p. 389-397.
3. Toole, G., H.B. Kaplan, and R. Kolter, *Biofilm formation as microbial development.*, in *Annu. Rev. Microbiol.* 2000. p. 49-79.
4. Hall-Stoodley, L., J.W. Costerton, and P. Stoodley, *Bacterial biofilms: from the Natural environment to infectious diseases*, in *Nat Rev Micro*. 2004. p. 95-108.
5. Huq, A., et al., *Biofilms in water, its role and impact in human disease transmission.*, in *Current Opinion in Biotechnology*. 2008. p. 244-247.
6. Molin, S. and T. Tolker-Nielsen, *Gene transfer occurs with enhanced efficiency in biofilms and induces enhanced stabilisation of the biofilm structure*, in *Current Opinion in Biotechnology*. 2003. p. 255-261.
7. Roberts, A.P., P. Mullany, and M. Wilson, *Gene transfer in bacterial biofilms.*, in *Meth. Enzymol.* 2001. p. 60-65.
8. Fux, C.A., et al., *Survival strategies of infectious biofilms.*, in *Trends in Microbiology*. 2005. p. 34-40.
9. Parsek, M.R. and P.K. Singh, *Bacterial biofilms: an emerging link to disease pathogenesis.*, in *Annu. Rev. Microbiol.* 2003. p. 677-701.
10. Pruden, A., *Balancing Water Sustainability and Public Health Goals in the Face of Growing Concerns about Antibiotic Resistance.*, in *Environ. Sci. Technol.* 2013.
11. Xi, C., et al., *Prevalence of antibiotic resistance in drinking water treatment and distribution systems.*, in *Applied and Environmental Microbiology*. 2009. p. 5714-5718.
12. Momba, M., et al., *An overview of biofilm formation in distribution systems and its impact on the deterioration of water quality*. 2000, Water Reseach Council.
13. Witte, W., *Ecological impact of antibiotic use in animals on different complex microflora: environment.*, in *International Journal of Antimicrobial Agents*. 2000. p. 321-325.
14. Ferreira da Silva, M., et al., *Antimicrobial resistance patterns in Enterobacteriaceae isolated from an urban wastewater treatment plant*, in *FEMS Microbiology Ecology*. p. 166-176.
15. Zhang, Y., et al., *Wastewater treatment contributes to selective increase of antibiotic resistance among Acinetobacter spp.*, in *Science of the Total Environment, The*. 2009, Elsevier B.V. p. 3702-3706.

Chapter 2

Literature Review: Components that contribute to natural transformation in water treatment and distribution system biofilms

2.1 Abstract

Bacterial pathogen resistance to antibiotics limits therapeutic options and increases morbidity and mortality.[1] Prevalence of resistance genes and resistant bacterial strains is increased in areas of heavy antibiotic use.[1, 2] Water treatment plants and distribution networks house bacterial biofilms, antibiotics and resistance genes.[3, 4] Thus, emergence and dissemination of antibiotic resistant bacteria from water systems can be due to the selective pressure of trace levels of antibiotics and from horizontal gene transfer of antibiotic resistance genes.[1, 5, 6] It is unknown if exposure to antibiotic resistant bacteria in the water is associated with increased risk of bacterial infection in the general population.[7] But, there is increasing evidence that clinically important resistance genes have emerged from environmental sources.[8] And in fact, water systems can serve as a reservoir for the spread of antibiotic resistance to opportunistic pathogens.[7] This chapter provides an overview of biofilm development and characteristics, summarizes evidence of antibiotics, antibiotic resistant genes and antibiotic resistant bacteria in water systems and ends with a focus on the physiologic properties and natural transformation of the model organism, *Acinetobacter baylyi* strain BD413.

2.2 Biofilms: A general introduction

Biofilms are interactive microbial communities formed by sessile aggregates of bacteria attached to organic or inert surfaces.[9-11] Whether composed of a single or multiple species, bacteria in a biofilm are encased within a matrix composed of water, extracellular DNA, secreted polymers, adsorbed nutrients and metabolites, cell lysis products and other detritus from the surrounding environment.[4, 10, 12] Biofilms are ubiquitous, especially in moist environments with sufficient nutrient flow and where attachment to a surface is possible.[10] Rather than being transient formations of settled planktonic cells, it is now widely accepted that biofilms are the preferred bacterial growth mode and exhibit distinct properties from their planktonic counterparts.[12-15] Thus, extrapolation from studies of planktonic cells may be severely limited.[16]

Biofilm development is a complex multifactorial process resulting in an ordered and, often heterogeneous, microbial community.[10, 12] Formation of the extra polysaccharide substance (EPS) is an integral component of this process. There are two general theories regarding general biofilm development.[17] The first is a two-step process. Bacteria attach to the surface via van der Waals forces, electrostatic forces and hydrophobic interactions. These cells are reversibly attached and can be removed via fluid shear forces. However, attachment can be strengthened through exo-polysaccharides or ligands that interact with the surface.[17] Some wild bacterial strains have a thick EPS layer surrounding the bacterial cell as well as thick protrusions or fimbriae that project out from the cell and through the EPS layer.[16] The fimbriae help to align bacterial cells with the surface and with one another while the EPS serves to irreversibly attach some cells to the surface.[17] Once cells

are irreversibly attached, the biofilm structure grows through cell division and also recruits other cells from the bulk fluid phase.[16, 18] The second theory involves a three-step process. In the first two steps, bacteria attach via van der Waals and electrostatic forces before permanently sticking on with the help of specific adhesion receptors.[17] Over time, the biofilm transforms into a structured community with the development of chemical gradients, water channels and internal nutrient availability.[15, 18, 19]

Biofilm maturation often results in a structure with an array of microenvironments. In thick biofilms, the cells in the upper layers exhibit aerobic activity reducing the oxygen available to the cells in the lower layers, next to the substratum. In addition, pH gradients have been noted in many biofilms, both in the vertical and horizontal zones. Biofilms also have an internal local availability of nutrients due to cell lysis and, in the case of some multi-species biofilms, due to the use of metabolites produced by one species and used as a nutrient by another. In some instances, heterotrophic bacteria surround primary producers and use their metabolic exudates.[18] Biofilm communities that have achieved physiological cooperation and work together as a unit are sometimes referred to as 'consortia'.[18]

2.3 Biofilms and antibiotic resistance

Mature biofilms can tolerate antibiotic agents at concentrations up to 1000 times that needed to kill genetically equivalent planktonic bacteria.[13, 18] Reduced susceptibility of biofilms to antibiotics is well documented, however there are several working hypotheses as to the cause.[20] The antibiotic may fail to fully penetrate the biofilm because of structural

barriers and/or consumption or neutralization reactions with the biomass.[21-25] Retarded

diffusion may also lead to biofilm regions with low substrate concentration levels and

metabolically inactive, less susceptible cells.[25, 26] Another hypothesis is that cells may turn

on a protective stress response upon exposure to high antibiotic concentrations or a

subpopulation of persistor cells may develop.[20] Alternatively, sessile cells may undergo a

physiological change upon surface adherence, resulting in a biofilm phenotype with

increased resistance.[25, 27] For instance, genes encoding efflux pumps may be differentially

expressed in biofilm cells versus planktonic cells. While these are all plausible theories, the

reality is that biofilm resistance seems to be a combination of several factors.[26, 28-31] In fact,

one species may have different resistance responses depending on the antibiotic agent

and/or biofilm properties.[20, 32]

Biofilms may acquire antibiotic resistance through the uptake of extracellular DNA

encoding resistance genes. A general assumption is that biofilms have high gene transfer

frequencies as compared to planktonic cells due to advantages afforded by the matrix,

close spatial orientation of the cells and increased genetic competence.[33-36] The matrix

concentrates exogenous DNA for efficient DNA uptake during natural transformation.

And, Roberts et al. (2001) conjectures that there are a variety of phenotypes displayed

among the closely packed cells with an increased likelihood of 'gene transfer'

phenotypes.[34, 37, 38] The close proximity of cells in a biofilm also facilitates cell-cell

communication.[10, 12, 39] This may increase genetic competence in instances where

competence induction is regulated via a quorum-sensing mechanism such as in Gram-

positive *Streptococcus mutans*.[40] Li et al. (2001) demonstrated that *S. mutans* cells

developed in a static system had 10- to 600-fold higher transformation frequencies than

their planktonic counterparts.[41] These results support the prevailing hypothesis regarding

higher transformation frequencies in biofilms versus planktonic cells. However, as

mentioned previously, competence development in streptococci is dependent on cell

density.[41] This hypothesis remains to be explored with other bacterial species with

competence pathways that may not be induced via a quorum-sensing mechanism.

2.4 Biofilm formation in water treatment & distribution systems

Biofilms are a common occurrence in water systems.[3, 4, 42] Approximately 10^7 cells (dead

or alive) remain per liter of water cleaned in even the most technologically advanced water

treatment facilities.[43] Cells that come through the process may be killed, reversibly injured

or may be unharmed. Thus the increase of bacteria in water networks, post treatment, can

be due to internal regrowth, after-growth and breakthrough growth. Regrowth refers to the

resuscitation and subsequent growth of cells that were reversibly injured in the treatment

process, after-growth is used to describe the growth of cells already present in the post-

treatment water distribution system and the term breakthrough growth denotes the

multiplication of cells that passed through the treatment process unharmed.[44] Xi et al.

(2009) found that the total heterotrophic plate count of bacteria in tap water samples was

lower than in the source water but still significantly higher than treated water, indicating

regrowth of bacteria in the drinking water distribution system.[7] A majority of viable post-

treatment cells adhere to the surface of the distribution pipes and storage tanks and form

biofilms. In fact, approximately 95% of the biomass in water systems is in the form of biofilms while less than 5% is found suspended in the bulk fluid.[44] Microbial cells are released into and contaminate the circulating water due to either the detachment of bacteria from the pipe and storage tank walls or the sloughing off of cells from the biofilm due to the shear forces of the bulk fluid.[43]

2.5 Presence of antibiotics in the general aqueous environment and in water treatment and distribution systems

Approximately 5500 tons of antibiotics are produced and purchased per year in the US and a majority of these compounds are excreted and can enter various stages of the urban water cycle as active metabolites. [2, 8, 45-52] While there are different sources of antibiotic pollution in the aqueous environment such as hospital waste and industrial pharmaceutical waste, a significant portion of antibiotic use in the US is for animal husbandry/ agricultural purposes.[45-48, 51, 53, 54] Antibiotics are administered as feed additives at sub-therapeutic levels, used to treat infections and are prophylactically sprayed on fruit trees.[46, 47, 55, 56] Antibiotics in manure used as fertilizer and pharmaceutical compounds used in animal farming practices can seep through the soil into surface water, ground water and potentially, drinking water.[51, 56, 57] Wastewater treatment plant (WWTP) disinfection procedures are not designed to efficiently remove antibiotics and treated effluent can contaminate receiving rivers.[8, 51, 58-61] Drinking water can also be affected by 'indirect potable reuse.' This term refers to situations when municipal water is recycled and treated effluents are used to augment drinking water sources or when a drinking water plant intake is downstream from

10

a wastewater effluent discharge point.[8, 52, 62] Trace levels of antibiotics have been found in finished drinking water, however there is scant research in this area.[7, 62]

2.6 Antibiotic resistant bacteria and antibiotic resistance genes in water treatment and distribution systems

Antibiotic resistant bacteria (ARB) and antibiotic resistance genes (ARGs) are fed into water systems from various sources and ARGs can further persist in these settings. Antibiotics in hospital and pharmaceutical plant effluents, treated municipal waste and agricultural runoff can lead to selection for antibiotic resistant bacteria in source water.[7, 56, 63] And, crude antibiotic preparations used on farms, manure from treated animals and human associated wastewaters contain both ARB and ARGs.[8, 45, 57, 59, 64, 65] Subsequent water treatment kills most of the bacterial cells but ARGs are still present in treated effluent and in distribution systems.[7, 8, 61] In addition, there is evidence that traditional disinfection procedures do not damage ARGs during the treatment process.[66] This extracellular DNA can remain stable for long periods of time, especially when associated with solid surfaces. DNA in this state is protected from environmental nucleases and can persist and retain its bacterial transforming abilities.[48, 67, 68]

2.7 Water treatment and distribution processes contribute to an increase in antibiotic resistant bacteria

Emergence and dissemination of ARB from water systems can be due to the selective pressure of trace levels of antibiotics and from horizontal gene transfer of ARGs.[1, 5, 6, 8] Research indicates that the treatment process in WWTPs contributes to an increase in

ARB, although the precise mechanism for this increase is not clarified.[1, 6] Zhang et al. (2009) found that the prevalence of *Acinetobacter* spp. isolates resistant to amoxicillin/ clavulanic acid, chloramphenicol or rifampicin progressively increased from raw influent samples to final effluent samples.[1] Ferreira da Silva et al. (2007) demonstrated a similar trend among WWTP *Enterobacteriaceae* isolates. Prevalence of resistance to ciprofloxacin and cephalothin significantly increased from *Escherichia* spp. isolated from raw influent to those isolated from treated effluent samples.[6] The same phenomenon is seen in drinking water systems. In two separate studies, Armstrong and colleagues found antibiotic resistant bacteria in drinking water treatment plant samples and in finished water samples.[69, 70] In fact, antibiotic resistant gram-negative organisms, including *Acinetobacter* spp., were more common in finished drinking water than in source waters.[69] Comparing source, finished and tap water samples, Xi et al. (2009) described heterotrophic plate count data that indicated a significant increase in resistance to chloramphenicol and rifampicin in tap water samples than in source water samples. And, there was a significant increase in resistance to tetracycline in tap water compared to source water and finished drinking water samples.[7]

The aforementioned study results suggest that water treatment and distribution systems can significantly impact the formation and spread of antibiotic resistant bacteria. Trace levels of antibiotics, presence of antibiotic resistant bacteria and resistance genes and high microbial densities in the form of biofilms lining pipes and storage tanks in water networks may create an environment that promotes gene transfer.[3, 44, 56, 63] In addition, water systems

link different environmental compartments and can therefore facilitate the spread of antibiotic resistant bacteria between these compartments.[1]

2.8 Model organism: *Acinetobacter baylyi* strain AC811

Acinetobacter baylyi strain BD413 is an ideal model organism for studying transformation, particularly in experiments conducted to assess the role of natural transformation in biofilms in the formation and spread of antibiotic resistant bacteria in water systems. *Acinetobacter* spp. are non-motile, coccobacilli bacteria that are capable of utilizing a wide variety of carbon sources and thus can be found in numerous environmental niches.[1, 71-73] In particular, members of this genus are found in soil, sewage, freshwater, and in drinking water systems.[44, 74, 75] The naturally competent *Acinetobacter baylyi* strain BD413, originally isolated from the soil, is particularly well suited for studying natural transformation.[76-78] BD413, also known as *Acinetobacter* sp. strain ADP1, has an extremely efficient transformation system and does not discriminate between homologous and heterologous DNA.[1, 71, 78-80] This strain exhibits high transformation frequencies in planktonic batch culture as well as in monoculture biofilms developed in once-through flow systems.[75, 77] In addition, it is transformable in groundwater and soil liquid with transformation frequencies as efficient as *in vitro* frequencies, even in the presence of indigenous microorganisms.[81]The ubiquity of this genus and evidence of high gene transfer between strains makes these microorganisms suitable for monitoring antibiotic resistance in the environment.[1, 53, 82] *Acinetobacter* sp. strain AC811 is a nonencapsulated

derivative of strain BD413 and is the recipient organism in a majority of the transformation experiments described in this work.[1, 79]

2.9 Overview of the *Acinetobacter baylyi* strain BD413 competence pathway

There are five genes in the BD413 competence pathway: *comB*, *comC*, *comE*, *comF* and *comP*.[71, 83-85] Respective transformation-deficient mutants indicate that all five gene products are essential for natural transformation. In particular, *comE* and *comF* mutants exhibited reduced transformation frequencies whereas *comB, comC* and *comP* mutants resulted in completely noncompetent phenotypes.[83-85] Amino acid sequences of ComB, ComE, ComF and ComP proteins are similar to prepilins, precursors of structural subunits of type IV pili.[84-86] And, ComC is similar to type IV pilus biogenesis or assembly factors.[83] Homologues of type IV pilus structures may be involved in natural transformation in various bacteria and there is no definitive conclusion as to whether type IV pilus structures are involved with DNA transformation. However, the presence of thick and thin fimbriae on the surface of *comB*, *comC*, *comE*, *comF* and *comP* mutants implies that these genes are not essential for pili development and that these two particular types of pilus structures are not involved in natural transformation in BD413.[71, 83-86] Instead, these competence proteins may be part of DNA translocating machinery. ComC and ComP are essential for DNA binding, with ComC located at the cell surface.[71, 83-86] ComC may be the basement protein or molecular usher for an oligomeric structure that transports DNA across the outer membrane, the periplasmic space and the cytoplasmic membrane.[71, 83, 84] ComB, ComE, ComF and ComP form this DNA shaft with ComP located in the outer

membrane.[71, 84-86] Double-stranded DNA binds to the surface of this structure and DNA enters the cell in a single-stranded form powered by ATP hydrolysis or an electrochemical gradient across the membrane.[85]

comB and *comP* expression profiles indicate that transformation machinery is present prior to competence induction. Induction of competence in *Acinetobacter baylyi* strain BD413 takes place after dilution of a stationary phase culture into fresh nutrient medium.[87] Cells remain competent during the exponential growth phase, decreasing thereafter.[86-88] Conversely, *comB* and *comP* expression peaks slightly after dilution of a stationary culture into fresh medium and then decreases across the exponential phase before peaking again in the late stationary phase.[85, 86, 89] Thus, *comB* and *comP* expression is not correlated with competence induction and is growth phase dependent. In fact, immediate competence of BD413 cells diluted into fresh medium is probably not due to induction of protein expression. This is supported by the finding that transformation of BD413 is not hindered by the protein synthesis inhibitor, chloramphenicol.[86, 88, 89] Most probably, DNA uptake machinery is already present in stationary cells and diluting these cells into fresh medium provides the requisite energy for DNA uptake.[85, 86, 89] Also, competence regulation may involve promoters that respond to environmental nutrient limitations or the energy charge of the cell as evidenced by higher levels of gene expression in the late stationary phase.[86]

2.10 Factors that affect transformation in *Acinetobacter baylyi* strain BD413 in planktonic and biofilm growth mode

Several studies have examined factors that affect transformation in *Acinetobacter baylyi* strain BD413 in both batch culture and biofilm growth modes. Palmen et al. (1993) found that BD413 transformation frequency increases with increasing concentration of both chromosomal and plasmid donor DNA; the frequency curve follows saturation kinetics.[77] Palmen and colleagues also studied the effect of incubation time with plasmid donor DNA on transformation frequency of BD413 batch culture cells. As expected, transformation frequency increases with longer incubation times.[77] Transformation frequency in strain BD413 also increases, in a biphasic pattern, as the donor DNA fragment size increases.[88] In particular, transformation of a modified BD413 strain with fragments larger than 1 kb resulted in high transformation frequencies.[88] Hendrickx et al. (2003) studied natural transformation in *Acinetobacter baylyi* strain BD413 biofilms developed in a once-through system.[75] Although *in situ* microscopy monitoring revealed new transformants in a 3-day old biofilm, younger cells are more readily transformed. Thus, biofilm age appears to affect transformation frequency.[75] Similar to batch culture experiment results, transformation frequency in BD413 biofilms increased as a function of influent plasmid DNA concentration. However the curve did not follow saturation kinetics since a saturation point was not reached in the tested donor DNA range.[75]

2.11 Transformation of *Acinetobacter baylyi* strain BD413 in the natural environment

Identification of resistance genes in the environment and use of genetically modified crops has prompted studies that characterize natural transformation in the environment. These

experiments are either conducted outside of the laboratory setting or in microcosms made up of materials recovered from the environment. BD413 served as the recipient organism in several transformation studies. Williams et al. (1996) found that BD413 recipient cells were transformed by whole cell lysate in filter matings incubated in the river and also when incorporated into the indigenous river epilithon. The authors also discovered that transformation frequencies of *in situ* filter matings increased with ambient river temperature.[90] Direct observation of horizontal gene transfer mechanisms in the environment is not always possible. However, microcosm studies offer the opportunity to study effects on transformation in the laboratory setting using materials recovered from the environment. Chromosomal DNA adsorbed to sand and sterilized groundwater aquifer material successfully transformed BD413 in respective microcosm settings. In fact, transformation efficiency with adsorbed DNA was as high as with DNA in solution.[68] Soil microcosm studies also produced detectable BD413 transformation frequencies. Antibiotic resistant cell lysate proved to be a viable source of transforming DNA for kanamycin-sensitive BD413 populations residing in sterile and non-sterile soil. Homologous sources were 4- to 16-fold more efficient for transformation in the sterile soil setting compared to heterologous DNA. And in the non-sterile soil setting, cell lysate from homologous sources transformed recipient cells at a frequency of $1.1 \times 10e^{-6}$ while BD413 did not uptake heterologous DNA at detectable rates. Further work clarified that cell lysates are available as transforming DNA for up to 4 days in sterile soil and for up to 8 hours in non-sterile soil.[91] Per these results, BD413 may appear to be recalcitrant to uptake of heterologous DNA. However, Watson and Carter (2008) found that there are several

external factors that may influence and even promote transformation.[67] In particular, transformation in soil environments is dependent on nutrient availability and on soil texture. Simulated root exudate promoted transformation in sterile soil microcosms containing antibiotic sensitive BD413 cells, whereas previous experiments sans root exudate did not produce any detectable transformation frequencies.[67] In addition, effects of tested environmental factors on transformation frequency varied according to soil type. Soils with a higher proportion of clay content had higher gene transfer rates.[67] *Acinetobacter baylyi* strain BD413 is prevalent in many environmental compartments and appears to be transformable in different settings under a wide range of conditions Thus, it can be viewed as a sentinel bacteria for gene transfer in an environment polluted with antibiotics and resistance genes.

2.12 Research implications

Biofilms form in water system pipes and storage tanks, representing a potential risk factor for the formation and spread of ARB.[3, 7, 42, 43, 92] There have been numerous studies documenting the increase in ARB post water treatment and distribution.[1, 6, 69, 70] In addition, several microcosm experiments identified factors that affect transformation in soil.[67, 91] However, there has been minimal work on natural transformation in biofilms developed in dynamic flow systems. In addition, only one study conducted by Li et al. (2001) has confirmed higher gene transfer frequencies in biofilm cells compared to their planktonic counterparts.[41] This dissertation addresses these gaps in knowledge by using a simplified laboratory model to assess transformation frequencies in biofilms developed in once-

through flow systems and exposed to varying antibiotic resistant donor DNA. We also

describe data comparing transformation frequencies and competence gene expression in

Acinetobacter baylyi strain BD413 biofilm and planktonic growth modes. Finally, we

present an agent-based model that incorporates the various natural transformation

processes. This model is used to look at factors that promote the formation and persistence

of antibiotic resistant bacteria in a single-species biofilm. In addition, this model has

numerous future applications as a stand alone computational tool and as an aide to drive

future laboratory work. This dissertation work not only has downstream implications

regarding water treatment procedures, water reuse and agricultural antibiotic use; it also

highlights the need to approach a multitier issue, such as this one, with an interdisciplinary

approach.

2.13 References

1. Zhang, Y., et al., *Wastewater treatment contributes to selective increase of antibiotic resistance among Acinetobacter spp.*, in *Science of the Total Environment, The*. 2009, Elsevier B.V. p. 3702-3706.
2. Pei, R., et al., *Effect of River Landscape on the sediment concentrations of antibiotics and corresponding antibiotic resistance genes (ARG)*, in *Water Research*. 2006. p. 2427-2435.
3. Berry, D., C. Xi, and L. Raskin, *Microbial ecology of drinking water distribution systems*, in *Current Opinion in Biotechnology*. 2006. p. 297-302.
4. Huq, A., et al., *Biofilms in water, its role and impact in human disease transmission.*, in *Current Opinion in Biotechnology*. 2008. p. 244-247.
5. Witte, W., *Ecological impact of antibiotic use in animals on different complex microflora: environment.*, in *International Journal of Antimicrobial Agents*. 2000. p. 321-325.
6. Ferreira da Silva, M., et al., *Antimicrobial resistance patterns in Enterobacteriaceae isolated from an urban wastewater treatment plant*, in *FEMS Microbiology Ecology*. p. 166-176.
7. Xi, C., et al., *Prevalence of antibiotic resistance in drinking water treatment and distribution systems.*, in *Applied and Environmental Microbiology*. 2009. p. 5714-5718.
8. Pruden, A., *Balancing Water Sustainability and Public Health Goals in the Face of Growing Concerns about Antibiotic Resistance.*, in *Environ. Sci. Technol.* 2013.
9. Dunne, W.M., *Bacterial adhesion: seen any good biofilms lately?*, in *Clin. Microbiol. Rev.* 2002. p. 155-166.
10. Singh, R., D. Paul, and R.K. Jain, *Biofilms: implications in bioremediation.*, in *Trends in Microbiology*. 2006. p. 389-397.
11. Toole, G., H.B. Kaplan, and R. Kolter, *Biofilm formation as microbial development.*, in *Annu. Rev. Microbiol.* 2000. p. 49-79.
12. Hall-Stoodley, L., J.W. Costerton, and P. Stoodley, *Bacterial biofilms: from the Natural environment to infectious diseases*, in *Nat Rev Micro*. 2004. p. 95-108.
13. Jefferson, K.K., *What drives bacteria to produce a biofilm?*, in *FEMS Microbiology Letters*. 2004. p. 163-173.
14. Costerton, J. and Z. Lewandowski, *Microbial biofilms*, in *Annual Reviews in …*. 1995.
15. Stewart, P.S. and M.J. Franklin, *Physiological heterogeneity in biofilms*, in *Nat Rev Micro*. 2008. p. 199-210.
16. Costerton, J.W., *Introduction to biofilm.*, in *International Journal of Antimicrobial Agents*. 1999. p. 217-21- discussion 237-9.
17. Palmer, J., S. Flint, and J. Brooks, *Bacterial cell attachment, the beginning of a biofilm*, in *J Ind Microbiol Biotechnol*. 2007. p. 577-588.
18. Blenkinsopp, S.A. and J.W. Costerton, *Understanding bacterial biofilms.* Trends in Biotechnology, 1991. **9**(1): p. 138-143.
19. Costerton, J.W., et al., *Biofilms, the customized microniche.*, in *J. Bacteriol.* 1994. p. 2137-2142.

20. Szomolay, B., et al., *Adaptive responses to antimicrobial agents in biofilms*, in *Environ Microbiol*. 2005. p. 1186-1191.
21. Chambless, J.D., S.M. Hunt, and P.S. Stewart, *A three-dimensional computer model of four hypothetical mechanisms protecting biofilms from antimicrobials.*, in *Applied and Environmental Microbiology*. 2006. p. 2005-2013.
22. Hunt, S.M., M.A. Hamilton, and P.S. Stewart, *A 3D model of antimicrobial action on biofilms*, in *Water Science & Technology*. 2005. p. 143-148.
23. COGAN, N., R. CORTEZ, and L. FAUCI, *Modeling physiological resistance in bacterial biofilms*, in *Bulletin of Mathematical Biology*. 2005. p. 831-853.
24. Donlan, R.M. and J.W. Costerton, *Biofilms: survival mechanisms of clinically relevant microorganisms.*, in *Clin. Microbiol. Rev.* 2002. p. 167-193.
25. Mah, T.F. and G.A. Toole, *Mechanisms of biofilm resistance to antimicrobial agents.*, in *Trends in Microbiology*. 2001. p. 34-39.
26. Roberts, M.E. and P.S. Stewart, *Modeling antibiotic tolerance in biofilms by accounting for nutrient limitation.*, in *Antimicrobial Agents and Chemotherapy*. 2004. p. 48-52.
27. Mah, T.-F., *Biofilm-specific antibiotic resistance*, in *Future Microbiology*. 2012. p. 1061-1072.
28. Walters, M.C., et al., *Contributions of Antibiotic Penetration, Oxygen Limitation, and Low Metabolic Activity to Tolerance of Pseudomonas aeruginosa Biofilms to Ciprofloxacin and Tobramycin*, in *Antimicrobial Agents and Chemotherapy*. 2003. p. 317-323.
29. Stewart, P.S., *Theoretical aspects of antibiotic diffusion into microbial biofilms.*, in *Antimicrobial Agents and Chemotherapy*. 1996. p. 2517-2522.
30. Stewart, P.S., *Biofilm accumulation model that predicts antibiotic resistance of Pseudomonas aeruginosa biofilms.*, in *Antimicrobial Agents and Chemotherapy*. 1994. p. 1052-1058.
31. Roberts, M.E., *Modelling protection from antimicrobial agents in biofilms through the formation of persister cells*, in *Microbiology*. 2005. p. 75-80.
32. Dodds, M.G., K.J. Grobe, and P.S. Stewart, *Modeling biofilm antimicrobial resistance.*, in *Biotechnol. Bioeng*. 2000. p. 456-465.
33. Molin, S. and T. Tolker-Nielsen, *Gene transfer occurs with enhanced efficiency in biofilms and induces enhanced stabilisation of the biofilm structure*, in *Current Opinion in Biotechnology*. 2003. p. 255-261.
34. Roberts, A.P., P. Mullany, and M. Wilson, *Gene transfer in bacterial biofilms.*, in *Meth. Enzymol*. 2001. p. 60-65.
35. Fux, C.A., et al., *Survival strategies of infectious biofilms.*, in *Trends in Microbiology*. 2005. p. 34-40.
36. Parsek, M.R. and P.K. Singh, *Bacterial biofilms: an emerging link to disease pathogenesis.*, in *Annu. Rev. Microbiol*. 2003. p. 677-701.
37. Lamont, R.J. and J.D. Bryers, *Biofilm-induced gene expression and gene transfer.*, in *Meth. Enzymol*. 2001. p. 84-94.
38. Wuertz, S., et al., *In situ quantification of gene transfer in biofilms.*, in *Meth. Enzymol*. 2001. p. 129-143.

39. Boles, B.R., M. Thoendel, and P.K. Singh, *Rhamnolipids mediate detachment of Pseudomonas aeruginosa from biofilms.*, in *Molecular Microbiology*. 2005. p. 1210-1223.
40. Senadheera, D. and D.G. Cvitkovitch, *Quorum sensing and biofilm formation by Streptococcus mutans.*, in *Adv. Exp. Med. Biol.* 2008. p. 178-188.
41. Li, Y.H., et al., *Natural genetic transformation of Streptococcus mutans growing in biofilms.*, in *J. Bacteriol.* 2001. p. 897-908.
42. Srinivasan, S., et al., *Factors affecting bulk to total bacteria ratio in drinking water distribution systems*, in *Water Research*. 2008. p. 3393-3404.
43. BATTE, M., *Biofilm responses to ageing and to a high phosphate load in a bench-scale drinking water system*, in *Water Research*. 2003. p. 1351-1361.
44. Momba, M., et al., *An overview of biofilm formation in distribution systems and its impact on the deterioration of water quality*. 2000, Water Reseach Council.
45. Josephson, J., *The Microbial "Resistome"*, in *Environ. Sci. Technol.* 2006. p. 6531-6534.
46. Martinez, J.L., *Environmental pollution by antibiotics and by antibiotic resistance determinants*, in *Environmental Pollution*. 2009, Elsevier Ltd. p. 2893-2902.
47. Aminov, R.I. and R.I. Mackie, *Evolution and ecology of antibiotic resistance genes*, in *FEMS Microbiology Letters*. 2007. p. 147-161.
48. Hong, P.Y., et al., *Environmental and Public Health Implications of Water Reuse: Antibiotics, Antibiotic Resistant Bacteria, and Antibiotic Resistance Genes*, in *Antibiotics*. 2013.
49. Jury, K.L., et al., *Antibiotic resistance dissemination and sewage treatment plants*, in *Current Research, Technology and Education Topics in Applied Microbiology and Microbial Biotechnology*. 2010. p. 509-519.
50. Heuer, H., H. Schmitt, and K. Smalla, *Antibiotic resistance gene spread due to manure application on agricultural fields.*, in *Current Opinion in Microbiology*. 2011. p. 236-243.
51. Kummerer, K., *Significance of antibiotics in the environment*, in *Journal of Antimicrobial Chemotherapy*. 2003. p. 5-7.
52. Le-Minh, N., et al., *Fate of antibiotics during municipal water recycling treatment processes*, in *Water Research*. 2010, Elsevier Ltd. p. 4295-4323.
53. Guardabassi, L., et al., *Antibiotic resistance in Acinetobacter spp. isolated from sewers receiving waste effluent from a hospital and a pharmaceutical plant.*, in *Applied and Environmental Microbiology*. 1998. p. 3499-3502.
54. Landers, T.F., et al., *A review of antibiotic use in food animals: perspective, policy, and potential.*, in *Public Health Rep*. 2012. p. 4-22.
55. van den Bogaard, A.E. and E.E. Stobberingh, *Antibiotic usage in animals: impact on bacterial resistance and public health.*, in *Drugs*. 1999. p. 589-607.
56. Allen, H.K., et al., *Call of the wild: antibiotic resistance genes in natural environments*. 2010, Nature Publishing Group. p. 1-9.
57. Schwartz, T., et al., *Detection of antibiotic-resistant bacteria and their resistance genes in wastewater, surface water, and drinking water biofilms*, in *FEMS Microbiology Ecology*. 2003, Wiley Online Library. p. 325-335.

58. Kim, S. and D.S. Aga, *Potential ecological and human health impacts of antibiotics and antibiotic-resistant bacteria from wastewater treatment plants.*, in *Journal of Toxicology and Environmental Health, Part B*. 2007. p. 559-573.

59. Martinez, J.L., *The role of natural environments in the evolution of resistance traits in pathogenic bacteria*, in *Proceedings of the Royal Society B: Biological Sciences*. 2009. p. 2521-2530.

60. Ding, C. and J. He, *Effect of antibiotics in the environment on microbial populations*, in *Appl Microbiol Biotechnol*. 2010. p. 925-941.

61. Zhang, X.-X., T. Zhang, and H.H. Fang, *Antibiotic resistance genes in water environment*, in *Appl Microbiol Biotechnol*. 2009, Springer. p. 397-414.

62. Jones, O.A., J.N. Lester, and N. Voulvoulis, *Pharmaceuticals: a threat to drinking water?*, in *TRENDS in Biotechnology*. 2005, Elsevier. p. 163-167.

63. Ash, R.J., B. Mauck, and M. Morgan, *Antibiotic resistance of gram-negative bacteria in rivers, United States.*, in *Emerging Infect. Dis*. 2002. p. 713-716.

64. D'Costa, V.M., E. Griffiths, and G.D. Wright, *Expanding the soil antibiotic resistome: exploring environmental diversity*, in *Current Opinion in Microbiology*. 2007. p. 481-489.

65. Aminov, R.I., *The role of antibiotics and antibiotic resistance in nature*, in *Environ Microbiol*. 2009. p. 2970-2988.

66. McKinney, C.W. and A. Pruden, *Ultraviolet disinfection of antibiotic resistant bacteria and their antibiotic resistance genes in water and wastewater.*, in *Environ. Sci. Technol*. 2012. p. 13393-13400.

67. Watson, S.K. and P.E. Carter, *Environmental influences on Acinetobacter sp. strain BD413 transformation in soil*, in *Biology and Fertility of Soils*. 2008, Springer. p. 83-92.

68. Chamier, B., M.G. Lorenz, and W. Wackernagel, *Natural Transformation of Acinetobacter calcoaceticus by Plasmid DNA Adsorbed on Sand and Groundwater Aquifer Material.*, in *Applied and Environmental Microbiology*. 1993. p. 1662-1667.

69. Armstrong, J.L., et al., *Antibiotic-resistant bacteria in drinking water.*, in *Applied and Environmental Microbiology*. 1981. p. 277-283.

70. Armstrong, J.L., J.J. Calomiris, and R.J. Seidler, *Selection of antibiotic-resistant standard plate count bacteria during water treatment.*, in *Applied and Environmental Microbiology*. 1982. p. 308-316.

71. Porstendörfer, D., U. Drotschmann, and B. Averhoff, *A novel competence gene, comP, is essential for natural transformation of Acinetobacter sp. strain BD413.*, in *Applied and Environmental Microbiology*. 1997. p. 4150-4157.

72. Guardabassi, L., A. Dalsgaard, and J.E. Olsen, *Phenotypic characterization and antibiotic resistance of Acinetobacter spp. isolated from aquatic sources.*, in *J. Appl. Microbiol*. 1999. p. 659-667.

73. Barbe, V., et al., *Unique features revealed by the genome sequence of Acinetobacter sp. ADP1, a versatile and naturally transformation competent bacterium.*, in *Nucleic Acids Res*. 2004. p. 5766-5779.

74. Juni, E., *Interspecies transformation of Acinetobacter: genetic evidence for a ubiquitous genus.*, in *J. Bacteriol.* 1972. p. 917-931.

75. Hendrickx, L., M. Hausner, and S. Wuertz, *Natural genetic transformation in monoculture Acinetobacter sp. strain BD413 biofilms.*, in *Applied and Environmental Microbiology.* 2003. p. 1721-1727.

76. Juni, E., *Genetics and physiology of Acinetobacter*, in *Annual Reviews in Microbiology.* 1978.

77. Palmen, R., et al., *Physiological characterization of natural transformation in Acinetobacter calcoaceticus.*, in *J. Gen. Microbiol.* 1993. p. 295-305.

78. Elliott, K.T. and E.L. Neidle, *Acinetobacter baylyi ADP1: Transforming the choice of model organism*, in *IUBMB Life.* 2011. p. 1075-1080.

79. Wu, J. and C. Xi, *Evaluation of Different Methods for Extracting Extracellular DNA from the Biofilm Matrix*, in *Applied and Environmental Microbiology.* 2009. p. 5390-5395.

80. Young, D.M., D. Parke, and L.N. Ornston, *Opportunities for genetic investigation afforded by Acinetobacter baylyi, a nutritionally versatile bacterial species that is highly competent for natural transformation.*, in *Annu. Rev. Microbiol.* 2005. p. 519-551.

81. Lorenz, M.G. and W. Wackernagel, *Bacterial gene transfer by natural genetic transformation in the environment.*, in *Microbiol. Rev.* 1994. p. 563-602.

82. Palmen, R. and K.J. Hellingwerf, *Acinetobacter calcoaceticus liberates chromosomal DNA during induction of competence by cell lysis.*, in *Curr. Microbiol.* 1995. p. 7-10.

83. Link, C., et al., *Identification and characterization of a novel competence gene, comC, required for DNA binding and uptake in Acinetobacter sp. strain BD413.*, in *J. Bacteriol.* 1998. p. 1592-1595.

84. Busch, S., C. Rosenplänter, and B. Averhoff, *Identification and characterization of ComE and ComF, two novel pilin-like competence factors involved in natural transformation of Acinetobacter sp. strain BD413.*, in *Applied and Environmental Microbiology.* 1999. p. 4568-4574.

85. Herzberg, C., A. Friedrich, and B. Averhoff, *comB , a novel competence gene required for natural transformation of Acinetobacter sp. BD413: identification, characterization, and analysis of growth-phase-dependent regulation*, in *Archives of Microbiology.* 2000. p. 220-228.

86. Porstendörfer, D., et al., *ComP, a pilin-like protein essential for natural competence in Acinetobacter sp. Strain BD413: regulation, modification, and cellular localization.*, in *J. Bacteriol.* 2000. p. 3673-3680.

87. Palmen, R., P. Buijsman, and K.J. Hellingwerf, *Physiological regulation of competence induction for natural transformation in Acinetobacter calcoaceticus*, in *Archives of Microbiology.* 1994, Springer. p. 344-351.

88. Palmen, R. and K.J. Hellingwerf, *Uptake and processing of DNA by Acinetobacter calcoaceticus--a review.*, in *Gene.* 1997. p. 179-190.

89. Seitz, P. and M. Blokesch, *Cues and regulatory pathways involved in natural competence and transformation in pathogenic and environmental Gram-negative bacteria.*, in *FEMS Microbiology Reviews*. 2013. p. 336-363.

90. Williams, H.G., et al., *Natural transformation in river epilithon.*, in *Applied and Environmental Microbiology*. 1996. p. 2994-2998.

91. Nielsen, K.M., K. Smalla, and J.D. van Elsas, *Natural transformation of Acinetobacter sp. strain BD413 with cell lysates of Acinetobacter sp., Pseudomonas fluorescens, and Burkholderia cepacia in soil microcosms.*, in *Applied and Environmental Microbiology*. 2000. p. 206-212.

92. LeChevallier, M.W., T.M. Babcock, and R.G. Lee, *Examination and characterization of distribution system biofilms.*, in *Applied and Environmental Microbiology*. 1987. p. 2714-2724.

Chapter 3

Evaluation of DNA transformation frequency in *Acinetobacter baylyi* AC811 biofilm and suspended culture

3.1 Abstract

Biofilms form in water distribution systems, coming in contact with potential donor DNA sources. The prevailing hypothesis is that frequency of gene transfer in biofilms is higher than that in corresponding planktonic counterparts, in part due to increased competence. Therefore, biofilms in water distribution systems may significantly contribute to the formation and spread of antibiotic resistant bacteria in water systems through natural transformation. To test the hypothesis regarding increased competence of biofilm cells, transformation frequencies in the biofilm and planktonic growth of *Acinetobacter* sp. strain AC811 with donor plasmid pWH1266 DNA carrying a tetracycline resistance marker were compared. Additionally, the underlying genetic mechanism responsible for observed differences was characterized. We demonstrate that detectable transformation frequencies are seen in *Acinetobacter* sp. strain AC811 biofilms developed in flow systems and exposed to varying donor DNA. Transformation frequencies ranged from 0 to $10e^{-4}$. We also compared DNA transformation frequencies in biofilm cells and overlying suspended cells grown in microtiter plates for 60 hours and in biofilm cells grown in a flow-cell system for 12, 24, 48 & 72 hours with planktonic cells grown in batch culture and

recovered at the exponential, early-stationary and late-stationary phases. The microtiter

experiment data show that the transformation frequencies of suspended cells were at least

10-fold higher than that of the biofilm cells. Similarly, the flow system experiment data

indicate that transformation frequencies of the planktonic samples at various growth stages

were approximately 10-fold higher than frequencies of corresponding biofilm samples. To

investigate whether the expression of competency components is differentially expressed

in both growth modes, qPCR was used to quantify the expression of the *comP* gene in

AC811. Comparison of *comP* gene expression trends in biofilm and planktonic cells

suggests that the ComP DNA uptake machinery is not synthesized to the same extent in

BD413 planktonic and biofilm cells, possibly accounting for observed transformation

frequency differences. The number of *comP* gene transcripts per AC811 biofilm cell

decreased over time. However, in a more complex pattern, number of *comP* gene

transcripts per planktonic cell decreased over the course of the exponential phase and then

increased to maximal levels in the stationary phase. The evidence indicates that BD413

planktonic cells are more competent than BD413 cells in the biofilm growth mode and that

the hypothesis regarding increased competence of biofilm cells may not be generalizable

across all bacterial species.

3.2 Introduction

Biofilms are interactive microbial communities formed by sessile clusters of bacteria

attached to organic or inert surfaces.[1-3] These bacterial aggregates are encased within a

matrix composed of water, polymeric substances including extracellular DNA produced by

the cells themselves, and other debris from the surrounding environment.[4-7] It is now widely accepted that biofilms are the preferred mode of bacterial growth and are ubiquitous in clinical, industrial and natural settings.[8-11] In particular, they adhere to the surface of water distribution pipes and storage tanks and form biofilms. Approximately 95% of the biomass in water systems is in the form of biofilms while less than 5% is found suspended in the bulk fluid.[12] Water networks can also be reservoirs of antibiotic resistant genes.[13-15] The presence of resistance determinants and high cell densities in this setting may induce horizontal gene transfer.[14]

Microbial biofilms are not simply a cluster of settled planktonic cells; they exhibit distinct properties from their free-floating counterparts.[16, 17] The complex biofilm structure and induced phenotype of the component cells is the result of a variation in gene regulation as compared to respective planktonic counterparts.[18-21] Furthermore, architectural features of and gene expression in biofilms may enhance gene transfer among biofilm cells.[2, 4, 11, 22] A general assumption is that biofilms have high gene transfer frequencies as compared to planktonic cells due to advantages afforded by the matrix, increased genetic competence, and close spatial orientation of the cells.[11, 21, 23] The matrix concentrates exogenous DNA for efficient uptake during natural transformation. Roberts et al. (2001) hypothesized that there are a variety of phenotypes displayed among the closely packed cells within a biofilm with an increased likelihood of 'gene transfer' phenotypes.[8, 18, 23] The close proximity of cells in a biofilm also facilitates cell-cell communication.[3, 4] This may increase genetic competence in instances where competence induction is regulated via a quorum-sensing

28

mechanism such as in Gram-positive *Streptococcus mutans*.[19] In *S. mutans*, the level of competence is higher in biofilm cells as compared to associated planktonic cells resulting in up to a 600-fold increase in transformation frequency of biofilm cells.[24] However, this phenomenon has not been demonstrated in other bacterial species.

In the current study, we assess the transformation frequency of monoculture *Acinetobacter baylyi* strain AC811 biofilms developed in a once-through flow system that have been exposed to donor DNA encoding antibiotic resistance. We also compare transformation frequencies and expression patterns of *comP*, a competence pathway gene, in *Acinetobacter baylyi* strain AC811 biofilm and suspended growth modes. *Acinetobacter* spp. are Gram-negative, non-motile, coccobacilli bacteria that are ubiquitous in the environment.[12, 25-28] AC811 is a derivative of *Acinetobacter baylyi* strain BD413, a naturally competent strain that is well suited for studying natural transformation.[29, 30] It has an extremely efficient transformation system and does not discriminate between homologous and heterologous DNA.[25] Thus far, five genes in the BD413 competence pathway have been identified and the expression of a portion of these has been characterized in planktonic batch culture cells.[25, 31, 32] There is no evidence that induction of competence in strain BD413 is regulated by a quorum-sensing mechanism.

Previous experiments have characterized transformation frequencies of *Acinetobacter baylyi* strain BD413 planktonic cells and biofilms developed in the lab setting.[33, 34] In a set of batch culture transformation experiments, Palmen et al. (1994) found that BD413 cells induced competence for natural transformation maximally after dilution of stationary phase

cells into fresh medium. Thus, transformation frequencies of BD413 cells with plasmid DNA were highest at the start of the exponential phase, decreased over the course of the exponential phase, and were undetectable in the stationary phase.[34] Hendrickx et al. (2003) studied the effect of biofilm age on transformation frequency in monoculture BD413 biofilms developed in once-through flow systems exposed to influent plasmid DNA.[33] The authors found that biofilm thickness reached a maximum after 48 h and remained at this level due to a steady state between lysis, detachment and growth functions.[33] Thus, 1-day old BD413 biofilms are still actively growing and accumulating mass while 3-day old biofilms could be considered mature biofilms.[33] Transformation frequencies in mature BD413 biofilms were lower than young biofilms.[33]

We expand on the work of Hendrickx et al. (2003) by evaluating DNA frequency in AC811 biofilms developed in a flow system with extracted genomic DNA in addition to plasmid DNA.[33] And, to our knowledge, this is the only study that compares transformation frequencies and competence gene expression between *Acinetobacter baylyi* biofilm and planktonic cells. We additionally characterize the expression pattern of a competence pathway gene, *comP,* in *Acinetobacter baylyi* strain AC811 biofilm cells. Finally, it is the only study to use a Gram-negative bacterium to test the hypothesis of increased genetic competence and gene transfer in biofilms as compared to free-floating cells.

3.3 Methods

3.3.1 Bacterial strains, plasmids & growth conditions.

Strains and plasmids used in this experiment are listed in Table 3.1. All strains were subcultured from frozen stock. Stocks were prepared from overnight batch cultures (240 rpm, 30 °C) grown in Luria-Bertani (LB) broth (BD Diagnostics, Franklin Lakes, NJ). Aliquots were then frozen with 70% glycerol and stored at -80 °C. Strains were routinely maintained on LB plates and LB medium supplemented with either 25 μg/ml kanamycin (Fisher Sci, Houston, TX), 50 μg/ml streptomycin (Sigma Aldrich, St. Louis, MO) or 5 μg/ml tetracycline (Sigma Aldrich, St. Louis, MO) was used to select for antibiotic resistant transformants. In the current study, a series of transformation experiments were conducted with recipient cells developed in different growth modes. *Acinetobacter* sp. strain AC811 served as the recipient strain in all transformation experiments. The nonencapsulated AC811 strain is a derivative of *Acinetobacter* sp. strain BD413 (also known as *Acinetobacter* sp. strain ADP1) and belongs to the *Acinetobacter baylyi* species.[30, 35]

Acinetobacter sp. strain AC811 biofilms developed in a flow-though system served as recipient cells in experiments assessing transformation frequency associated with influx of genomic DNA, plasmid DNA and PCR amplified DNA product.[8] Genomic DNA was isolated from streptomycin resistant (strep^r) strain *Acinetobacter* sp. strain AC323 and a tetracycline resistant (tet^r) *Acinetobacter* sp. environmental isolate. Plasmid pWH1266, carrying a tet^r marker, was isolated from *Acinetobacter* sp. strain AC1499. And, a 1kb

DNA segment containing a kanamycin resistance (kan^r) gene flanked by sequences homologous to the recipient AC811 strain was obtained through PCR amplification of the appropriate region in the AC811 *comP* mutant strain (AC811Δ*comP*::km). *A. baylyi* strain AC811 and AC811Δ*comP*::km were used as the recipients in transformation frequency experiments comparing competence of biofilm and free-floating cells. The donor DNA in these genetic transformation experiments was the plasmid pWH1266 carrying a tet^r marker.

3.3.2 Preparation and storage of transforming DNA.

All plasmid DNA was extracted using the QIAprep Spin Miniprep Kit (50) (QIAGEN, Valencia, CA) and all genomic DNA was obtained with the Wizard SV Genomic DNA Purification System (Promega, Madison, WI) following protocols as described in the respective manuals (Promega, Madison, WI). DNA sample concentrations were determined using the Nanodrop 1000 (Thermo Scientific, Hanover Park, IL) and were subsequently stored at -80 °C.

The following primers were used to amplify the 1000 bp fragment from the AC811Δ*comP*::km strain: F' CTAAGAACAAATTGTGTGAG ; R' GATTTACTTGAAATCGCGCC (IDT, Coralville, IA). Primer stocks (100 μM) were stored at -80 °C. The PCR reaction was conducted by adding 1μl of extracted AC811Δ*comP*::km genomic DNA (20 ng/μl) into a microcentrifuge tube and then adding 39.75 μl sterile water, 5 μl 10X GoTaq Buffer (Promega, Madison, WI), 2.0 μl dNTP mix (40 mM), .25 μl GoTaq DNA polymerase (Promega, Madison, WI), and 1 μl of each

primer (20 µM). PCR reactions to amplify the 1000 bp DNA fragment were performed as follows: 95 °C (10 min), 30 cycles of 94 °C (1 min), 42 °C (30 sec), 72 °C (30 sec), and 72 °C (10 min) for final extension. PCR amplified product was purified using the QIAquick PCR product purification kit (QIAPREP, Valencia, CA). Amplified products were quantified on the Nanodrop 1000.

3.3.3 Screening of antibiotic resistant transformants in experiments assessing transformation frequency of AC811 biofilms developed in once-through flow systems and exposed to influent genomic and plasmid donor DNA.

Kanamycin, streptomycin and tetracycline sensitive AC811 cells were grown in biofilms developed in a once flow-through system and were exposed to the previously described donor DNA. Post incubation, appropriate biofilm and effluent sample dilutions were spread onto fresh LB medium plates and onto LB medium plates supplemented with either kanamycin (25 µg/ml), streptomycin (50 µg/ml) or tetracycline (5 µg/ml) to capture transformants. After 24 h incubation at 30 °C, transformation frequencies were obtained by calculating the ratio of transformants to the total viable cell count.

3.3.4 Screening of tet^r transformants in experiments comparing transformation frequencies of AC811 cells in biofilm and suspended growth modes.

Tetracycline-sensitive AC811 cells developed under varying growth conditions were incubated with pWH1266 donor DNA in polystyrene microtiter plate wells. Post incubation, appropriate dilutions were spread onto fresh LB medium plates and onto LB medium plates supplemented with tetracycline (5 µg/ml) to capture transformants. After 24

h incubation at 30 °C, transformation frequencies were obtained by calculating the ratio of transformants to the total viable cell count.

3.3.5 Transformability of AC811.

Plate transformation experiments were conducted to confirm the transformability of AC811 with the previously described donor DNA. In brief, a mixture of 100 μl of an 8 h AC811 planktonic broth culture and 10 μl of a 2 μg/ml donor DNA solution was placed onto an LB plate. Post incubation at 30 °C for 6 h, the cells were scraped off and diluted into 1 ml 1X PBS. Appropriate dilutions were spread onto fresh LB medium plates and onto LB medium plates supplemented with antibiotic to capture transformants. After 24 h incubation at 30 °C, transformation frequencies were obtained by calculating the ratio of transformants to the total viable cell count. These experiments also verified that transformants were able to grow on the appropriate selective plates.

3.3.6 Evaluation of transformation frequency in AC811 biofilms, developed in a once-through flow system, with genomic and plasmid donor DNA.

AC811 biofilms were grown in silicon tubes in a once-through flow system using methods described previously.[8] 10% LB growth media was continuously pumped through the system at a constant flow rate of 30 ml/h with the aid of a multi-channel pump (Ismatec 12Ch peri pump, Fisher Sci, Houston, TX). Thus, multiple biofilms could be developed in parallel. Initially, the system was inoculated with 1 ml of an 8 h AC811 batch culture and

media flow was paused for 3 h to allow for bacterial attachment. Flow was then resumed at 7 ml/h for 1 h and then increased to 30 ml/h thereafter.

AC811 biofilms were grown for 72 h in the flow-system. At that time point, 2 μg/ml donor DNA solutions made up in minimal M9 media (64 g/L Na_2HPO_4, 15 g/L KH_2PO_4, 2.5 g/L NaCl, 5.0 g/L NH_4Cl, 1M $MgSO_4$, 1M $CaCl_2$) were added to the system at a flow rate of 7 ml/h over the course of 1 h. As discussed previously, multiple biofilms may be developed in parallel and donor DNA was only administered once for each distinct channel. After donor DNA addition, the flow rate was maintained at 7 ml/h for 1 h and then increased to 30 ml/h thereafter.

Post DNA addition, effluent was collected at the 24 h and 48 h time points and the biofilm biomass was scraped off the silicone tubing and collected at the 72 h time point. All samples were homogenized (~17,000 rpm, TH Homogenizer, Omni International, Marietta, GA) and plated appropriately. Transformation frequencies were calculated as described above. Baseline effluent was collected prior to the addition of donor DNA solution to each biofilm channel in the flow-system. Baseline samples were plated as described above to check for a potential spontaneous mutation rate to the tested antibiotics. In addition, with each biofilm run there was at least one channel to which no DNA was added to serve as a negative control. Concurrent with the addition of the donor DNA solution to the biofilm flow-system, aliquots of the donor DNA were spread onto LB agar plates and incubated at 30°C for at least 24 h to check for possible contamination of the extracted donor DNA solution with any remaining live cells of the source resistant strain.

3.3.7 Comparison of transformation frequencies of biofilms developed in a static system with transformation frequencies in overlying suspended cells.

AC811 static biofilms were grown at room temperature for a period of 60 h in Costar 6-well microtiter plates (Fisher Sci., Houston, TX) through a 1:10 inoculation of 10% LB media with an 8 h batch culture. Biofilm biomass and suspended cells grown in one well were separated resulting in one biomass sample and one suspended cell sample. These samples were subsequently homogenized (~17,000 rpm) and incubated with pWH1266 plasmid at a final concentration of 0.4 μg/ml for 6 h (Figure 3.1A). Donor pWH1266 DNA was added to another microtiter plate well at a final concentration of 0.4 μg/ml. After a 6 h incubation period, the combined mixture of biofilm biomass and overlying suspended cells was homogenized (~17,000 rpm) to disperse the cells (Figure 3.1B). Finally, pWH1266 DNA was added to yet another microtiter plate well at a final concentration of 0.4 μg/ml. After a 6 h incubation period, the biofilm biomass was separated from the overlying suspended cells resulting in separate biofilm biomass and suspended cell solutions. The biofilm biomass and suspended cell samples were then homogenized to disperse the cells (~17,000 rpm), (Figure 3.1C). All homogenized samples were plated appropriately and transformation frequencies were calculated as described above.

3.3.8 Comparison of transformation frequencies of biofilms developed in a static system with transformation frequencies in planktonic batch culture cells.

AC811 static biofilms were grown at room temperature for a period of 60 h in Costar 6-well microtiter plates (Fisher Sci., Houston, TX) through a 1:10 inoculation of 10% LB media with an 8 h batch culture. The overlying suspended cells were removed and the

remaining biofilm biomass was homogenized (~17,000 rpm). Biofilm cells were counted

using the Haussner Brightline Counting Chamber as per manufacturer instructions

(Hausser Sci., Horsham, PA). Samples in the range of 10^8 cells/ml were incubated with

donor DNA for 2 h and for 6 h at a final concentration of 0.4 μg/ml. AC811 planktonic

cells were grown at room temperature in batch culture mode in 10% LB for approximately

8 h to capture them in the exponential phase. Cells were counted and samples in the range

of 10^8 cells/ml were incubated with donor DNA for 2 h and for 6 h at a final concentration

of 0.4 μg/ml. Post incubation, all samples were plated appropriately and transformation

frequencies were calculated as described above.

3.3.9 Comparison of transformation frequencies of biofilms developed in a flow system with transformation frequencies in planktonic batch culture cells.

AC811 biofilms were grown in silicon tubes in a once-through flow system using methods

described previously.[8] 10% LB growth media was continuously pumped through the

system at a constant flow rate of 30 ml/h with the aid of a multi-channel pump (Ismatec

12Ch peri pump, Fisher Sci, Houston, TX). Initially, the system was inoculated with an 8 h

AC811 batch culture and media flow was paused for 3 h to allow for bacterial attachment.

Flow was then resumed at 7 ml/h for 1 h and then increased to 30 ml/h thereafter.

Biofilms were grown in the flow system for 12, 24, 48 and 72 h at room temperature.

AC811 batch culture cells were also grown in 10% LB at room temperature. Planktonic

cells were recovered at the exponential (8 h), early stationary (10 h), and late stationary

phases (12 h). At each biofilm or planktonic sampling time point, cells were homogenized (~17,000 rpm) and then counted using the Haussner Brightline Counting Chamber as per manufacturer instructions (Hausser Sci, Horsham, PA). Samples in the total cell count range of ~10^8 cells/ml were incubated with pWH1266 DNA in microtiter plate wells at a final concentration 0.4 μg/ml for 2 h and for 6 h. Post incubation, all samples were plated appropriately and transformation frequencies were calculated as described above.

3.3.10 Confirmation of the role of the *comP* gene in the AC811 transformation pathway.

Transformation experiments were conducted with a *comP* mutant of strain AC811 (AC811Δ*comP*::km) to confirm the necessity of the ComP protein in natural transformation. AC811Δ*comP*::km biofilms were grown in static systems for 60 h and in flow systems for 12, 24, 48 & 72 h, under growth conditions similar to those above. These biofilm samples and their planktonic counterparts were homogenized (~17,000 rpm) and then counted using the Haussner Brightline Counting Chamber (Hausser Sci, Horsham, PA). Samples in the total cell count range of ~10^8 cells/ml were incubated with pWH1266 DNA in microtiter plate wells at a final concentration 0.4 μg/ml for 2 h and for 6 h. Post incubation, all samples were plated appropriately and transformation frequencies were calculated as described above.

3.3.11 Sample collection and storage for downstream RNA extraction.

12, 24, 48 & 72 h AC811 biofilms were developed in the flow-system in 10% LB at room temperature using methods described above. AC811 batch culture cells were also grown in 10% LB at room temperature and recovered at 4, 6, 8, 10 & 12 h. At each biofilm or planktonic sampling time point, samples were immediately dispersed in RNAlater (Applied Biosystems/ Ambion, Austin, TX) per manufacturer instructions and homogenized (~17,000 rpm). Samples were further processed following RNAlater manual guidelines with aliquots set aside to be quantified using the Haussner Brightline Counting Chamber (Hausser Sci, Horsham, PA). All quantified biofilm and planktonic cell samples were stored at -80 º C for total RNA extraction.

3.3.12 RNA isolation and reverse transcription.

Total RNA was isolated via the hot-phenol method previously described followed by an RNAse-free DNAse I digestion (8U/ 100 ul) (Promega, Madison, WI).[36] Integrity of extracted RNA was verified by running the RNA in a precast 2% agarose E-gel (Invitrogen, Carlsbad, CA) and total RNA concentration was quantified on the Nanodrop 1000 spectrophotometer. Quantified extracted total RNA was stored at -80 °C. cDNA was reverse transcribed from 1 μg total RNA using the High Capacity cDNA Reverse Transcription Kit (Applied Biosystems, Carlsbad, CA) following protocols described in associated manuals. cDNA was quantified on the Nanodrop 1000 and subsequently stored at -80 °C.

3.3.13 Standard curve set-up.

The following desalted primers were used to amplify a 110 bp fragment of the target *comP*

gene: F' ATGAATGCACAAAAGGGTTT ; R' GCACGGACTGTATAATCTGT (IDT,

Coralville, IA). Primer stocks (100 μM) were stored at -80 °C. The PCR reaction was

conducted by adding 1μl of extracted AC811 genomic DNA (20 ng/μl) into a

microcentrifuge tube and then adding 34.75 μl sterile water, 10 μl 5X GoTaq Buffer

(Promega, Madison, WI), 1.0 μl dNTP mix (40 mM), .25 μl GoTaq DNA polymerase

(Promega, Madison, WI), and 1 μl of each primer (20 μM). PCR reactions to amplify the

110 bp *comP* gene fragment were performed as follows: 95 °C (10 min), 30 cycles of 94

°C (1 min), 42 °C (30 sec), 72 °C (30 sec), and 72 °C (10 min) for final extension. PCR

amplified product was purified using the QIAquick PCR product purification kit

(QIAPREP, Valencia, CA). Amplified products were quantified on the Nanodrop 1000 and

number of gene copies per ng DNA, for each sample, was calculated through a series of

mathematical conversions.

3.3.14 qRT-PCR rxn.

Optimized qRT-PCR reactions were completed on the Mastercycler realplex[2] (Eppendorf,

Westbury, NY) using SYBR Green fluorescence detection technology. Each 25μl real-time

PCR reaction mixture consisted of 12.5 μl 2X SYBR Green Master Mix (Applied

Biosystems, Carlsbad, CA), .25 μl of forward primer (20 μM), .25 μl of reverse primer (20

μM), 1.0 μl cDNA template, and 11.0 μl DNAse, RNAse free water. Real-time PCR

reactions were performed as follows: 95 °C (10 min), 30 cycles of 94 °C (1 min), 42 °C

(30 sec), 72 °C (30 sec), and 72 °C (10 min) for final extension. The fluorescence

measuring point was set at the annealing step. All qPCR reactions were run with a duplicate standard curve ranging from $10^2 - 10^8$ gene copies/ μl of the *comP* gene fragment and absolute numbers of *comP* gene transcripts were extrapolated from standard curve Ct values. Appropriate calculations were completed to obtain number of *comP* gene transcripts/ cell for all biofilm and planktonic samples.

3.4 Results

3.4.1 Exposure to amplified PCR product, plasmid DNA and genomic DNA encoding resistance genes results in detectable transformation frequencies in single species biofilms developed in once-through flow systems.

AC811 biofilms were developed in once-through flow systems for 72 h after which they were exposed to influent donor DNA for 1 h. Effluent samples were collected at the baseline, 24 h and 48 h time points and biofilm cells were scraped from the tube at the 72 h time point. Baseline samples were collected prior to exposure to donor DNA and each multi-channel run included one negative control tube to which no donor DNA was added. Undetectable transformation frequencies in all baseline and negative control samples indicate that there is no baseline spontaneous mutation rate or contamination. Results from Figure 3.2 indicate that transformation frequencies in effluent and cell samples from biofilms exposed to amplified PCR products are at least 10-fold higher than respective time point samples from biofilms exposed to pWH1266 plasmid DNA. In general, there were detectable transformation frequencies in biofilms exposed to PCR amplified product, plasmid DNA and genomic DNA.

3.4.2 Transformation frequencies of biofilms grown in a static system are at least 10-fold lower than transformation frequencies of the overlying suspended cells.

AC811 static biofilms were developed in microtiter plate wells for 60 h after which samples were processed as previously described (Figure 3.1A-C). Two biological replicates, both with three technical replicates, were completed for each of five transformation experiments represented in Figure 3.3. The average transformation frequency of suspended cells (S) homogenized prior to incubation with pWH1266 plasmid DNA carrying a tet^r resistance gene is 2.8×10^{-4}. Surprisingly, this is approximately 10-fold higher than the 2.6×10^{-5} transformation frequency of biofilm biomass cells (B) also homogenized prior to incubation with donor DNA. The fold-difference is decreased to 3-fold when comparing the transformation frequencies of biofilm biomass cells (B sep), that were incubated with donor DNA prior to homogenization, with suspended cells (S). Homogenization disrupts biofilm architecture and may inhibit any advantages provided by an intact matrix. Therefore, it is expected that biofilm cells that were homogenized prior to incubation with the plasmid DNA have lower transformation frequencies compared to biofilm cells that were left intact before incubation with donor DNA. There is a significant decrease ($p < 0.01$) of transformation frequencies in biofilm samples (B & B sep) compared to that of the suspended cell sample (S).

3.4.3 Transformation frequencies of AC811 biofilms developed in a static system are at least 10-fold lower than transformation frequencies of AC811 planktonic batch culture cells.

AC811 static biofilms were developed in microtiter plates for 60 h and AC811 planktonic cells were grown in batch culture mode and captured in the exponential phase (8 h). Isolated biofilm and planktonic cells were then homogenized and counted. Approximately 10^8 cells of each type were incubated with plasmid donor DNA for 2 h and for 6 h. Two biological replicates were completed for transformation experiments shown in Figure 3.4. For each biological replicate, transformation frequencies were averaged across three technical replicates. As seen in Figure 3.4, transformation frequencies of planktonic batch culture cells are at least 10-fold higher than transformation frequencies in biofilm cells for both the 2 h and 6 h incubation periods – contrary to the general hypothesis regarding increased competence of biofilm cells. However, the increase in transformation frequency for planktonic cells as compared to biofilm cells is only significant ($p < 0.01$) for the 6 h incubation data. The average transformation frequency of AC811 biofilm cells incubated with pWH1266 donor DNA for 2 h is 4.7×10^{-5} and for 6 h is 7.2×10^{-5}. Transformation frequencies of AC811 planktonic cells incubated with donor DNA for 2 h and 6 h are 1.1×10^{-3} and 8.6×10^{-3}, respectively. The viable cell count data indicates that the increase in transformation frequencies for both planktonic cells and biofilm cells is attributed to the longer incubation time with the donor DNA as opposed to post incubation growth.

3.4.4 Transformation frequencies of AC811 planktonic batch culture cells are as much as 10-fold higher than transformation frequencies of AC811 biofilms developed in a flow-system.

12, 24, 48 and 72 h BD413 biofilms were developed in a flow-system and AC811 cells grown in planktonic batch culture mode were captured at the exponential (8 h), early stationary (10 h) and late stationary phases (12 h). All samples were homogenized and counted and equivalent numbers of total cells were incubated with donor DNA for 2 h and 6 h incubation periods. Two biological replicates were completed for all respective transformation experiments. For each biological replicate, transformation frequencies were averaged across three technical replicates as seen in Figure 3.5.

Appropriate transformation frequency comparisons of planktonic batch culture cells and of biofilm cells developed in a dynamic flow system can be made based on growth stage. By definition, planktonic batch cultures are actively growing in the exponential phase and reach a maximal, steady growth level upon entry into stationary phase. And, according to Hendrickx et al. (2003), 1-day old AC811 biofilms are still actively growing and accumulating mass while 3-day old biofilms could be considered mature biofilms.[33] In the present study, transformation frequencies of planktonic exponential phase cells (8h) are higher than young (12 h & 24 h) biofilms for both the 2 h and 6 h incubation periods. The same pattern is seen when comparing transformation frequencies of early and late stationary phase planktonic cells with mature biofilms (48 h & 72 h). The difference between planktonic and biofilm transformation frequencies is most apparent in the 6 h incubation results. There is approximately a 10-fold transformation frequency difference

between planktonic exponential phase cells and 12 h biofilms. This difference increases to more than 10-fold when comparing planktonic exponential phase cells with a 24 h biofilm. Similarly, early stationary planktonic batch culture cells that have incubated with donor DNA for 6 h are approximately 10-fold higher than 48 h biofilms and late stationary planktonic batch culture cells are more than 10-fold higher than 72 h biofilms. Again, these results are surprising considering the general consensus that biofilm cells are more competent than their planktonic counterparts.

Despite the noted 10-fold differences, only a portion of these transformation frequency comparisons is statistically significant. In particular, exponential planktonic cells incubated for 2 h with donor DNA have significantly ($p < .05$) higher transformation frequencies than 24 h biofilm cells incubated with donor DNA for 2 h. Planktonic cells captured during the early stationary phase and incubated with donor DNA for 6 h display significantly ($p < 0.01$) increased transformation frequencies than 48 h biofilm cells incubated with donor DNA for the same time period. Finally, late stationary planktonic cells incubated with donor DNA for 2 h have significantly higher transformation frequencies ($p < .05$) than comparable 72 h biofilm transformation frequencies and late stationary planktonic cells incubated with donor DNA for 6 h have significantly ($p < 0.01$) increased transformation frequencies than 72 h biofilm cells incubated with donor DNA for 6 h.

3.4.5 The ComP protein is necessary for natural transformation in *Acinetobacter baylyi* strain AC811 and contributes to the differential transformation frequency between biofilm cells and their planktonic counterparts.

Competence factor, ComP, is necessary for natural transformation in strain AC811. It allows for the binding to and uptake of exogenous DNA.[25] Transformation frequency experiments with AC811 *comP* mutant biofilms grown in static systems and in flow-systems and with their respective planktonic counterparts were conducted. Resultant undetectable transformation frequencies indicate that the ComP protein is an essential component of the BD413 transformation pathway (data not shown). We also investigated *comP* gene expression in biofilms and their planktonic counterparts using quantitative PCR. Total RNA was extracted from quantified AC811 biofilms developed in flow-systems and planktonic batch culture cells. Samples were run alongside standard curves in quantitative PCR experiments to obtain absolute quantification of the number of *comP* gene transcripts per cell. Forward and reverse primers were consistently run between 90-99% efficiency. Two biological replicates, with three technical replicates, were run for each biofilm and planktonic time point. Variance of technical replicate Ct values were < .56 for all samples.

Results in Figure 3.6 show that the number of *comP* gene transcripts per AC811 biofilm cell decrease over time. In a more complex pattern, number of *comP* gene transcripts per planktonic cell decrease over the course of the exponential phase and then increase to maximal levels in the stationary phase. The patterns seen in the planktonic cells are consistent with the literature and comparison of the biofilm and planktonic *comP*

expression data may elucidate previously described results.[31] In particular, qPCR results indicate that the number of comP gene transcripts per late phase planktonic cell is significantly higher (p < .05) than the number of *comP* gene transcripts per mature biofilm cell. This suggests that the DNA uptake machinery is not synthesized to the same extent in BD413 planktonic and biofilm cells, possibly accounting for observed transformation frequency differences.

3.5 Discussion

Biofilms in water distribution systems may significantly contribute to the formation and spread of antibiotic resistant bacteria in water systems through natural transformation. Our initial approach to this multitier question involved the use of a simplified laboratory biofilm model to assess the transformation frequency in biofilms and in detached effluent cells with donor DNA of different formats. We also compared transformation frequencies of and expression of a competence pathway component in biofilm and planktonic cells to substantiate the general claim of increased competence in the biofilm state.[23]

Exposure of monoculture AC811 biofilms to strep[r], tet[r] and kan[r] donor DNA resulted in detectable transformation frequencies in both the detached cells in effluent from the once-through flow system and in biofilm cells collected from the flow cell. These results indicate that transformation events can occur in a simplified laboratory model of a water distribution pipe under nutrient limited conditions similar to environmental conditions in water distribution systems in most developed countries.[37] In addition, detectable

transformation frequencies occur in biofilms exposed to tet[r] plasmid donor DNA. This is especially significant since many known antibiotic resistance genes in the environmental resistome are found on plasmids.[38]

Transformation frequency differences between biofilms exposed to the various DNA types in the once-through flow system experiments may be attributed to varying influent resistance determinant concentration and resistance mechanisms. Although the overall concentration of donor DNA fed into the influent was the same across the different types of donor DNA, the absolute concentrations of the respective resistance gene may have differed. For instance, the concentration of the resistance determinants in amplified PCR product was probably higher than the concentration of resistance genes in extracted genomic DNA. In addition, the number of steps to gene expression may explain the difference in transformation frequencies in biofilms exposed to plasmid donor DNA with those exposed to extracted genomic DNA from a tet[r] environmental isolate. Plasmid encoded tetracycline resistance on pWH1266 is expressed by the transformed host cell. However, assuming that resistance is not present on an extra-chromosomal plasmid in the environmental isolate, resistance expression would have to be preceded by uptake and integration of the determinant into the host cell chromosome. This may explain the lack of detectable transformants with the environmental isolate genomic DNA.

Hendrickx et al. (2003) also obtained detectable transformation frequencies for biofilms developed in a multi-channel flow system, but frequencies from that study were at least 10-

fold higher than our results.[33] Methods differences between the Hendrickx et al. (2003) study and our study hamper comparisons. In the Hendrickx et al. (2003) study, after initial inoculation with *Acinetobacter sp.* strain BD413, flow cells were exposed to donor DNA during 1 h of continuous flow with donor plasmid DNA. Transformation frequencies were calculated *in situ* via quantitative microscopy for 24 and 72 h biofilms and respective frequencies on the order of 10^{-2} and 10^{-4} were found.[33] Our study results indicate a transformation frequency of 3.45 x 10^{-5} in biofilms 72 h post exposure to 1 h continuous flow with plasmid DNA. As stated previously, this difference in results probably stems from protocol differences. Hendrickx and colleagues developed a biofilm in rich LB broth and assessed transformation frequency through a noninvasive method resulting in high transformation frequencies at a 10-fold lower donor DNA concentration and in much younger biofilms.[33] In comparison, we developed our biofilms under nutrient starvation conditions and biofilms were grown for 72 h, exposed to donor DNA and then plated 72 h post exposure to donor DNA. Transformation frequency in biofilms can decrease with age.[33] In addition, comparisons of *in situ* and plating techniques show 1000-fold higher conjugation rates with quantitative microscopy versus plating results.[39] Regardless of the discrepancy with the Hendrickx et al. (2003) results, our study still adds to the modest literature in this area. In addition, transformation frequencies of biofilms exposed to donor DNA, other than plasmid DNA, are detectable in the same system and under the same growth conditions.

Our results contradict the prevailing hypothesis regarding higher gene transfer rates in biofilms as well as transformation frequency work by Li et al. (2001) done with *Streptococcus mutans*.[23, 24] Surprisingly, in all experiments comparing biofilm and planktonic transformation frequencies in this study, AC811 biofilm transformation frequencies were lower than respective planktonic transformation frequencies. When making the appropriate comparisons, frequencies of planktonic cells were approximately 10-fold higher than biofilm frequencies. Given the close proximity of cells, the advantages of the extracellular matrix and the assumption of increased competence – it is reasonable to expect higher gene transfer rates in biofilms compared to planktonic cells.[18, 23] However, this has only been demonstrated by Li et al. (2001) with Gram-positive *Streptococcus mutans*.[24] Transformation frequencies in *Streptococcus mutans* biofilms were up to 600-fold higher than corresponding planktonic cells.[24] The disparity between our results and those of Li et al. (2001) may be explained by a difference in competence pathway induction between *Streptococcus mutans* and *Acinetobacter baylyi* strain AC811. *S. mutans* competence is regulated via a quorum sensing mechanism. *S. mutans* cells secrete competence stimulating peptide and threshold concentrations of this peptide trigger a series of events resulting in the up regulation of genes that govern competence. The aggregation of cells in a biofilm facilitates cell-cell interactions, such as quorum sensing, and the high density of cells would allow for concentrations of signaling molecules to approach threshold levels. In contrast, competence induction in *Acinetobacter baylyi* does not correlate with up regulation of genes in the competence pathway.[31, 40] To our knowledge only five genes in the *Acinetobacter baylyi* competence pathway have been identified:

comB, *comE*, *comF*, *comC* and *comP*.[25, 31, 32] The ComP protein is thought to function in binding and uptake of DNA.[31] In a study monitoring *comP* gene expression in planktonic batch culture via a *comP::lacZ* reporter construct – *comP* expression initially decreased over the course of the exponential phase and then began to increase to maximal levels during the transition from late exponential phase to stationary phase and beyond.[31] Interestingly, the expression of *comP* did not correlate with transformation frequencies of *Acinetobacter baylyi* cells with donor DNA. Transformation frequencies decreased over the course of the exponential phase to minimal levels in the stationary phase. Thus, *comP* transcription is growth dependent but does not correlate with competence development.[31] In fact, it may be that components necessary for DNA uptake are synthesized long before they are needed.[31]

Although *comP* gene expression does not seem to correlate with competence induction, comparison of the AC811 biofilm and planktonic batch culture *comP* gene expression patterns may elucidate an underlying reason for the observed transformation frequency differences seen between the two growth modes. Our study results show that *comP* expression reached maximal levels in the stationary phase of BD413 planktonic cells, similar to results previously found by Porstendorfer et al. (2000).[31] Whereas, the number of *comP* gene transcripts per cell decreased as the BD413 biofilm matured. Porstendorfer et al. (2000) saw an initial increase in transformation frequency immediately after inoculating fresh medium with stationary phase BD413 batch culture cells.[31] This led to the possible conclusion that DNA uptake apparatus is already synthesized prior to maximal

competence induction.[31] Mature biofilms are similar to stationary phase planktonic batch cultures. The number of *comP* gene transcripts per cell in 10 h and 12 h (stationary phase) planktonic batch cultures is significantly ($p < .05$) higher than those in 48 h and 72 h (mature) BD413 biofilms. This suggests that the DNA uptake machinery is not synthesized to the same extent in BD413 planktonic and biofilm cells, possibly accounting for observed transformation frequency differences.

Patterns of transformation frequencies were similar to those previously seen in the literature.[33, 41] *Acinetobacter baylyi* batch culture cells exhibit the highest competence during the exponential phase with competency decreasing thereafter.[25, 41] This is reflected in planktonic batch culture transformation frequencies in Figure 3.5. The same results show higher transformation frequencies in young biofilms compared to biofilms 24 h and older. Hendrickx et al. (2003) first showed this phenomenon in single species *Acinetobacter baylyi* biofilms developed in flow systems.[33] With some notable exceptions, the transformation frequency experiments in this paper involved sample homogenization prior to incubation with donor DNA. Homogenization not only avoids structural effects that may influence transformation frequency, it facilitates more accurate quantification of biofilm and planktonic cell numbers. Transformation frequencies of biofilms developed in static and flow-systems and their planktonic counterparts were compared. The physiologic and structural features of a biofilm may be dependent on the growth system used to develop the biofilm. Studies done by Hendrickx et al. (2003) indicate that the overlying

suspended cells inhibited the *in situ* transformation of *Acinetobacter baylyi* biofilms grown in static systems.[33]

Although our results indicate that AC811 planktonic cells are more competent than BD413 biofilm cells – this in no way diminishes the very real role of transformation in biofilms in the spread of antibiotic resistant genes in the environment. Transformation is a complex process influenced by numerous factors such as donor DNA, resistance gene type and the recipient strain. Therefore, it would be imprudent to draw general conclusions of transformation in biofilms based on current study results alone. In addition, the focus of this paper as well as many previous studies has been on the cellular components of the transformation pathway. However, biofilm architecture plays an important role in transformation, particularly advantages conferred by the extracellular matrix.[23] AC811 biofilms developed in a static system and incubated with donor DNA with an intact matrix displayed higher transformation frequencies than biofilm cells that were homogenized before incubation with transforming DNA. Future research should focus on structural features of biofilms and their effect on transformation. It is also important to recognize that transformation is only one of the mechanisms that bacteria use to acquire genes from other bacterial cells and the environment. High gene transfer rates in biofilms are due to conjugation and transduction mechanisms in addition to natural transformation.[18]

Table 3.1 Strains & plasmids

Strain or plasmid	Experimental function	Source or reference
Acinetobacter sp. strains		
AC811	Recipient Strain*	Vaneechoutte et al. (2006)
AC1499	Harbors plasmid pWH1266	Hunger et al. (1990)
AC811 Δ*comP*::km	*comP* mutant of AC811, contains a 1 kb fragment with a kan^r gene	Xi Lab
AC323	Donor DNA*, strep^r	Juni (1969)
Tet^r environmental isolate	Donor DNA*, tet^r	Xi Lab
Plasmids		
pWH1266	Donor DNA*, non-mobile, Tet^r	Hunger et al. (1990)

* with regards to transformation experiments
(kan^r) kanamycin resistance
(strep^r) streptomycin resistance
(tet^r) tetracycline resistance
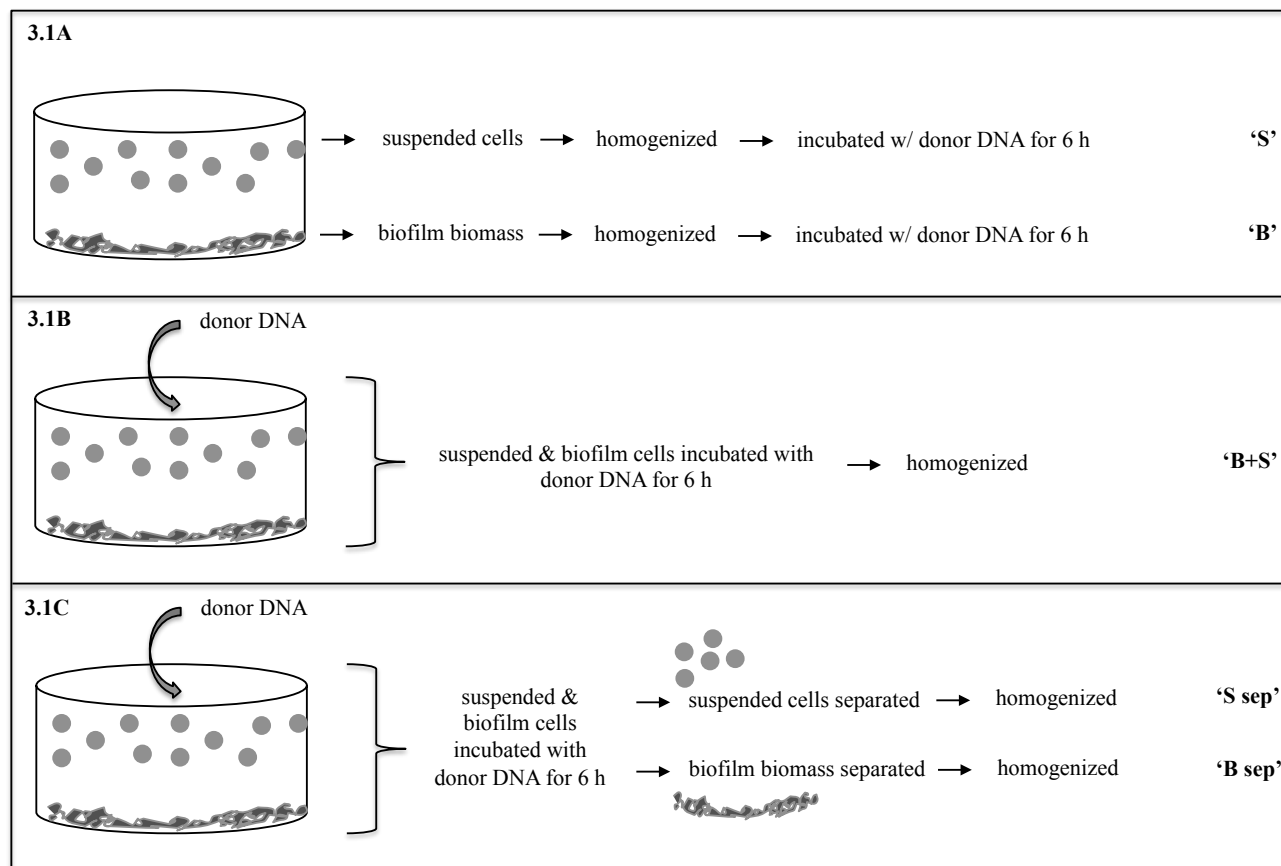
Figure 3.1: Processing of static biofilm samples. (A) Biofilm biomass and overlying suspended cells were isolated from one another, homogenized and incubated with donor DNA. These are samples 'B' & 'S', respectively. **(B)** Biofilm biomass and overlying suspended cells were incubated with the donor DNA together and then homogenized. This is sample 'B+S'. **(C)** Biofilm biomass and overlying suspended cells were incubated with the donor DNA together, separated into the two components and then homogenized. These are samples 'B sep' & 'S sep', respectively. All static biofilms were grown for 60 h and all samples were incubated for 6 h with pWH1266 donor DNA at a final concentration of .4 µg/ml. Transformation frequencies were calculated as previously described.
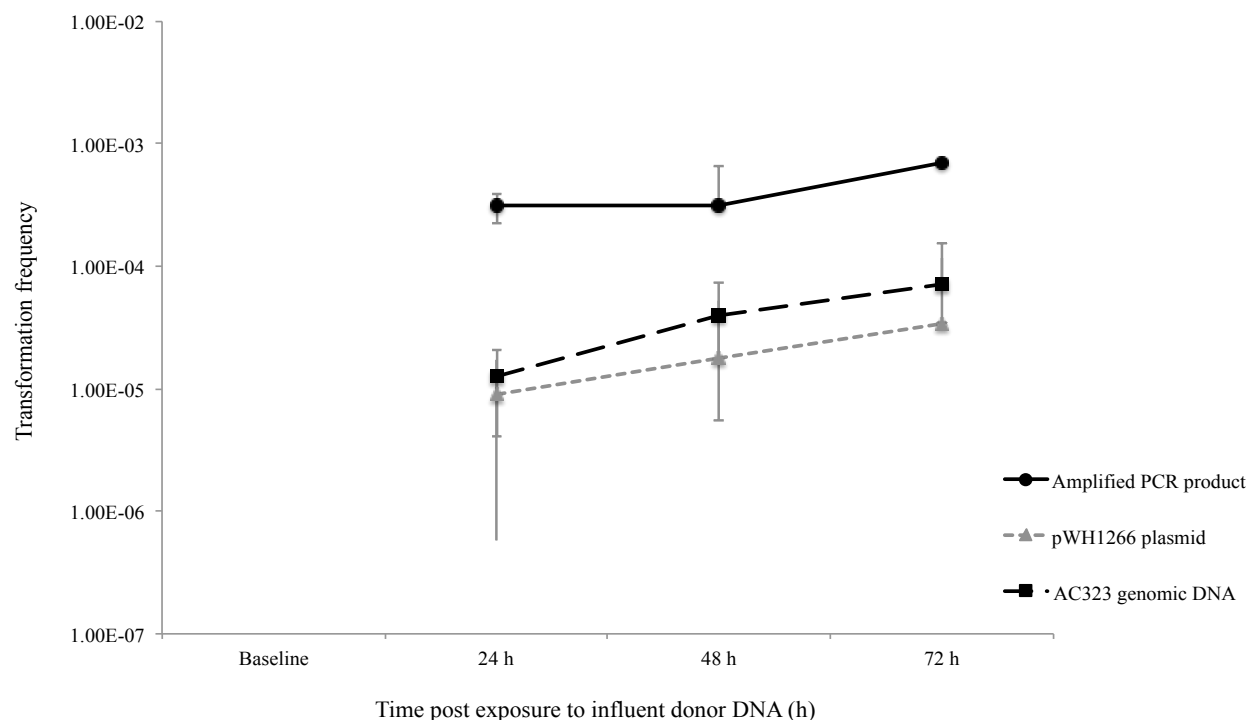
Figure 3.2: Transformation frequency of BD413 biofilms grown in a once-through flow system exposed to various types of donor DNA. 72 h *A. baylyi* strain BD413 biofilms developed in a flow though system served as recipient cells in experiments assessing transformation frequency associated with influx of genomic DNA, plasmid DNA and PCR amplified DNA product. Genomic DNA was isolated from streptomycin resistant strain AC323 and a tetracycline resistant *Acinetobacter* sp. environmental isolate. Plasmid pWH1266, carrying a tetracycline resistant marker, was isolated from *Acinetobacter calcoaceticus* strain 1499. And, a 1kb DNA segment containing a kanamycin resistance gene flanked by sequences homologous to the recipient BD413 strain was obtained through PCR amplification of the appropriate region in the BD413 *comP* mutant strain (BD413Δ*comP*::km). Transformation experiments conducted with the tetracycline resistant genomic donor DNA did not produce any detectable transformation frequencies. All transformation experiments were conducted twice; each with three technical replicates. Negative control experiments with no donor DNA in the influent indicated no detectable spontaneous mutation rate to any of the tested antibiotics. Baseline samples were collected prior to the addition of donor DNA to check for a baseline mutation rate. Transformation frequencies were calculated from effluent
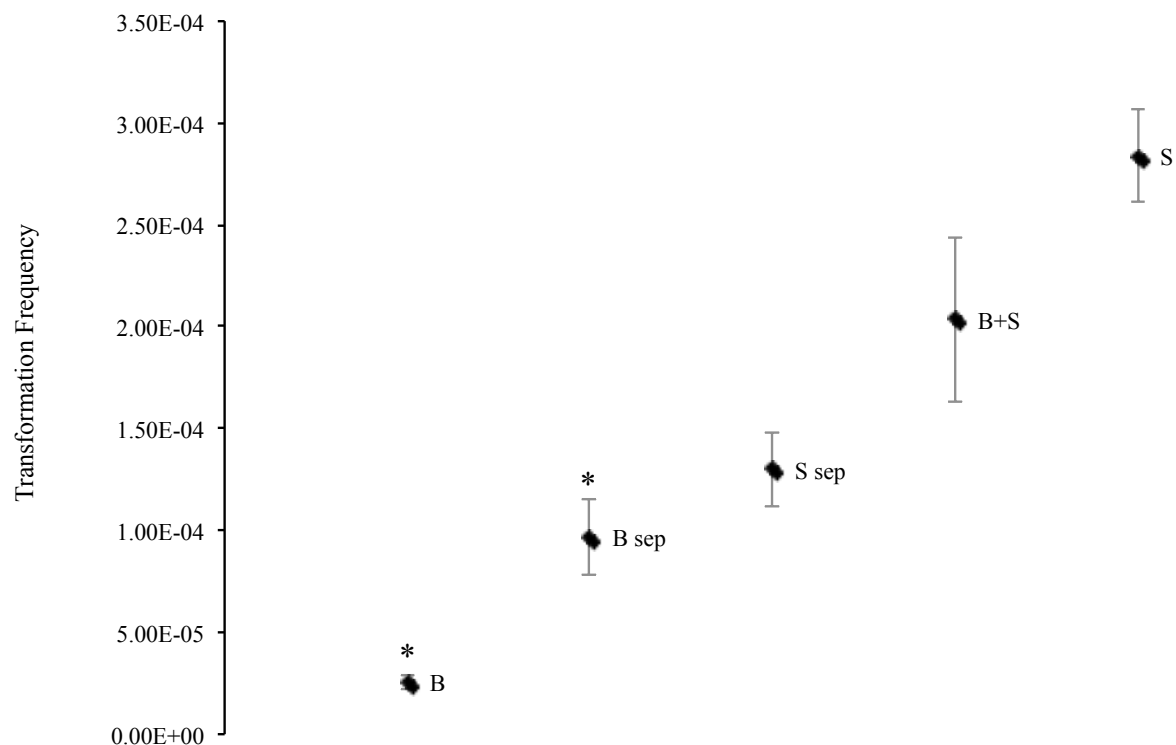
Figure 3.3: Transformation frequency of BD413 biofilms grown in the static system and the overlying suspended cells. (S) suspended cells were isolated from the biofilm biomass and incubated with DNA and transformation frequency was calculated post incubation; (B+S) biofilm biomass and suspended cells were incubated with DNA together before transformation frequency was calculated in the total sample; (S sep) biofilm biomass and suspended cells were incubated with DNA together before transformation frequency was calculated in the isolated suspended cell component; (B sep) biofilm biomass and suspended cells were incubated with DNA together before transformation frequency was calculated in the separated biofilm biomass component; (B) the biofilm biomass was isolated from the overlying suspended cells and incubated with DNA and transformation frequency was calculated post incubation. Symbol * indicates significant decrease (p<0.01) of transformation frequencies in biofilm samples (B & B sep) compared to that of the suspended cell sample (S). Negative control experiments with no donor DNA indicated no detectable spontaneous mutation rate. All biofilm biomass and suspended samples were incubated with pWH1266 plasmid donor DNA (at a final concentration of 0.4 µg/ml) for a period of 6 h. Two biological replicates, each with three technical replicates, were completed for each sample.
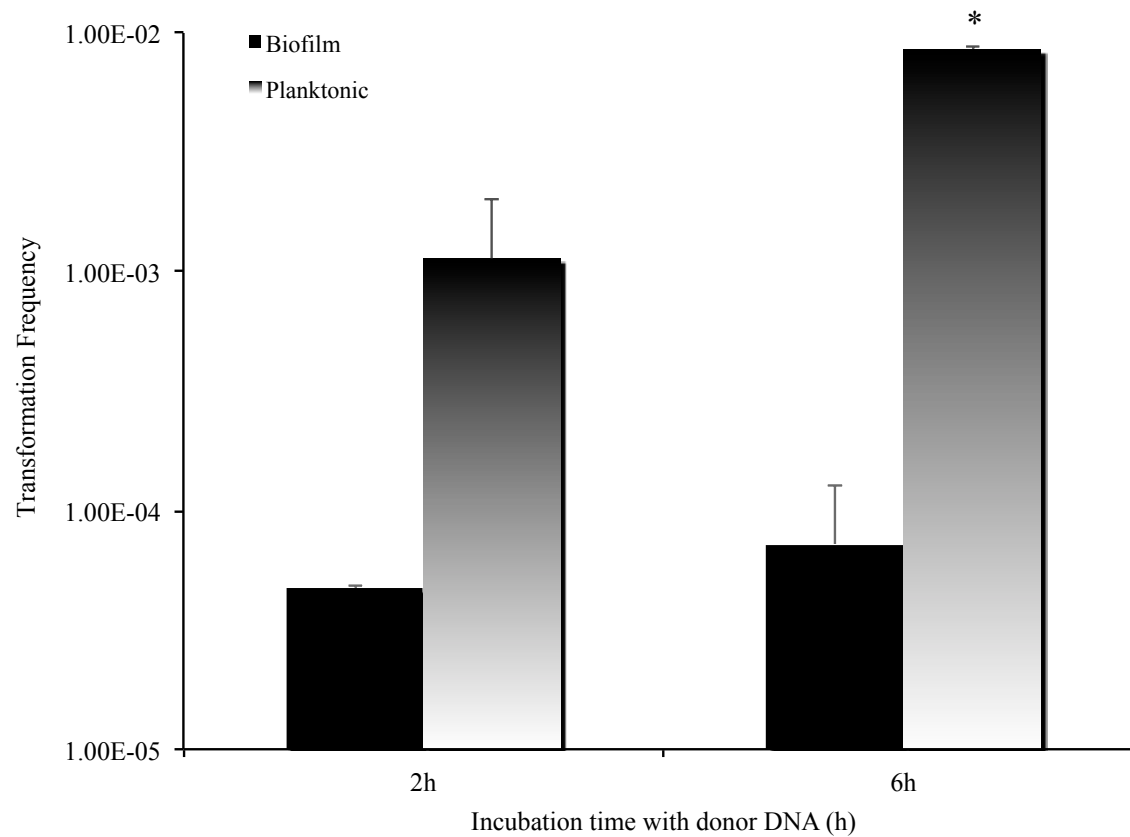
Figure 3.4: Transformation frequencies of BD413 biofilms grown in static systems and 8h BD413 planktonic batch culture cells incubated with pWH1266 donor DNA. Biofilm and planktonic cell numbers in the range of 10^8 cells were incubated with the donor DNA at a final concentration of 0.4 ug/ml and were incubated for 2 h and for 6 h. Negative controls indicated that there was no detectable spontaneous mutation rate of tetracycline resistance. Two biological replicates, each with three technical replicates, were completed for each sample. Symbol * indicates significant increase ($p<0.01$) of planktonic cell transformation frequency compared to that of microtiter biofilm cells incubated with donor DNA for the same incubation time.
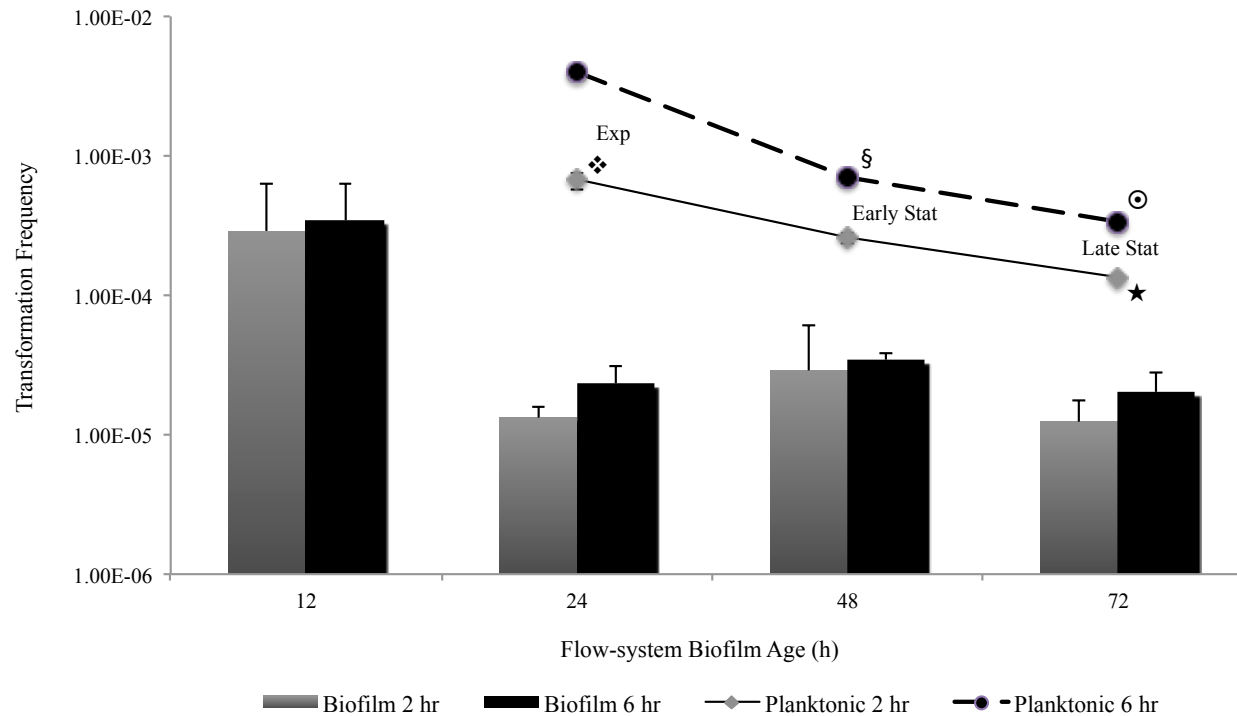
Figure 3.5: Transformation frequencies of BD413 biofilms grown in flow-systems and planktonic batch culture cells (recovered at the mid-exponential (8 h), early stationary (10 h) and late stationary (12 h) phases) incubated for 2 h and for 6 h with plasmid pWH1266 donor DNA. Biofilm and planktonic cells in the range of 10^8 cells were incubated with donor DNA at a final concentration of 0.4 μg/ml. Negative controls indicated that there was no baseline spontaneous mutation rate to tetracycline in either the biofilm biomass samples or the planktonic batch culture samples. Symbol ❖ indicates significant increase (p<0.05) in transformation frequency of exponential planktonic cells incubated with donor DNA for 2 h compared to that of 24 h biofilm incubated with donor DNA for the same incubation time. Symbol § indicates significant increase (p<0.01) in transformation frequency of early stationary planktonic cells incubated with donor DNA for 6 h compared to that of 48 h biofilm cells incubated with donor DNA for the same incubation time. Symbol ★ indicates significant increase (p<0.05) in transformation frequency of late stationary planktonic cells incubated with donor DNA for 2 h compared to that of 72 h biofilm cells incubated with donor DNA for the same incubation time. And, Symbol ⊙ indicates significant increase (p<0.01) in transformation frequency of early stationary planktonic cells incubated with donor DNA for 6 h compared to that of 72 h biofilm incubated with donor DNA for the same incubation time.
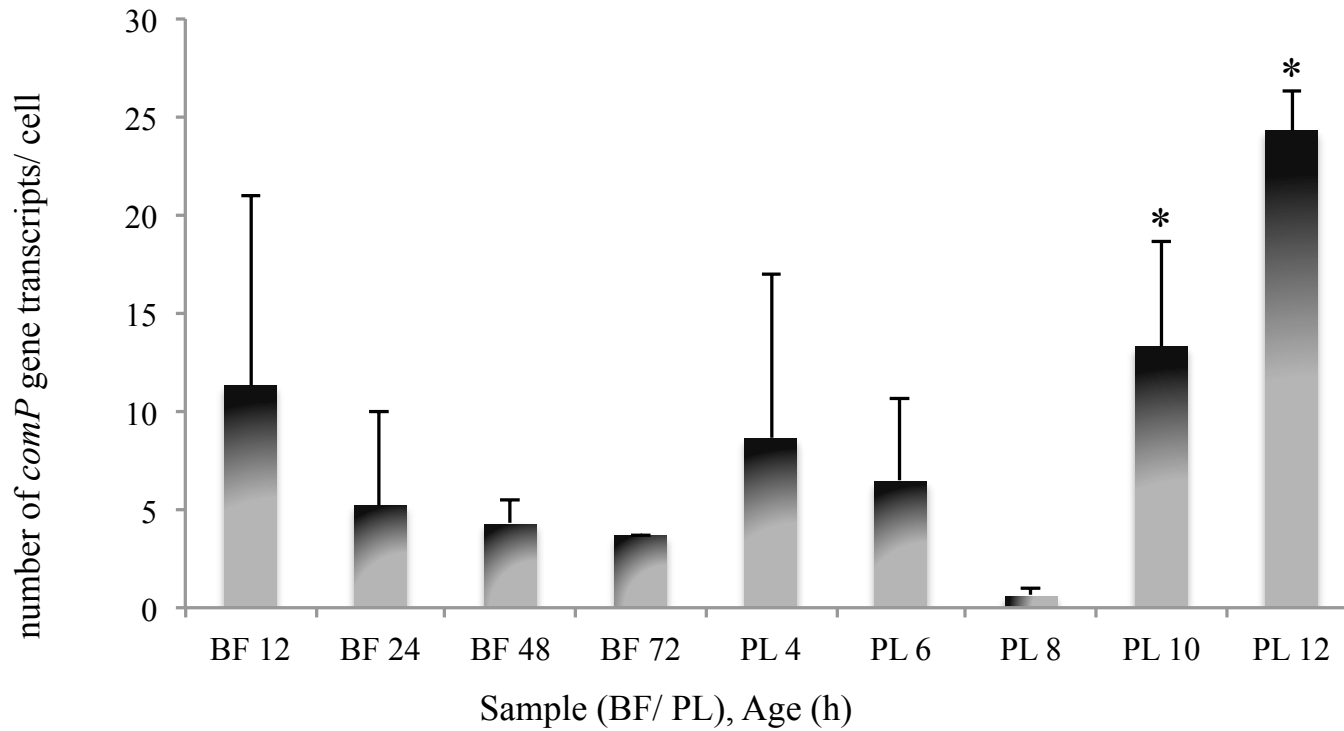
Figure 3.6: Real-time PCR results calculating absolute quantification of *comP* gene transcripts/ cell for BD413 biofilm(BF) and planktonic (PL) batch culture cells. Two biological replicates, with three technical replicates, were run for each biofilm and planktonic time point. No template negative controls indicated no contamination of cDNA. Symbol * indicates significant increase ($p < .05$) of gene transcripts/ cell in late phase planktonic cells (PL 10 & PL 12) compared to those in mature biofilms (BF 48 & BF 72).

3.6 References

1. Dunne, W.M., *Bacterial adhesion: seen any good biofilms lately?*, in *Clin. Microbiol. Rev.* 2002. p. 155-166.
2. Mah, T.F. and G.A. Toole, *Mechanisms of biofilm resistance to antimicrobial agents.*, in *Trends in Microbiology*. 2001. p. 34-39.
3. Boles, B.R., M. Thoendel, and P.K. Singh, *Rhamnolipids mediate detachment of Pseudomonas aeruginosa from biofilms.*, in *Molecular Microbiology*. 2005. p. 1210-1223.
4. Singh, R., D. Paul, and R.K. Jain, *Biofilms: implications in bioremediation.*, in *Trends in Microbiology*. 2006. p. 389-397.
5. Hall-Stoodley, L., J.W. Costerton, and P. Stoodley, *Bacterial biofilms: from the Natural environment to infectious diseases*, in *Nat Rev Micro*. 2004. p. 95-108.
6. Huq, A., et al., *Biofilms in water, its role and impact in human disease transmission.*, in *Current Opinion in Biotechnology*. 2008. p. 244-247.
7. Blenkinsopp, S.A. and J.W. Costerton, *Understanding bacterial biofilms.* Trends in Biotechnology, 1991. **9**(1): p. 138-143.
8. Wuertz, S., et al., *In situ quantification of gene transfer in biofilms.*, in *Meth. Enzymol.* 2001. p. 129-143.
9. Costerton, J.W., *Introduction to biofilm.*, in *International Journal of Antimicrobial Agents*. 1999. p. 217-21- discussion 237-9.
10. Costerton, J.W., et al., *Biofilms, the customized microniche.*, in *J. Bacteriol.* 1994. p. 2137-2142.
11. Molin, S. and T. Tolker-Nielsen, *Gene transfer occurs with enhanced efficiency in biofilms and induces enhanced stabilisation of the biofilm structure*, in *Current Opinion in Biotechnology*. 2003. p. 255-261.
12. Momba, M., et al., *An overview of biofilm formation in distribution systems and its impact on the deterioration of water quality*. 2000, Water Reseach Council.
13. Xi, C., et al., *Prevalence of antibiotic resistance in drinking water treatment and distribution systems.*, in *Applied and Environmental Microbiology*. 2009. p. 5714-5718.
14. Pruden, A., *Balancing Water Sustainability and Public Health Goals in the Face of Growing Concerns about Antibiotic Resistance.*, in *Environ. Sci. Technol.* 2013.
15. Zhang, X.-X., T. Zhang, and H.H. Fang, *Antibiotic resistance genes in water environment*, in *Appl Microbiol Biotechnol*. 2009, Springer. p. 397-414.
16. Costerton, J. and Z. Lewandowski, *Microbial biofilms*, in *Annual Reviews in ....* 1995.
17. Jefferson, K.K., *What drives bacteria to produce a biofilm?*, in *FEMS Microbiology Letters*. 2004. p. 163-173.
18. Lamont, R.J. and J.D. Bryers, *Biofilm-induced gene expression and gene transfer.*, in *Meth. Enzymol.* 2001. p. 84-94.
19. Senadheera, D. and D.G. Cvitkovitch, *Quorum sensing and biofilm formation by Streptococcus mutans.*, in *Adv. Exp. Med. Biol.* 2008. p. 178-188.

20. Wuertz, S., S. Okabe, and M. Hausner, *Microbial communities and their interactions in biofilm systems: an overview.*, in *Water Sci. Technol.* 2004. p. 327-336.

21. Fux, C.A., et al., *Survival strategies of infectious biofilms.*, in *Trends in Microbiology.* 2005. p. 34-40.

22. Parsek, M.R. and P.K. Singh, *Bacterial biofilms: an emerging link to disease pathogenesis.*, in *Annu. Rev. Microbiol.* 2003. p. 677-701.

23. Roberts, A.P., P. Mullany, and M. Wilson, *Gene transfer in bacterial biofilms.*, in *Meth. Enzymol.* 2001. p. 60-65.

24. Li, Y.H., et al., *Natural genetic transformation of Streptococcus mutans growing in biofilms.*, in *J. Bacteriol.* 2001. p. 897-908.

25. Porstendörfer, D., U. Drotschmann, and B. Averhoff, *A novel competence gene, comP, is essential for natural transformation of Acinetobacter sp. strain BD413.*, in *Applied and Environmental Microbiology.* 1997. p. 4150-4157.

26. Guardabassi, L., A. Dalsgaard, and J.E. Olsen, *Phenotypic characterization and antibiotic resistance of Acinetobacter spp. isolated from aquatic sources.*, in *J. Appl. Microbiol.* 1999. p. 659-667.

27. Juni, E., *Interspecies transformation of Acinetobacter: genetic evidence for a ubiquitous genus.*, in *J. Bacteriol.* 1972. p. 917-931.

28. Palmen, R. and K.J. Hellingwerf, *Acinetobacter calcoaceticus liberates chromosomal DNA during induction of competence by cell lysis.*, in *Curr. Microbiol.* 1995. p. 7-10.

29. Juni, E., *Genetics and physiology of Acinetobacter*, in *Annual Reviews in Microbiology.* 1978.

30. Vaneechoutte, M., et al., *Naturally transformable Acinetobacter sp. strain ADP1 belongs to the newly described species Acinetobacter baylyi.*, in *Applied and Environmental Microbiology.* 2006. p. 932-936.

31. Porstendörfer, D., et al., *ComP, a pilin-like protein essential for natural competence in Acinetobacter sp. Strain BD413: regulation, modification, and cellular localization.*, in *J. Bacteriol.* 2000. p. 3673-3680.

32. Busch, S., C. Rosenplänter, and B. Averhoff, *Identification and characterization of ComE and ComF, two novel pilin-like competence factors involved in natural transformation of Acinetobacter sp. strain BD413.*, in *Applied and Environmental Microbiology.* 1999. p. 4568-4574.

33. Hendrickx, L., M. Hausner, and S. Wuertz, *Natural genetic transformation in monoculture Acinetobacter sp. strain BD413 biofilms.*, in *Applied and Environmental Microbiology.* 2003. p. 1721-1727.

34. Palmen, R., P. Buijsman, and K.J. Hellingwerf, *Physiological regulation of competence induction for natural transformation in Acinetobacter calcoaceticus*, in *Archives of Microbiology.* 1994, Springer. p. 344-351.

35. Juni, E. and A. Janik, *Transformation of Acinetobacter calco-aceticus (Bacterium anitratum).* in *J. Bacteriol.* 1969. p. 281-288.

36. Lin-Chao, S. and H. Bremer, *Effect of the bacterial growth rate on replication control of plasmid pBR322 in Escherichia coli.*, in *Mol. Gen. Genet.* 1986. p. 143-149.

37. Boe-Hansen, R., et al., *Monitoring biofilm formation and activity in drinking water distribution networks under oligotrophic conditions.*, in *Water Sci. Technol.* 2003. p. 91-97.

38. Allen, H.K., et al., *Call of the wild: antibiotic resistance genes in natural environments*. 2010, Nature Publishing Group. p. 1-9.

39. Hendrickx, L. and S. Wuertz, *Investigating in situ natural genetic transformation of Acinetobacter sp. BD413 in biofilms with confocal laser scanning microscopy*, in *Genetic Engineering: Principles and Methods*. 2004, Springer. p. 159-173.

40. Herzberg, C., A. Friedrich, and B. Averhoff, *comB , a novel competence gene required for natural transformation of Acinetobacter sp. BD413: identification, characterization, and analysis of growth-phase-dependent regulation*, in *Archives of Microbiology*. 2000. p. 220-228.

41. Palmen, R., et al., *Physiological characterization of natural transformation in Acinetobacter calcoaceticus.*, in *J. Gen. Microbiol.* 1993. p. 295-305.

Chapter 4

Development and use of an agent-based model to assess the effect of resistance gene burden value on the persistence of resistant bacteria in a biofilm exposed to donor DNA and varying antimicrobial concentrations

4.1 Abstract

Microbial biofilms are aggregates of bacterial cells attached to a surface. They often form in dynamic flow environments, such as water distribution pipes. Biofilms encounter resistance determinants in these same compartments and obtain resistance properties through horizontal gene transfer mechanisms such as natural transformation. Various factors can affect the persistence of resistant bacteria in water system biofilms such as antibiotic selective pressure and the metabolic burden imposed by acquired resistance genes. This chapter details the development and use of an extended version of the iDynoMiCS model. In particular, this extended agent-based model is used to assess the effect of resistance gene burden value on the persistence of resistant bacteria in a biofilm exposed to donor DNA and varying antimicrobial concentrations. Several trends are apparent in simulations results. Bacteria harboring no cost and low cost fitness genes will persist in the absence of selective pressure and increasing antimicrobial concentration in

the influent promotes increased resistance expansion within the single-species biofilm. In addition, the use of this extended model to study additional research questions is discussed.

4.2 Introduction

Biofilms are the preferred growth mode for many bacterial species and are ubiquitous in both natural and clinical settings.[1, 2] Horizontal gene transfer (HGT) mechanisms allow bacteria to acquire new genetic features for persistence in a wide range of environments.[3] In particular, competent organisms can uptake and integrate extracellular DNA encoding resistance genes through the process of natural transformation.[4] Resistance genes may incur a fitness cost and can proliferate through both natural transformation and clonal expansion.[5, 6] Resistance expansion can also be affected by antibiotic pressure. It is widely accepted that the advent of antibiotics advanced therapeutic options as well as initiated new selective pressures on existing bacterial populations.[6-10] Prevailing opinion is that antibiotics in various settings cause resistance expansion and resistant bacteria may persist even if the selection pressure is removed.[9-14] In this study, we focus on the effect of resistance gene burden value on the persistence of resistant bacteria in a biofilm exposed to donor DNA and varying antimicrobial concentrations.

Resistance expansion in the environment most likely occurs due to antibiotic selective pressure, influx of resistant bacteria and HGT.[15] Antibiotics are mainly used for clinical and agricultural purposes, polluting those settings as well as land areas fertilized with antibiotic contaminated manure.[6] A significant portion of these compounds is only slightly

modified post treatment and is excreted into sewage as active metabolites and 30-90% of administered veterinary antibiotics are excreted into manure.[16-18] Additionally, pharmaceutical compounds are released into the environment post wastewater treatment and contaminate receiving rivers.[6, 8, 9] Antibiotic resistance determinants have been found in crude antibiotic preparations used on farms and in human-associated wastewater.[6, 19] The selection of and increase in resistant bacteria due to antibiotics is seen in both soil and aquatic environments. Application of contaminated manure may promote the spread of resistance genes in soil.[18, 20] And, studies indicate an increase in antibiotic resistance downstream from sewage treatment plants.[16, 21, 22] Antibiotic selective pressures also appear to play a role in resistance gene maintenance in other water systems.[16, 23, 24]

It is clear that antibiotic usage has promoted the spread of resistant bacteria. However, resistance expansion is a complex process influenced by many factors, such as the biological cost of fitness.[9] Bacterial antibiotic resistant phenotypes can be achieved by chromosomal DNA mutations, conjugation, mobile genetic elements or the focus of our study, transformation.[25, 26] While some resistance genes confer no cost or even improve an organism's fitness, most incur a cost that is usually observed as a reduced bacterial growth rate.[5, 26, 27] Studying the interaction between antibiotic use and burden value can provide information on resistance stability in the presence and absence of antibiotic.[28-30] Frequency and rate of increase of resistant bacteria within a bacterial population is assumed to be directly related to the antibiotic pressure and inversely related to the fitness cost of the resistant gene.[5, 28, 29, 31]

There are a modest number of experiments on burden cost. At present, *in vitro* fitness experiments have mainly been evaluated in pairwise competition of isogenic strains or wild-type and resistant strains.[28, 29, 32] Generally, experiments conducted in a drug free environment show that acquired resistance is associated with a negative fitness cost.[33-37] However, a majority of this research focuses on fitness cost of R plasmids, mobile genetic elements and chromosomal mutations. Bacterial transformation with extracellular DNA readily occurs in the environment and is the mechanism for emergence of penicillin resistance in *S. pneumonia* and *N. gonorrhoae*.[38, 39] Despite this, there appear to be no studies assessing the fitness cost of extracellular resistance determinants integrated into the host chromosome. This may be because the burden is negligible in these instances or because respective host strains are difficult to isolate. Finding appropriate samples for comparison and conducting *in vitro* studies can be a difficult and time consuming endeavor. In addition, burden values may be dependent on experimental conditions making it problematic to compare study results.[28] Thus, pairwise competition experiments set in chemostats or batch cultures and results may not be relevant to a biofilm environment.

While it is possible to assess the effect of burden cost on resistant bacterial spread in a biofilm developed in the laboratory setting and exposed to influent donor DNA and antimicrobial, such experiments would be labor intensive for several reasons. Donor DNA encoding antibiotic resistance and conferring varying burden cost would have to be identified and isolated, biofilm experiments would have a finite run time before contamination might set in and resistant cells would have to be identified through a non-invasive technique that wouldn't disrupt the biofilm structure. In addition, testing a range

of burden cost values and a range of influent antimicrobial concentrations ,with the appropriate number of technical replicates, would require completing multiple laboratory experiments. A theoretical, agent-based model offers an attractive alternative. Simulations can be run for as long as needed, a wide range of burden cost values can be explored and model images can provide an overview of resistant cell placement in the biofilm. In addition, trends from model simulation results can drive laboratory experiment settings such as the range of tested influent antimicrobial concentration.

The development of mathematical models has extended the study of HGT and biofilms beyond laboratory *in vitro* experimentation.[40] Study of HGT has primarily focused on conjugation dynamics in microbial communities. Some of the earliest conjugal plasmid transfer models applied a mass action approach to all system components, biological and chemical.[40-45] However, models have advanced over the years by uncoupling reactions that occur at the biologic level from the system level and by extending study to surface attached communities.[40, 46, 47] Models studying microbial communities have seen a parallel development from the earliest cellular automaton frameworks. The individual-based Dynamics of Microbial Communities Simulator (iDynoMiCS) is open source software that simulates the growth of individual microbes and subsequent biofilm development in a dynamic aquatic environment.[48] In an individual-based model (IbM), individuals or agents are modeled explicitly with population behavior emerging from low-level, agent interactions.[48] Thus, IbM's are an appropriate choice for modeling microbial biofilms. iDynoMiCS decouples bacterial reactions from solute level reactions, includes separate

reactions for bacterial growth and maintenance and produces both biofilm image and quantitative output.[48]

In this work, we study the effect of both selective pressure and resistance gene fitness cost on the spread and persistence of resistant bacteria within a single-species biofilm. We have developed an extension to the base iDynoMiCS model to explore this association. Our extended model includes transformation and antimicrobial inhibition mechanisms as they occur at the individual cell level embedded within an iBM framework for biofilm growth. The model organism is a heterotroph based on *Acinetobacter baylyi*. *A. baylyi* is a naturally competent widespread heterotroph capable of taking up environmental DNA.[11, 21, 49] Members of this genus are found in soil, sewage, freshwater, and in drinking water systems.[50-52] This strain exhibits high transformation frequencies in planktonic batch culture as well as in monoculture biofilms developed in once-through flow systems.[51, 53] The ubiquity of this genus and evidence of high gene transfer between strains makes these microorganisms suitable for monitoring antibiotic resistance in the environment.[21, 54, 55] To our knowledge, this is the only agent-based model that incorporates natural transformation along with biofilm development. Thus, this extended model is a tool for testing hypotheses that may be difficult to conduct *in vitro* and could also be used to drive future laboratory work.

4.3 Model Overview

The model description below follows the Overview, Design concepts and Details (ODD) protocol developed by Grimm et al. (2006) and is limited to processes associated with transformation and antimicrobial inhibition.[56] The current model is an extension of the individual-based Dynamics of Microbial Communities Simulator (iDynoMiCS) software that provides an ibM simulation of biofilm growth.[40, 48]

4.3.1 Purpose.

The purpose of the current model is to simulate DNA uptake, transformation and antimicrobial inhibition of bacterial growth in single-species biofilms to observe the effect of varying antimicrobial exposure and fitness burden values on the spread of an antibiotic resistance gene within the biofilm.

4.3.2 State variables and scales.

The basic agent in this model is a heterotrophic bacterium chiefly characterized by resistance type with properties that include a resistance switch threshold and amount of DNA taken up from the surrounding environment. Resistant and non-resistant DNA is present in this model in three forms: capsule DNA, particulate DNA and soluble DNA. Resistant and non-resistant capsule DNA are bacterial properties that track the respective DNA type taken up from the environment. Two additional agents, resistant and non-resistant particulate DNA, are the result of bacterial lysis. The distinguishing property between these two agents is that resistant particulate DNA encodes a metabolic burden and

additional metabolic reactions. Bacteria and particulate DNA agents all take up space in the model world. However there is no interaction between these two agents. Particulate DNA undergoes a solubilization reaction resulting in the solute: soluble DNA. Soluble DNA is the only form of DNA that can be taken up by bacteria agents. An antimicrobial solute is also present in the model, in addition to those already present in the iDynoMiCS base model.[48] The solute field and computation domain are treated as in Lardon et al. (2011).[48] The growth substrate or nutrient media in the base iDynoMiCS model is COD (chemical oxygen demand). It is essentially a carbon energy source for heterotrophic agents. In the present model, COD and nutrient media are interchangeable. Figure 4.1 is a model algorithm depicting program flow of bacteria agents and the role of capsule DNA, particulate DNA and soluble DNA in the transformation process; Figure 4.1b provides a succinct overview of the three DNA types in the model.

4.3.3 Process overview and scheduling.

The computational domain consists of three regions: a biofilm composed of bacteria agents, the general bulk compartment which encompasses the entire computational domain, and a boundary layer between the biofilm and the overlying bulk liquid. Solute concentrations in the bulk compartment stay fixed based on user set values. However, solute concentrations in the boundary layer and within the biofilm vary due to diffusion reactions and agent metabolic reactions, respectively. Solute concentrations in all three computational domain regions are updated at the start of each global time-step.[48] Several agent time steps are completed in one global time step. In the current model, the global

71

time step is .2 h and the agent time step is .01 h. Thus, 20 agent time steps are completed within 1 global time step. This falls in line with reasoning that agent level reactions occur faster than reactions at the global level such as the diffusion of solutes. In fact, it is assumed that global level values are constant during the smaller agent intervals.[57] It is also important to note that model output files are produced every hour of the simulation. 1 output file is equivalent to 5 global time steps and to 100 agent time steps.

At the start of the agent time step, all growth and maintenance reactions are computed and the bacteria agent size (cell radius and biomass) is updated. If the bacterial cell has approached the division radius value, it will divide to form two new clones. A fraction of bacteria agents that reach the death threshold will lyse and release particulate DNA, the remaining will stay dormant until they have access to substrate. Similarly, a portion of bacteria that have taken up enough resistant soluble DNA to hit the resistant switch threshold will become resistant agents; the rest will remain non-resistant for the duration of the simulation. Pressure-driven movements are then applied to all agents along with local shoving to minimize agent overlap, and the resultant agent locations are updated. Once the agent time-steps are completed, the end of the global time-step is marked by removal of agents detached from the biofilm due to erosion effects applied to the entire biofilm structure.[40, 48] The agent time-step for the current model is laid out in Figure 4.1. Agent processes that are a modification of or are in addition to the base iDynoMiCS model described by Lardon et al. (2011) are described below.[48]

72

4.3.3.1 *Biofilm structure development.* The model organism for this HGT model is *Acinetobacter baylyi*, a Gram-negative aerobic heterotrophic bacterial species.[49, 53] The overall shape of *Acinetobacter* spp. biofilms is not detailed in the literature. However an organism from the same order, *Pseudomonas aeruginosa*, appears to form mushroom-shaped biofilm structures.[58, 59] Several agent and environmental model parameters govern bacterial growth and therefore, influence biofilm shape. Included among these are maximal bacteria growth rate (μ^G_{max}) and maintenance rate (μ^{NR}). All bacteria agents undergo growth and maintenance reactions. These two metabolism reactions respectively convert substrate into additional cellular biomass or deplete biomass. Cellular biomass, in turn, affects the cell radius value.

The effects of modifying various parameter values on biofilm structure are illustrated in *Supplemental* Figures 1a-f. Values resulting in mushroom-shaped biofilm structures were set as the default as seen in Tables 4.1 & 4.2. In addition, the bacterial growth rate (μ^G_{max}) and maintenance rate (μ^{NR}) default values are similar to corresponding heterotrophic growth values in previous studies.[48, 60, 61] Long-term biofilm growth in *Supplemental* Figure 2 shows the development of mushroom structures into finger-like structures that eventually detach. This fingering instability phenomenon has been shown in previous biofilm models.[62]

4.3.3.2 *Bacterial lysis.* All bacteria agents have a cell radius property. This value changes according to cell metabolism and bacteria divide or die when an agent reaches threshold

cell radius values. Following Lardon et al. (2011) dead agents are subsequently removed from the simulation.[48] However in the current model, cells that approach the death radius can either lyse or become dormant. Biofilms, even single-species biofilms, are a heterogeneous population.[63, 64] Cells can vary in their response to local nutrient and chemical concentrations resulting in inactive or dead cells.[63, 65] Following cell death, a subpopulation of biofilm cells can lyse and release genomic DNA.[64, 66] In this model, cells near the death radius threshold have a probability of lysis [P(lysis)]. Thus, a subset of these cells lyse and release genomic DNA (represented by the particulate DNA agent). The remainder may lyse in subsequent time steps if they continue to hover near the death radius. These cells are most likely located in nutrient poor regions of the biofilm and will continue to decrease in size due to starvation and a maintenance cost.[63, 65] Therefore, these dormant cells are not completely void of all metabolic reactions but it is highly unlikely they will uptake substrate or divide. The default value for P(lysis) was chosen to reflect non-extreme behavior (*Supplemental* Figures 3a-b).

4.3.3.3 *Transformation.* Natural transformation in bacterial species is the active uptake and integration of donor DNA.[67] *Acinetobacter baylyi* has a particularly efficient transformation system and can uptake and process homologous as well as foreign DN*A*.[68-71] In addition, *A. baylyi* is common in water and soil environments making it an appropriate choice for modeling transformation in a flow system.[26, 39] To our knowledge, the current model is the only agent-based model with transformation functions.

Additionally, this HGT model is limited to transformation with chromosomal DNA and therefore does not include plasmid spread dynamics.

Three forms of DNA are present in the model: capsule, particulate and soluble DNA. Capsule DNA is a bacterial property that tracks the amount and type of DNA taken up. Upon lysis, resistant bacterial cells release a portion of their host genomic DNA along with any contents of the resistant capsule. The amount of DNA present in the non-resistant capsule is considered to be negligible and therefore, unaccounted for post-lysis. Non-resistant bacterial cells undergo a complimentary sequence of events. Resultant extracellular DNA is now a particulate DNA agent labeled as resistant or non-resistant depending on the gene profile of the original lysed bacterial cell. Particulate DNA and bacteria both occupy space in the model world but there is no interaction between the two. In fact, bacteria cannot uptake particulate DNA. Particulate DNA dissolves into the surrounding liquid environment forming soluble DNA, a solute that is the only form of genetic material accessible to bacteria. Figure 4.1b provides an overview of the three DNA types found in the model.

DNA released from lysed cells and soluble DNA solution fed into the bulk influent are the only sources of genetic material for transformation in the model biofilm. Since lysed DNA dissolves to form soluble DNA these two donor sources are essentially the same. However, the surrounding bulk liquid immediately dilutes local concentrations of solute formed from cell lysate whereas the user can preset the concentration of resistant and/or non-resistant

soluble DNA solution fed into the bulk influent. This is similar to transforming recipient

cells with whole cell lysate with an unknown concentration of the resistant marker versus

transforming cells with a purified resistant DNA solution.

Regardless, both crude cell lysate and purified DNA efficiently transform *Acinetobacter*

spp. in laboratory and environmental settings.[39, 68, 72, 73] In particular, Hendrickx et al. (2003)

demonstrated detectable transformation frequencies in *Acinetobacter baylyi* biofilms

developed in a laboratory flow cell.[51] Similar to our model world set-up, the single species

biofilm was surrounded by bulk fluid and exposed to an influent flow of purified plasmid

DNA with a resistance marker.[51] Transformation of *Acinetobacter* spp. in the environment

may be due to environmental donor DNA that retains its bacterial transforming abilities for

extended time periods when adhered to sediment particles.[74] While there is no

representation of such particles in the current model, it is assumed that the transforming

ability of resistant DNA does not vary with time.

Even in a highly transformable organism such as *Acinetobacter baylyi*, transformation is a

regulated process with multiple steps and is treated as such in the model. However, in the

absence of adequate quantitative transformation parameters, processes are coupled with

well-established model kinetics. Thus, bacteria agents uptake soluble DNA through the

same mechanisms for bacterial growth previously described by Lardon et al. (2011).[48]

The kinetic reaction, describing uptake of COD and subsequent increase in bacterial

biomass, is also used to characterize uptake of soluble DNA and increase in the DNA

capsule contents (Table 4.3). Thus, the maximum rate of soluble DNA uptake (μ^D_{max}) and

the soluble DNA saturation constant (κ_{DNA}) are equivalent to their growth reaction counterparts (μ^{G}_{max} & κ_{COD}) (Table 4.1). There is a minor drawback to using a Monod equation to describe soluble DNA uptake kinetics as is illustrated in *Supplemental* Figures 4a-c. Rate of soluble DNA uptake will maximize as the biofilm is saturated with donor DNA. This then decreases the amount of DNA available to cells located in the lower biofilm strata and leads to a decrease in overall transformation frequency. There will therefore be a slight dip in the transformation frequency curve before the uptake rate is stabilized.

As discussed before, internalized resistant extracellular DNA is tracked in the resistant capsule. When this capsule value approaches a user preset resistant switch threshold (Th$_{res}$) the respective bacteria agent has a probability [P(resistant)] of expressing the resistance gene. Transformation frequencies of *Acinetobacter baylyi* batch cultures and monoculture biofilms vary with the concentration of donor DNA.[51, 53, 75] Frequency curves often plateau when recipient cells are saturated with DNA; therefore we assume that there must also be a donor DNA concentration below which transformants are undetectable represented by the Th$_{res}$. *Supplemental* Figure 5 shows the influence of the Th$_{res}$ parameter value on the transformation frequency curve in a single-species biofilm. We assumed a default value for Th$_{res}$ based on *in vitro* transformation frequency experiments (unpublished results). This setting also proved to be the most sensitive parameter value for transformation frequencies in young biofilms.

Transformation with chromosomal DNA is dependent not only on uptake but also on functional integration of donor DNA into the host chromosome.[76] Thus, a sub-population of cells that approach the Th_{res} has a probability of transformation [P(resistant)]. Transformed cells express the resistance gene and the remainder will remain non-resistant for the duration of the simulation. Successful recombination events vary as a function of the organism and only .1% of internalized DNA fragments are successfully recombined into the *Acinetobacter baylyi* host chromosome.[6] *Supplemental* Figures 4a-c illustrate the effect of changing this parameter value on the overall transformation frequency curve and the range of the data values. The default P(resistant) value was set to .02. This was the lowest effective value the parameter could be set to. In addition, considering the low percent of recombined internalized fragments and the fact that transformation is a multifactorial process – this seems to be a reasonable assumption.

There is usually a fitness cost associated with acquired antibiotic resistance.[5] Expression of foreign genes can place a significant metabolic burden on the recombinant host cell resulting in, but not limited to, a decreased growth rate.[5, 11, 77] This has been shown for antibiotic resistant *Acinetobacter spp.* and an organism from the same order: *Pseudomonas aeruginosa.*[11, 78] Seoane and colleagues found that the growth rate of *P. putida* cells carrying a plasmid is decreased on the order of 10% compared to growth of plasmid free cells.[79] Merkey et al. (2011) used iDynoMiCS to study plasmid invasion in biofilms and set the maintenance rate of resistant bacteria to 5% based on these findings. In the current model, resistant bacteria agents experience an additional metabolic drain above the

baseline maintenance cost of their nonresistant counterparts. The rate of this reaction (μ^R) is equal to 0-20% of the growth rate (μ^G_{max}). We assume that the metabolic burden associated with plasmid carriage is much higher than with chromosomally integrated DNA however a wide metabolic burden value range ensures a more comprehensive analysis. There are instances when antibiotic resistance improves fitness or has no effect at all.[10, 80] The former case will not be addressed in this model and the latter can be addressed by setting μ^R to 0%.

4.3.3.4 *Antimicrobial Inhibition.* Numerous antibiotics are available to control or eradicate bacterial infections and they are usually classified according to the mode of antagonistic action.[81] While the antimicrobial target(s) and mechanism(s) are often well understood, the bacterial response may not be since it usually involves various genetic and biochemical pathways.[81] Antibiotic interaction at the biofilm level is also fraught with uncertainties. Reduced susceptibility of biofilms to antibiotics has been well documented however there are several working hypotheses as to the cause.[82] The antimicrobial may fail to fully penetrate the biofilm because of structural barriers and/or consumption or neutralization reactions with the biomass.[83-85] Retarded diffusion may also lead to biofilm regions with low substrate concentration levels and metabolically inactive, less susceptible cells.[86] Alternatively, cells may turn on a protective stress response upon exposure to high antimicrobial concentrations or a subpopulation of persistor cells may develop.[82] While these are all plausible theories, the reality is that biofilm resistance seems to be a

combination of several factors.[86-90] In fact, one species may have different resistance

responses depending on the antimicrobial agent and/or biofilm properties.[82, 91]

Incorporating new code into the base model to account for a hypothesized or known

mechanism would introduce unnecessary complexity. Present model goals only require a

general inhibitory pressure. In addition, antimicrobial interaction with bacterial cells on the

individual and biofilm levels appears to be a complex process with many unknowns. Thus,

similar to transformation processes, inhibition follows model kinetics from the validated

base iDynoMiCS model (Table 4.3).[48] Antimicrobial is treated as a model solute with the

maximal antimicrobial inhibition rate (μ^I_{max}) and the antimicrobial saturation constant (κ_{Ab})

equivalent to their growth reaction counterparts (μ^G_{max} & κ_{COD}) (Table 4.1). However,

COD uptake increases bacterial biomass whereas antimicrobial uptake decreases biomass

(Table 4.3). Antibiotics are often classified according to whether they inhibit cell growth

(bacteriostatic) or induce cell lysis (bacteriolytic).[81] Bacteria agents increase y biomass

units per x COD units taken up, decrease y biomass units per x bacteriostatic antimicrobial

units taken up and decrease $>y$ biomass units per x bacteriolytic antimicrobial units taken

up. Therefore, static drugs directly offset bacterial growth and lytic drugs decrease biomass

at a greater magnitude than the increase in biomass concurrent with COD uptake.

Although no particular inhibition mechanism is explicitly represented in the present model,

antimicrobial effects and diffusion at the biofilm level are consistent with previous work.

Dose response curves in *Supplemental* Figures 6a & 6c are similar to results of a study

examining the dose response of *Pseudomonas aeruginosa*.[92] Chambless et al (2006) studied biofilm antimicrobial resistance using the computer model, BacLAB.[83] Antimicrobial concentration profiles were constructed for two hypothetical resistance mechanisms: limited antimicrobial penetration of the biofilm structure and stress response resulting in resistance. While the number of live versus dead cells and location of cells varied, the substratum antimicrobial concentration was approximately 10% of the overlying bulk fluid concentration in both.[83] The same pattern was seen in antimicrobial plot contours produced from test simulations (data not shown).

4.3.4 Design concepts.

4.3.4.1 *Emergence*. Transformation frequencies over time and discernible patterns of transformants at the biofilm level are a result of individual bacterium behavior.

4.3.4.2 *Fitness.* Resistance gene expression imposes a metabolic burden on the host bacterium.

4.3.4.3 *Adaptation.* Bacteria expressing the resistance gene can withstand antimicrobial growth inhibition effects.

4.3.4.4 *Prediction.* This model is a predictive tool to assess trends of transformation frequencies and patterns of transformants in biofilms in varying environments. However, raw model data may not be equivalent to laboratory results.

4.3.4.5 *Sensing*. Bacteria cannot estimate the concentration of nutrients or DNA in their surrounding environment and cannot differentiate between resistant and non-resistant soluble DNA.

4.3.4.6 *Stochasticity*. None in addition to that described in Lardon et al. (2011).[48]

4.3.4.7 *Collectives*. The biofilm is tracked as a collective entity to update the delineation between the biofilm and surrounding liquid in the computational domain as described by Lardon et al. (2011) and by Merkey et al. (2011).[40, 48]

4.3.4.8 *Observation*. Information about the bacteria and particulate agents is updated and saved at pre-set time intervals. The same occurs for bulk compartment concentrations.

4.3.5 Details.

4.3.5.1 *Initialization*. The number, type and placement of bacteria agents as well as initial concentrations of all solutes in the bulk compartment are specified in the XML protocol document. S_{bulk} and S_{in} parameters exist for all model solutes in the XML document and set the initial bulk fluid concentration and the influent concentration, respectively. Simulations testing hypotheses regarding resistance gene spread in a biofilm exposed to varying environmental antimicrobial concentrations and a range of resistance gene burden values read in a grown biofilm. To develop this initial structure at least 10 non-resistant bacterial agents are randomly placed in a defined region of the computational domain. Soluble DNA solute is added to simulations as the source of resistant DNA and antimicrobial may be applied to test for its effects.

4.3.5.2 *Input*. Many of the input parameters are the default values described by Lardon et al. (2011). The exceptions are listed in Table 4.1. Default environmental parameters are listed in Table 4.2 and model processes/ reactions are shown in more detail in Table 4.3.

4.3.5.3 *Simulations.* All experiments are simulated for 792 hours, which includes 72 hours of initial attachment and uninhibited biofilm growth followed by 720 hours of constant antimicrobial exposure. Initial unchallenged 72-hour biofilms are composed entirely of nonresistant bacteria. These 72-hour biofilms are exposed to continuous soluble resistant DNA ($10e^{-3}$ g.L^{-1}) and antimicrobial (0 g.L^{-1} – $10e^{-3}$ g.L^{-1}) in the influent. The effects of a range of metabolic burden values (0-.140 h^{-1}) are examined within these continuous antimicrobial treatment simulations. Table 4.4 provides an overview of all the model simulations.

4.3.5.4 *Submodels.* Only transformation and antimicrobial inhibition related extensions of the iDynoMiCS model are discussed here; refer to Lardon et al (2011) for a complete description of the iDynoMiCS model.[48]

4.3.6 Data analysis.

iDynoMiCS saves a set of output files describing the agents and solutes written at user set time points, mainly agent_State files, POV-Ray files and env_State files.[48] The agent_State file lists the properties of each agent in the simulation, including the resistance profile. A MATLAB routine is used to analyze these state files and provide numbers of resistant and nonresistant bacteria at intervals over the course of the simulation. These data are used to construct total resistant cell/ total cell curves and the biomass curves presented in the results section. Each set of simulation conditions is repeated five times; each run with a unique seed number. Biofilm images are visualized from both the POV-Ray and

agent_State results files. POV-Ray files are rendered into images using Mega-POV software and provide a detailed pictorial of the overall biofilm structure, sizes of component bacterial cells and the location of any resistant cells. However, POV-Ray images do not provide a measure of biofilm height. MATLAB plots of agent_State files render biofilm images with height along the y-axis. Unlike the POV-ray files, agent sizes are not representative of actual size and bacterial agents are not color-coded based on resistance profile. By overlapping both POV-Ray images and MATLAB plots, we can visually divide POV-Ray rendered images into three biofilm strata (≤ 40 μm, 40 μm $< x \leq 80$ μm, and > 80 μm). MATLAB analysis of agent_State files provides number of resistant and nonresistant bacteria by stratum. As stated previously, all simulations conditions are repeated five times. However, biofilm images in the results section are not an average of the repeat simulations but are representative images from one of the five repeat simulations.

4.3.7 Assumptions.

There were several assumptions made during model development either for simplicity or to minimize computational burden. Competence in *Acinetobacter baylyi* varies with cellular growth phase.[93] However, in the current model, DNA uptake and integration are only dependent on the immediate environmental concentration of soluble DNA and the P(resistant) value. We assume that all cells are competent for the duration of the simulation. In addition, the particulate DNA solubilization rate was set to a low rate and no

lag period exists for resistant gene expression. Finally, there are no compensatory mechanisms. Once cells become resistant, they cannot revert back to a susceptible state.

4.4 Results

This study explores the association between resistance burden value and persistence of resistant bacteria in biofilms. We ran simulations exposing nonresistant biofilms to a constant exposure of both resistant soluble DNA ($10e^{-3}$ $g.L^{-1}$) and varying antibiotic concentrations ($0-5e^{-3}$ $g.L^{-1}$). Within each set of simulations, we looked at the effect of increasing the resistance gene burden value. The tested antimicrobial range and influent resistant soluble DNA concentration was set based on previous tests. *Supplemental* Figure 6c indicates that the inhibition effects are first apparent at antibiotic influx concentrations greater than $10e^{-4}$ $g.L^{-1}$ and that there are virtually no live cells at antimicrobial concentrations greater than and including $10e^{-2}$ $g.L^{-1}$. Burden value effects may be overshadowed by antimicrobial inhibition reactions at these high antibiotic influx concentrations making it difficult to tease out trends. So, the highest antibiotic concentration tested was $5e^{-3}$ $g.L^{-1}$. Simulations were also run with no antibiotic exposure to observe the base ratio of resistant bacterial cells/ total bacterial cells over time in a simulated environment with no antimicrobial pollution. A constant application of resistant soluble DNA is applied in all simulations as well. *Supplemental* Figure 4c indicates that an influent donor DNA concentration of $10e^{-3}$ $g.L^{-1}$ produced a mid-range transformation frequency. In essence, we could be reasonably sure this non-saturating value would not result in any extreme behavior.

Several data trends are consistent with prevailing assumptions regarding antibiotic exposure and resistance expansion. [9-14] As seen in Figure 4.2a, resistant bacteria with no cost or low cost fitness genes persist in the absence of antibiotic. However, resistant bacteria with a metabolic burden higher than .007 h^{-1} are outcompeted by their susceptible counterparts. While there is progressively no overlap between the 0 h^{-1} and .007 h^{-1} curves in the absence of antibiotic, the gap between these two curves lessens as the antibiotic influx concentration increases. Results in Figures 4.3a, 4.4a, 4.5a & 4.6a imply that frequency and rate of increase of resistant bacteria appears to be directly related to increase in antibiotic pressure. Cells harboring resistance genes with burden values .021 h^{-1} and .035 h^{-1} appear to persist long-term once the biofilm is exposed to $2.5e^{-3}$ $g.L^{-1}$ influent antimicrobial. And, bacterial cells with resistance genes that have a burden cost of .070 h^{-1} appear to persist longer under exposure to antimicrobial concentrations greater than $2.5e^{-3}$ $g.L^{-1}$. However, there are no conditions in the tested antibiotic exposure range that promote the expansion of resistant bacteria with a .140 h^{-1} metabolic burden value.

Results also indicate that for some tested conditions, data patterns only emerge once simulations are run for the appropriate amount of time. For instance, there is no visible trend among the resistant cell/ total cell ratio curves for the different metabolic burden values in younger biofilms at antibiotic influx concentrations of 1.25 e^{-3} g/L and lower. This does not apply to biofilms exposed to higher antibiotic concentrations where the resistant cell/ total cell curves diverge earlier.

The data in Figures 4.3a, 4.4a, 4.5a & 4.6a are presented in a different format in Figures 4.7a-o and in Figures 4.8a-o. Figures 4.7a-o depict the absolute numbers of resistant cells, nonresistant cells and total cells over time while Figures 4.8a-o plot the numbers of resistant cells by location within the biofilm. Results in Figures 4.7a, d, g, j & m show a rise in the number of resistant cells over time as the influent antibiotic concentration increases. At an antimicrobial concentration of $2.5e^{-3}$ g.L^{-1} and above, there is an increase in resistant cells regardless of the metabolic burden value. However, at lower concentrations, we only see an increase in resistance cells with a fitness cost of 0 h^{-1} and .007 h^{-1}. Nonresistant cells over time plots appear to be roughly similar across antimicrobial exposures groups for concentrations $1.25 \ e^{-3}$ g.L^{-1} and lower. And, the various metabolic burden curves appear to almost overlap within each of these same antimicrobial exposure groups. However, the metabolic burden curves begin to separate out within the $2.5e^{-3}$ g.L^{-1} and the $5.0 \ e^{-3}$ g.L^{-1} antibiotic exposure groups. It would appear that the resistant cell population is high enough to siphon off growth resources, thus stunting overall proliferation of the nonresistant cell population. In general, there is a drop in the number of nonresistant cells between 240-288 h after which the curve appears to flatten out. The exception to this trend are the simulation results of exposing a nonresistant biofilm to resistant DNA and $5e^{-3}$ g.L^{-1} antibiotic. In this case, the drop in nonresistant cells occurs at an earlier time point between 144-240 h except for the .140 h^{-1} metabolic burden curve. This curve drops at $\sim$ 264 h and stabilizes at a higher number of nonresistant cells compared to biofilms housing resistant cells with lower fitness costs. Figure 4.6a implies that resistant cells with a .140 h^{-1} fitness cost are outcompeted by susceptible cells early on

(~ 312 h). This would allow the remaining nonresistant population to grow unabated.
Figures 4.7 c, f, i, l & o chart total cells over time and these results closely mirror
nonresistant cell curves in Figures 4.7b, e, h, k & n. Figures 4.8a-o plot the resistant cells
by location in the biofilm. The metabolic burden curves appear to cluster together within
each of the antibiotic exposure groups. But, there is a pattern in the location of resistant
cells over time. The number of resistant cells located above 80 μm peaks before 240 h but
this increase fails to persist over time. In contrast, resistant cells located between 40-80 μm
and below 40 μm are more predominant in older biofilms. This is not due to an increased
penetration of the structure by resistant cells over time. Figures 4.2b-c, 4.3b-c, 4.4b-c,
4.5b-c & 4.6b-c indicate that a majority of the biofilm structure falls below 80 μm after
240 h, so the location of any resistant cells is limited by biofilm height.

As described previously in the Model Overview section, MegaPOV is auxiliary software
that can further analyze iDynoMiCS output files. In particular, biofilm images can be
rendered using MegaPOV and resistance cell type is indicated by color. It was not possible
to create a composite figure by overlapping images from repeat simulations, instead
Figures 4.2b-c, 4.3b-c, 4.4b-c, 4.5b-c & 4.6b-c are compilations of biofilm structures that
are most representative of the average resistant cell total data displayed alongside each
biofilm image. Each set of simulation conditions was repeated 5 times, each time with a
different seed value. There are instances when one simulation run may bias the results
average. This is the case with the 0 h^{-1} maintenance value results in Figures 4.5b-c and
with the .007 h^{-1} maintenance value results in Figures 4.6b-c. In both these instances,

average total resistant cell values are influenced by outlier simulation results. Despite this, some general inferences may be drawn from biofilm structure development under the varying simulation conditions. As noted previously, there is a drop in nonresistant cells between the 120 -240 h time points. This decrease in cell count may be a combined result of antimicrobial inhibition, detachment of cells and erosion effects. These biofilm images imply that resistance expansion within the biofilm structure increases as antimicrobial influx concentration rises and thus, the number of resistant cells that detach also increases. Higher antimicrobial concentrations seem to promote dispersal of resistant cells from the biofilm into the surrounding environment. It is also important to specify that image resolution limits the display of cells with an extremely small cell radius value. This would account for images that seem to not be tethered to the inert substratum when in fact, there is a layer of dormant and starved cells in the substrate poor region.

4.5 Discussion

Acquired resistance in bacteria is usually associated with a metabolic burden. The fitness cost amount can impact the rate of resistance development, stability of resistance and the rate at which frequency of resistance might decrease in the absence of antibiotic pressure.[5, 37] In particular, frequency and rate of increase of resistant bacteria within a bacterial population is assumed to be directly related to the antibiotic pressure and inversely related to the fitness cost of the resistant gene.[5, 28, 29, 31] It is generally assumed that a decrease in selective pressure will benefit the susceptible bacteria and allow them to displace resistant strains.[27] The exception to this generalization is bacteria harboring low cost or no cost

resistance mechanisms. These bacteria will persist even in the absence of antibiotic.[10, 14] The model results presented in this paper support these general assertions. Additionally, extended iDynoMiCS model simulation results suggest that magnitude of antibiotic selection pressure may allow for the persistence of more virulent resistance genes and generally affect the type and frequency of resistance genes circulating in the resistome. Study results imply that trends seen in clinical and *in silico* studies can also be seen at the microbial biofilm level. Although model set-up and parameter values do not exactly replicate conditions in the natural environment, this extended model can still be exploited to study additional hypotheses outside of the laboratory setting.

Our model investigates a wide range of metabolic burden values (0-.140 h^{-1}) and the magnitude may correlate with the method of acquired resistance.[37] Merkey et al. (2011) set the plasmid metabolic burden rate at 5% of the maximal bacterial growth rate, which translates to .035 h^{-1} in our model.[40] We assume that plasmid carriage imposes a higher fitness cost compared to genes integrated into the bacterial chromosome. Thus maintenance rates in the lower end of the tested range of values, such as .007 and 0 h^{-1}, may be representative of resistance acquired through transformation with extracellular DNA. Bacteria with these resistance genes persist in the absence of antimicrobial pressure. In contrast, bacteria harboring resistance genes with a fitness cost higher than .007 h^{-1} have a truncated life span in a drug-free environment. Acquired resistance can increase bacterial virulence in some instances.[94] Assuming that genes that increase bacterial virulence also have a high fitness cost, model results indicate that these genes can persist under certain

conditions. In particular, the frequency of high cost resistance genes increases as antibiotic selection pressure increases. As stated previously, we assume that low cost and no cost resistance genes are most likely the result of the main resistance mechanism under study, transformation. However, this does not necessarily rule out the possibility that there are high cost resistance genes integrated into bacterial chromosomes. The ephemeral nature of high cost resistance genes may decrease the likelihood that such resistance determinants are detected in the environment and/or studied in a laboratory setting. The extended iDynoMiCS model allows us to demonstrate trends in the absence of appropriate bacterial strains for *in vitro* experiments.

Model simulation results suggest that influent antibiotic concentration may affect the type and frequency of resistance genes circulating in the resistome, a reservoir of antibiotic resistant determinants. It can also affect HGT of these genes into pathogenic bacteria.[10, 19, 95, 96] Environmental microbes house a wide array of resistance genes, and some of these same genes can be found in pathogenic organisms. There is evidence that the antibiotic resistant mechanisms in nosocomial pathogens have their origins in the environmental resistome.[27, 97, 98] Furthermore, commensal bacteria can serve as a vector for transmission of resistance genes between the environment and clinical settings.[7] The potential effect of antibiotics on the make-up of the resistome and downstream mobilization of these genes into clinically significant bacteria signals that antibiotic research should expand focus to nonpathogenic organisms, such as our model organism – *A. baylyi*. Additionally methods

to remove excreted antibiotic metabolic compounds should be improved so as to reduce the total antibiotic circulating in the environment.

Trends in the extended iDynoMiCS model results are consistent with results from previous clinical and *in silico* studies, in addition to the *in vitro* studies previously discussed in the introduction section. Unsurprisingly, some of the earliest observations of antibiotic resistance occurred in clinical settings.[99, 100] Nosocomial infections are a significant burden to the healthcare delivery process and resistant infections are an increasing threat.[101] As a result, there are a number of studies establishing a clear relationship between increased antimicrobial use and emergence of resistant strains.[102-106] While there are examples of successful interventions – a correlation between reduced prescribing and reduced resistance does not always hold.[102] Theoretical models developed at both the human host and bacterial agent levels also indicate long-term negative effects of prolific antibiotic use. To study the impact of human antibiotic consumption on resistance frequency, Levin (2002) developed an SIR model. This open population model showed a rapid rise in resistance frequency following a small increase in antimicrobial consumption. However, effects of reduced antibiotic use were much slower indicating the persistence of resistance long after drug cessation.[107] A population genetics model using parameters derived from epidemiologic surveillance data of resistant isolates and community drug consumption produced similar results. In this case, constant antimicrobial exposure resulted in a sigmoidal rise in resistance. Successful interventions reduced the total numbers of resistant pathogens but did not fully reverse antibiotic effects.[12, 108] Although the results are not as

92

conclusive, the same trends are seen in a model with bacterial level state variables.[109] This mechanistic model attempted to explain the high densities of resistant bacteria in aquatic settings impacted from anthropogenic tetracycline use. Authors ruled out the possibility that environmental resistant populations are due to a high influx of resistant bacteria from wastewater that then do not grow in the receiving water body. Instead, model results indicated that it is more likely that there is a negligible input of resistant bacteria that then grow under selective pressure or exogenous bacteria transfer resistance to the local population allowing them to survive antibiotic exposure.[109]

Although stated previously, it is important to reiterate that this model can provide information on trends and cannot supplant quantitative data. Model development is an ongoing process and parameters may be modified as new *in vitro* data emerges. At present, there are several limitations with the current model extension. To our knowledge, this is the first agent-based model to incorporate transformation. This is coupled with the fact that transformation is a multifactorial process with several unknown parameters.[26, 110] Thus, in the absence of good measurements, we used *a priori* knowledge to choose biologically meaningful parameters. Despite this, we did find that transformation curves produced by the model had a limited range as seen in *Supplemental* Figures 4a-c. In all three figures, the shape follows the typical *Acinetobacter baylyi* transformation curve but there are no detectable transformants below the $10e^{-5}$ g.L^{-1} soluble DNA influent concentration.[51] This is most probably due to a low total cell count. Increasing the computational grid size will allow for more bacteria agents and extend the detectable transformation frequency range.

However, this will also increase the computation time and the required memory. *Supplemental* Table 1 lists the total cell count and computation time for several grid sizes. Depending on the chosen grid size, additional parameter adjustments may have to be made to ensure a realistic initial biofilm structure. Additionally, present study experiments are based on an initial 72 hr. mushroom shaped heterotrophic nonresistant biofilm. However, biofilm structure is affected by nutrient and environmental conditions and on-going research implies that *Acinetobacter* spp. biofilms may not form mushroom structures (unpublished results).[2] Repeating simulation conditions using initial biofilms with varying structures could expand current study results. Influent antimicrobial concentrations used in the model are much higher than those found in the environment or used in *in vitro* lab experiments. Our main concern was to include a selective pressure that has a varied effect with changing concentration so the actual concentration was not a concern. Finally, this paper presents the results of simulations that include exposure to a constant influent of resistant DNA. Biofilms in dynamic flow systems may not encounter a constant supply of resistance determinants. In fact, resistant DNA influx may occur in intervals. However, the initial application of this extended iDynoMiCs model used the most simple simulation settings. This included a constant application of antimicrobial and resistant soluble DNA. Future work can and should include more realistic settings for antimicrobial and resistant soluble DNA influx. Despite these limitations, it is our assertion that this is a reliable model for trend estimation since the current model is an extension of the vigorously validated iDynoMiCS model, transformation and antimicrobial inhibition reactions are

based on iDynoMiCS kinetic equations, and assumptions are informed from peer-reviewed literature and laboratory observations.[48]

The current model lends itself to studying various hypotheses without any significant source code modifications. Current experiments look at the effects of constant antimicrobial exposure and resistant soluble DNA across different burden values. However, input of antibiotics in the real world may occur in a single pulse or multiple pulses.[9] It would be interesting to examine the effect of antimicrobial cessation, post prolonged exposure, on the resistance make-up of the biofilm. The antibiotic can also be applied in predefined intervals. Initial biofilm structures may be exposed to pulsing antibiotic alone, or concomitant and/or alternating with resistant soluble DNA. The strength of the antibiotic can also be easily manipulated. The antimicrobial in study simulations offsets growth however the strength or toxicity can be easily changed in the .xml protocol document. Properties of the initial biofilm may also affect the frequency of resistance and location of resistant cells. Running simulations with initial biofilms that vary in age and or location of resistant cells within the structure may offer additional insights.

Additional but somewhat more significant source code modifications would expand the utility of the model. These include: a compensatory mechanism, the ability to use antimicrobial as a growth substrate and growth phase dependent competence. It has been shown that bacteria can ameliorate the cost of acquired resistance with compensatory mutations. These mutations can restore or even improve fitness.[5, 13, 27] The current model

can be amended to include a mutation rate that allows a portion of the resistant bacteria population to maintain resistance but with no fitness cost. Bacteria have other means of persisting in a hostile environment. For instance, some soil bacteria species can subsist on antibiotics, even using them as their sole carbon source.[7] A growth reaction using antimicrobial as a substrate can be specified in the .xml protocol document to account for this. The model could also be expanded to include bacterial cell competence. As previously mentioned, an assumption of the current model is that bacterial cells are competent for the duration of their life span. However, competence induction in *Acinetobacter baylyi* is induced after the transition from lag phase to exponential growth phase and decreases thereafter.[111] If this level of complexity is necessary, it could be achieved by manipulating the source code. The uptake of soluble DNA reaction could be tied to bacterial cell age, only occurring during a specific age period.

This extension of the iDynoMiCS model has numerous applications that would extend research beyond the laboratory setting. Hypotheses can be tested for lengthy periods of time without the potential contamination issues that abound in a lab setting. The model can also be a tool to drive laboratory research and examine ongoing research questions such as mechanisms of biofilm resistance to antimicrobials and methods to promote biofilm dispersal. In addition, it expands the study of HGT. Conjugation dynamics have been extensively studied with *in vitro* and agent-based models such as the iDynoMiCS extension developed by Merkey et al. (2011).[40] Transformation studies are fewer in comparison. This may be because the relative contribution of conjugation to antibiotic

resistance expansion is higher than that of natural transformation mechanisms. However, in depth study of natural transformation is essential to obtain a complete picture of resistance expansion in the environment.

Table 4.1: Default agent parameter values

Parameter	Symbol	Value	Units	Source
Maximal bacteria growth rate	μ^G_{max}	.7	h^{-1}	1,2,3
Maximal antimicrobial inhibition rate	μ^I_{max}	.7	h^{-1}	Assumed
Maximal DNA uptake rate	μ^D_{max}	.7	h^{-1}	Assumed
Saturation constant for COD	κ_{COD}	2.5e-4	$g.L^{-1}$	4
Saturation constant for antimicrobial	κ_{Ab}	2.5e-4	$g.L^{-1}$	Assumed
Saturation constant for soluble DNA	κ_{DNA}	2.5e-4	$g.L^{-1}$	Assumed
Maintenance rate of bacteria	μ^{NR}	.0133	h^{-1}	1,2,3
Fitness burden of resistant gene	μ^R	(0-.140)*	h^{-1}	5,6
Resistance switch threshold	Th_{res}	1	fg	7
Probability of transformation	P(resistant)	2	%	8
Probability of lysis	P(lysis)	1	%	Assumed
Biomass density	$\rho_{biomass}$	150	$g.L^{-1}$	3
Capsule density	$\rho_{capsule}$	10,000#	$g.L^{-1}$	Assumed

Sources values: Noguera & Picioreanu (2004)[1], Rittmann et al. (2004)[2], Lardon et al. (2011)[3], default value in idynomics example[4], Merkey et al. (2011)[5], Seone et al. (2010)[6], unpublished lab results[7], Martinez (2009)[8]

This accounts for any additional burden associated with expressing the resistance gene. Thus resistant bacteria will have a baseline maintenance rate similar to their nonresistant counterparts plus metabolic burden.*

In the base iDynoMiCS model, agents are made up of several compartments including inert biomass, active biomass and capsular EPS. In this modified model, the capsular compartment keeps track of soluble DNA that has been taken up from the surrounding liquid environment. Cellular division is dictated by cell radius which increases as cell biomass increases. To make sure cell division is based on increase in biomass from uptake of nutrient media and not from uptake of soluble DNA, the capsule density was set at 10,000 $g.L^{-1}$.#

Table 4.2: Default environmental parameter values

Parameter	Symbol	Value	Units
Influent nutrient media concentration	COD_{in}	$10e^{-3}$	$g.L^{-1}$
Constant bulk concentration	isConstant	False	n/a
Erosion rate	κ_{Det}	$5e^{-4}$	$(\mu m.h)^{-1}$
Biofilm max thickness	max_{Th}	200	μm

Please refer to *Supplemental Figures* 1a-f for an explanation of the environmental parameters and the chosen default values.

Table 4.3: Overview of model reactions

Process	Δ biomass	capsule	COD	soluble DNA	antimicrobial	Kinetic Expression
	Mass		**Solute** (S_{COD}, S_{Ab}, S_{DNA})			
Bacteria growth on COD	1.0		-1.5			$\mu = \mu^G_{max} \dfrac{S_{COD}}{\kappa_{COD} + S_{COD}} X$
Antimicrobial inhibition of non-resistant bacteria	-1.0*				-1.5	$\mu = \mu^I_{max} \dfrac{S_{Ab}}{\kappa_{Ab} + S_{Ab}} X$
Uptake of soluble DNA		1.0		-1.5		$\mu = \mu^D_{max} \dfrac{S_{DNA}}{\kappa_{DNA} + S_{DNA}} X$
Maintenance of nonresistant bacteria	-1.0					$\mu = \mu^{NR}_{max} X$
Fitness burden of resistant gene	-1.0					$\mu = \mu^R_{max} X$
DNA solubilization		-1.0		1.0		$\mu = \mu^S_{max} X$

Decrease in biomass units due to antimicrobial inhibition may be increased when simulating a stronger (i.e. bacteriolytic) antimicrobial. In the table above, the inhibiting effect of the antimicrobial directly offsets bacterial cell growth.*

Table 4.4: Overview of simulations

Ab_{in}[§] (g.L^{-1}) [constant application]	DNA_{in}[❖] (g.L^{-1}) [constant application]	Resistance maintenance rate (h^{-1})[°]	
0	10e-3	0.000	
		.007	
		.021	Range of maintenance
		.035	rate values used for all
		.070	experiments
		.140	
10e-4	10e-3		
1.25e-3	10e-3		
2.5e-3	10e-3		
5.0e-3	10e-3		

Concentration of antimicrobial in the influent [§]

Concentration of resistant soluble DNA in the influent [❖]

Expressing the resistance gene imposes a metabolic burden on the host bacterium. Burden values are expressed as a percentage of the growth rate (μ^G_{max}). Thus, the maintenance rate of resistant bacteria is actually the baseline maintenance rate (μ^{NR}) plus an additional burden value cost.[°]
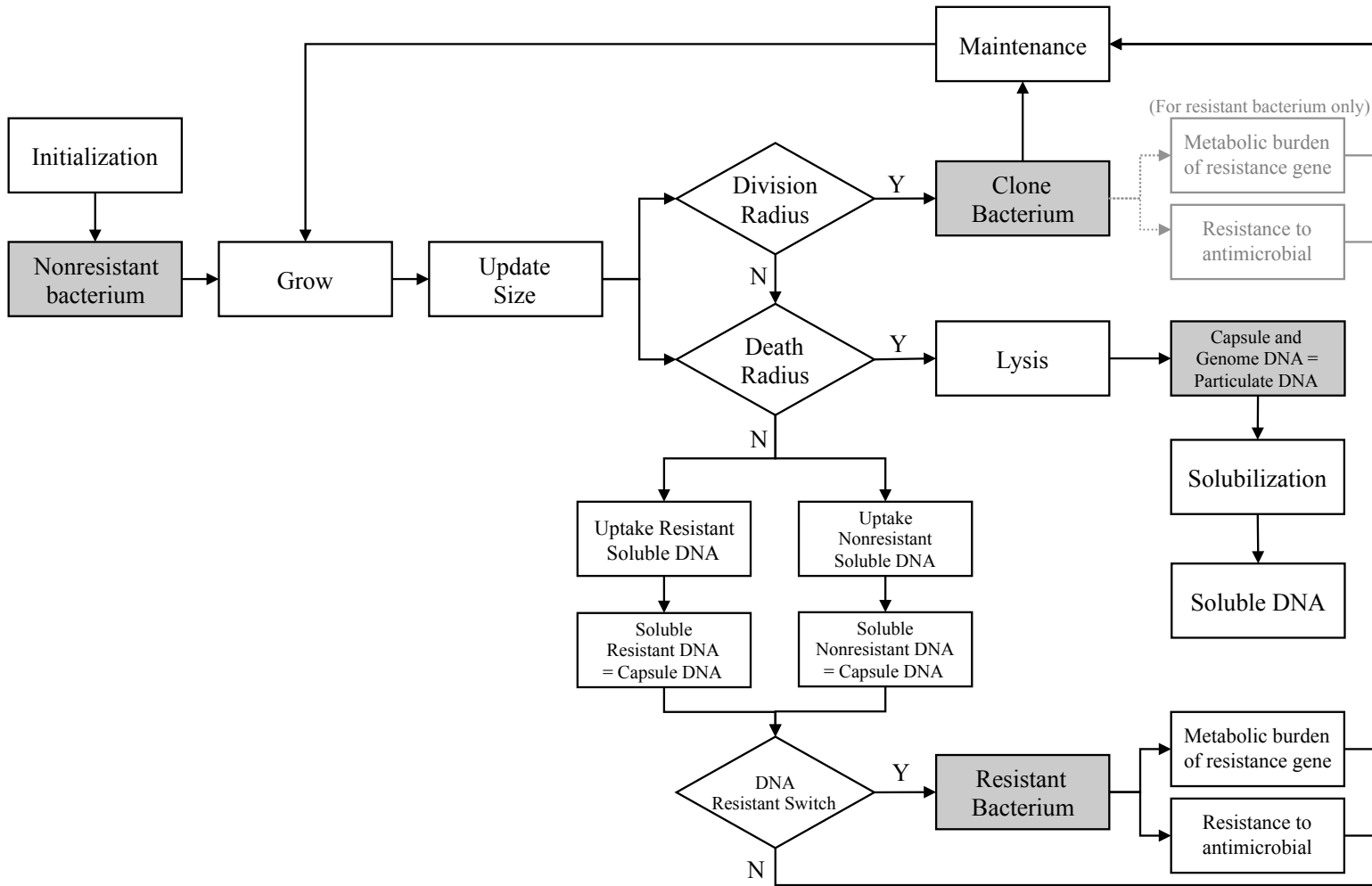
Figure 4.1. Transformation & antimicrobial inhibition model algorithm. Model algorithm depicting the flow of transformation and inhibition processes completed every agent time step. The dark grey shaded boxes represent model agents.
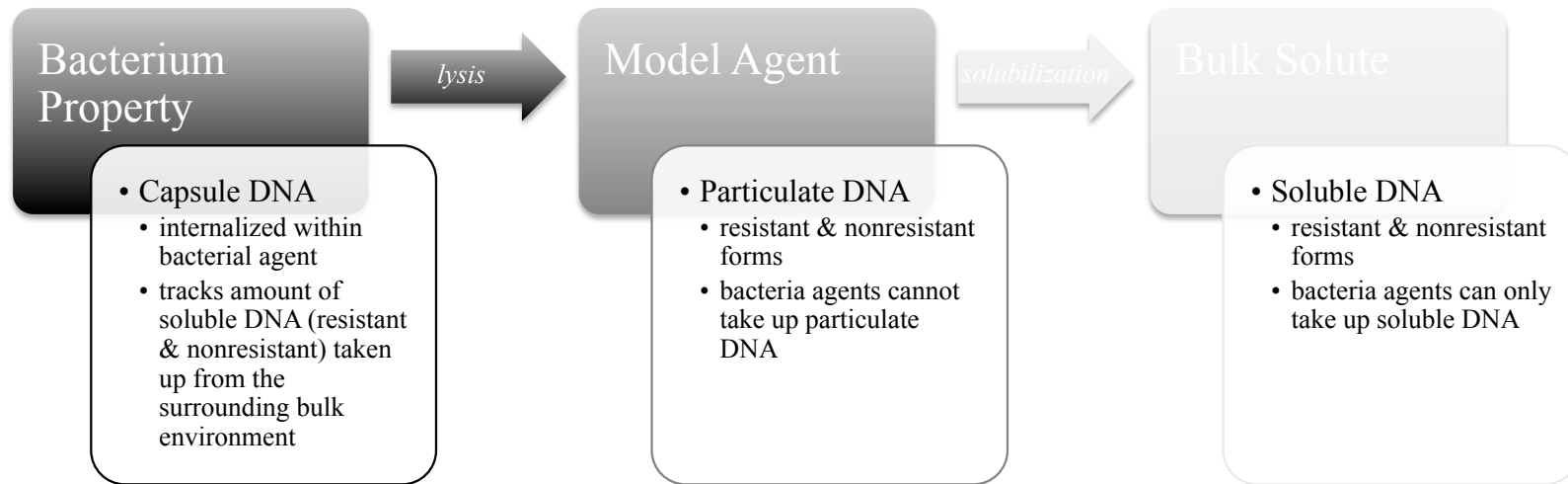
Figure 4.1b. Overview of DNA in the model. DNA is present in three forms: as a bacterial property (capsule DNA), as a model agent (particulate DNA) and as a solute in the bulk compartment (soluble DNA). Arrows between compartments denote model processes.

Figure 4.2a: Effect fitness burden value on the persistence of resistant cells in a biofilm in the absence of antimicrobial exposure. A 3-day nonresistant biofilm was developed in $10e^{-3}$ g.L^{-1} influent nutrient media. This initial biofilm was then exposed to a constant concentration of $10e^{-3}$ g.L^{-1} resistant soluble DNA in the influent. In the current model all bacteria, regardless of resistance make-up, experience a baseline maintenance reaction. However, expressing the resistance gene imposes a metabolic drain on the host bacterium and resistant bacteria undergo an additional maintenance reaction to account for this added cost. The rate of this reaction (μ^R) is a percentage of the bacteria growth rate (μ^G_{max}). In the figure above, resistant bacteria cell/ total bacteria cell curves are charted for μ^R values 0 - .140 h^{-1}. Simulations were run for 30 days and data points are an average of 5 runs; each run had a distinct seed value. Due to the high volume of data points, standard deviations are only graphed for a subset of the values.

Biofilm Age (h)

0	# res. [SD]	120	# res. [SD]	240	# res. [SD]	360	# res. [SD]	
	0 [0]		13.8 [30.3]		0 [0]		.2 [.4]	h >80
0	0 [0]		14.8 [13.5]		5.6 [12.5]		17.2 [35.2]	40 < h ≤ 80
	0 [0]		8.6 [2.3]		19.4 [9.5]		28.2 [21.1]	h ≤ 40
	0 [0]		2.2 [4.9]		0 [0]		0 [0]	h >80
.007	0 [0]		15.2 [17.5]		5.6 [12.0]		2.6 [5.8]	40 < h ≤ 80
	0 [0]		7.6 [3.0]		10 [3.9]		5.8 [4.4]	h ≤ 40
	0 [0]		0 [0]		0 [0]		0 [0]	h >80
.021	0 [0]		8.4 [10.0]		0 [0]		0 [0]	40 < h ≤ 80
	0 [0]		5.2 [2.8]		3.2 [2.3]		.4 [.9]	h ≤ 40
	0 [0]		0 [0]		0 [0]		0 [0]	h >80
.035	0 [0]		3.6 [1.7]		.2 [.4]		0 [0]	40 < h ≤ 80
	0 [0]		7 [3.7]		1.6 [1.5]		.2 [.4]	h ≤ 40
	0 [0]		1.4 [3.1]		0 [0]		0 [0]	h >80
.070	0 [0]		2.6 [1.7]		0 [0]		0 [0]	40 < h ≤ 80
	0 [0]		4.2 [1.3]		0 [0]		0 [0]	h ≤ 40
	0 [0]		0 [0]		0 [0]		0 [0]	h >80
.140	0 [0]		1.2 [1.1]		0 [0]		0 [0]	40 < h ≤ 80
	0 [0]		3 [2.6]		1.4 [.9]		0 [0]	h ≤ 40

Maintenance rate of resistant bacteria (μNR, h-1)

Biofilm height (μm)

Figure 4.2b: Biofilm images: effect of fitness burden value on the persistence of resistant cells in a biofilm in the absence of antimicrobial exposure (0-360h). A 3-day nonresistant biofilm was developed in $10e^{-3}$ g.L^{-1} influent nutrient media. This initial biofilm was then exposed to a constant concentration of $10e^{-3}$ g.L^{-1} resistant soluble DNA in the influent. In the figure above, images of biofilm development over time are displayed for μ^R values 0 - .140 h^{-1}, with each row representing a different μ^R value. Nonresistant cells are blue and resistant cells are red. The total numbers of resistant cells are listed by biofilm height to the right of each respective biofilm image. Total resistant cell data are presented as averages with associated standard deviations. Simulations were run for 30 days and data pts are an average of 5 runs; each run had a distinct seed value. However the images above are from a single, representative simulation.

Biofilm Age (h)

480	# res. [SD]	600	# res. [SD]	720	# res. [SD]	
0	.8 [1.8]		0 [0]		0 [0]	h >80
	23.3 [51.9]		10.4 [23.2]		2 [4.5]	$40 < h \leq 80$
	28.2 [34.7]		22.2 [31.0]		20.6 [32.8]	$h \leq 40$
.007	0 [0]		0 [0]		0 [0]	h >80
	.2 [.4]		0 [0]		0 [0]	$40 < h \leq 80$
	3.2 [2.2]		1.2 [.8]		1.4 [.5]	$h \leq 40$
.021	0 [0]		0 [0]		0 [0]	h >80
	0 [0]		0 [0]		0 [0]	$40 < h \leq 80$
	.4 [.9]		0 [0]		0 [0]	$h \leq 40$
.035	0 [0]		0 [0]		0 [0]	h >80
	0 [0]		0 [0]		0 [0]	$40 < h \leq 80$
	.2 [.4]		0 [0]		0 [0]	$h \leq 40$
.070	0 [0]		0 [0]		0 [0]	h >80
	0 [0]		0 [0]		0 [0]	$40 < h \leq 80$
	0 [0]		0 [0]		0 [0]	$h \leq 40$
.140	0 [0]		0 [0]		0 [0]	h >80
	0 [0]		0 [0]		0 [0]	$40 < h \leq 80$
	0 [0]		0 [0]		0 [0]	$h \leq 40$

Maintenance rate of resistant bacteria ($\mu_N R h^{-1}$)

Biofilm height (μm)

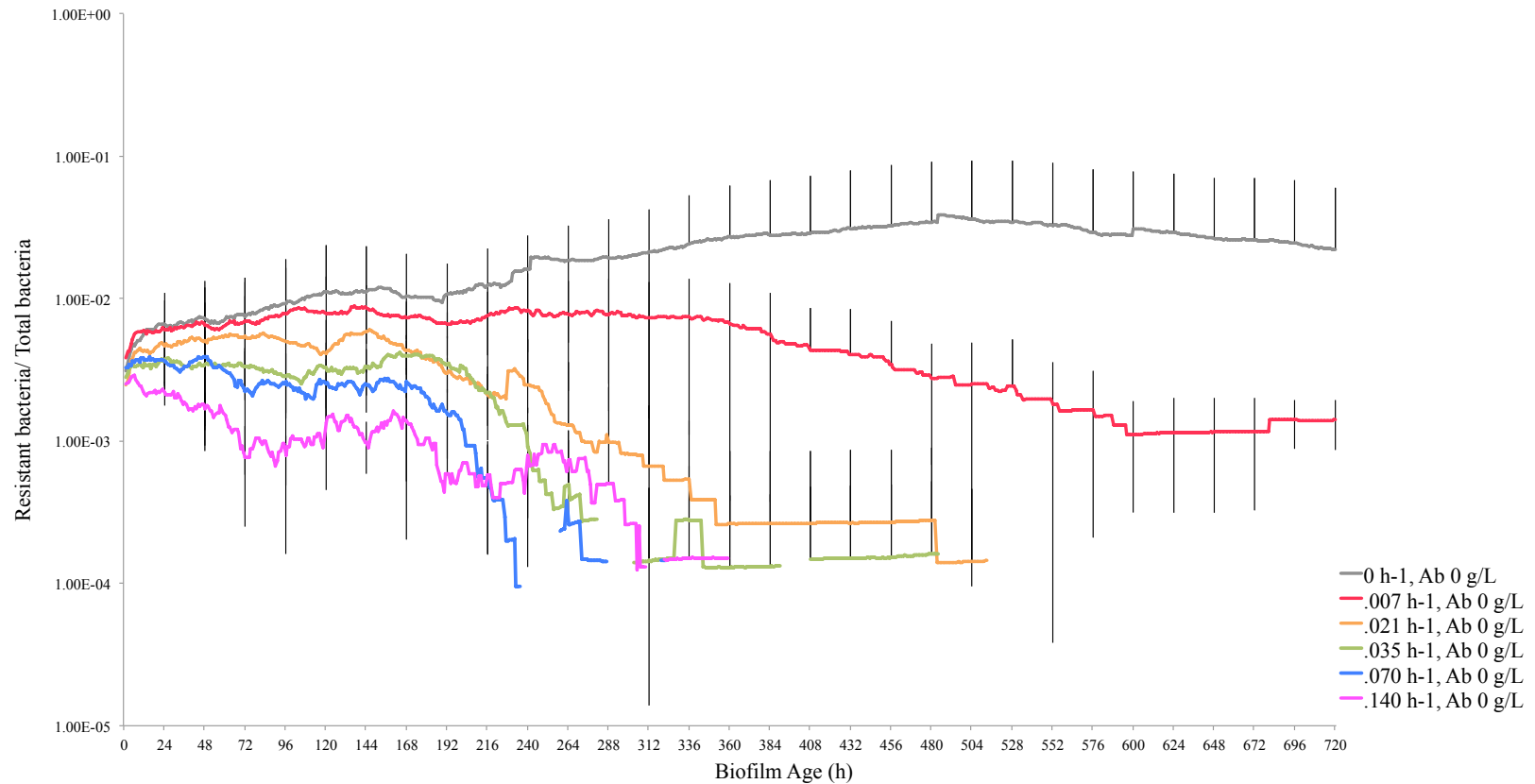**Figure 4.2c: Biofilm images: effect fitness burden value on the persistence of resistant cells in a biofilm in the absence of antimicrobial exposure (480-720h).** A 3-day nonresistant biofilm was developed in $10e^{-3}$ g.L^{-1} influent nutrient media. This initial biofilm was then exposed to a constant concentration of $10e^{-3}$ g.L^{-1} resistant soluble DNA in the influent. In the figure above, images of biofilm development over time are displayed for μ^R values 0 - .140 h^{-1}, with each row representing a different μ^R value. Nonresistant cells are blue and resistant cells are red. The total numbers of resistant cells are listed by biofilm height to the right of each respective biofilm image. Total resistant cell data are presented as averages with associated standard deviations. Simulations were run for 30 days and data points are an average of 5 runs; each run had a distinct seed value. However the images above are from a single, representative simulation.

Figure 4.3a: Effect fitness burden value on the proportion of resistant cells in a biofilm exposed to $10e^{-4}$ g/L antimicrobial. A 3-day nonresistant biofilm was developed in $10e^{-3}$ g.L^{-1} influent nutrient media. This initial biofilm was then exposed to a constant concentration of $10e^{-3}$ g.L^{-1} resistant soluble DNA & $10e^{-4}$ g/L antimicrobial in the influent. In the current model all bacteria, regardless of resistance make-up, experience a baseline maintenance reaction. However, expressing the resistance gene imposes a metabolic drain on the host bacterium and resistant bacteria undergo an additional maintenance reaction to account for this added cost. The rate of this reaction (μ^R) is a percentage of the bacteria growth rate (μ^G_{max}). In the figure above, resistant bacteria cell/ total bacteria cell curves are charted for μ^R values 0 - .140 h^{-1}. Simulations were run for 30 days and data points are an average of 5 runs; each run had a distinct seed value. Due to the high volume of data points, standard deviations are only graphed for a subset of the values.
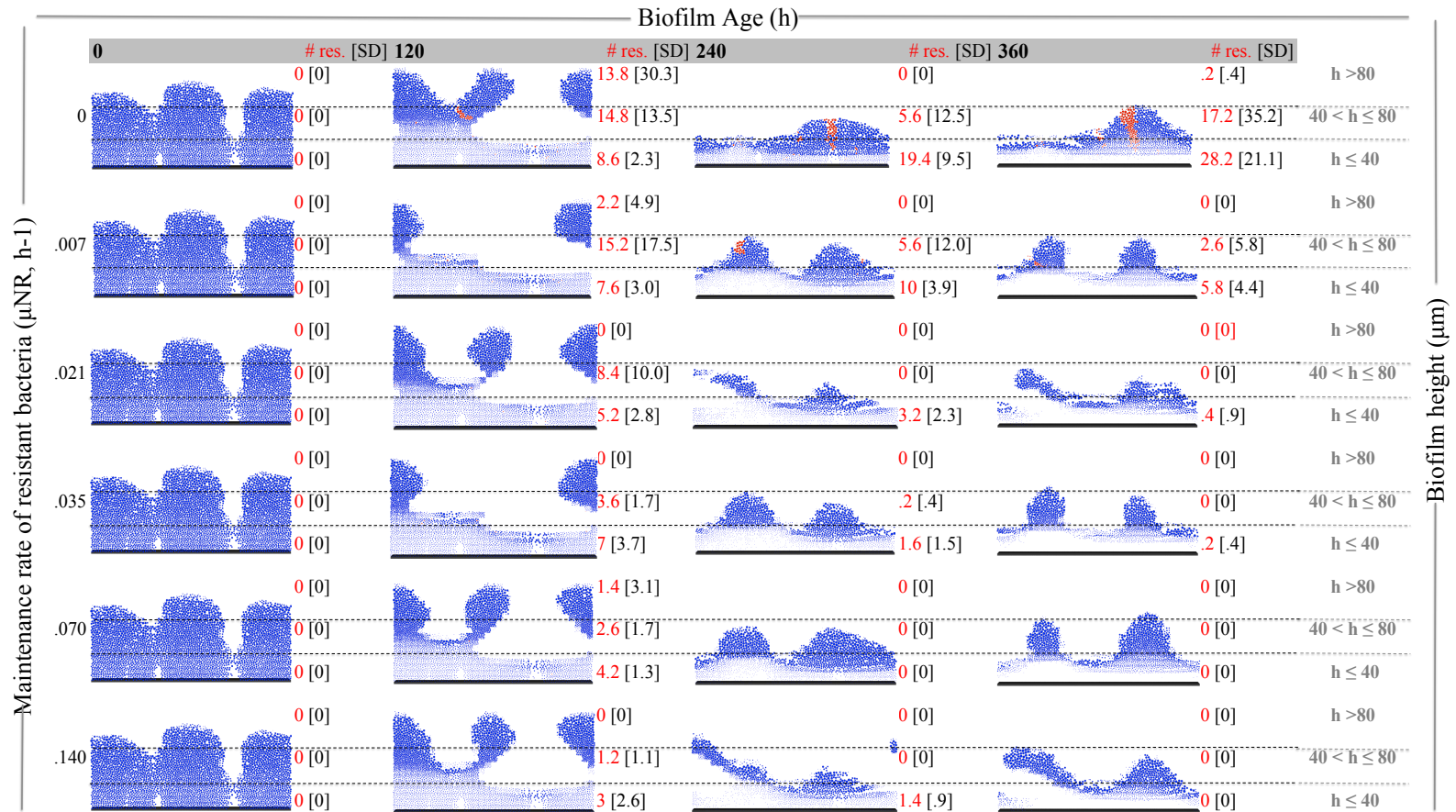
Biofilm Age (h)

Maintenance rate of resistant bacteria (μNR, h-1)

	0	# res. [SD] 120	# res. [SD] 240	# res. [SD] 360	# res. [SD]	
0		0 [0]	83 [92]	18.8 [42]	3.2 [7.2]	h >80
		0 [0]	37 [27.6]	35.4 [33.6]	69.2 [81.4]	40 < h ≤ 80
		0 [0]	9.2 [1.3]	31.6 [16.6]	68.6 [24.8]	h ≤ 40
.007		0 [0]	33.4 [46.4]	9 [20.1]	7.4 [10.3]	h >80
		0 [0]	27 [30.1]	69.6 [74.5]	70.8 [98.7]	40 < h ≤ 80
		0 [0]	7.2 [2.4]	18.6 [14.5]	26.4 [34.1]	h ≤ 40
.021		0 [0]	9.6 [21.5]	0 [0]	0 [0]	h >80
		0 [0]	10.8 [15.9]	.4 [.5]	0 [0]	40 < h ≤ 80
		0 [0]	5.4 [1.3]	6.2 [3.8]	0 [0]	h ≤ 40
.035		0 [0]	13.6 [30.4]	0 [0]	0 [0]	h >80
		0 [0]	7.2 [5.1]	0 [0]	0 [0]	40 < h ≤ 80
		0 [0]	6 [4]	2.2 [2.2]	.4 [.9]	h ≤ 40
.070		0 [0]	0 [0]	0 [0]	0 [0]	h >80
		0 [0]	1.4 [1.1]	0 [0]	0 [0]	40 < h ≤ 80
		0 [0]	4 [1.2]	2.6 [2.9]	0 [0]	h ≤ 40
.140		0 [0]	0 [0]	0 [0]	0 [0]	h >80
		0 [0]	1.8 [1.6]	0 [0]	0 [0]	40 < h ≤ 80
		0 [0]	2.8 [1.9]	1 [1.7]	0 [0]	h ≤ 40

Biofilm height (μm)

Figure 4.3b: Biofilm images: effect fitness burden value on the proportion of resistant cells in a biofilm exposed to $10e^{-4}$ g/L antimicrobial (0-360h). A 3-day nonresistant biofilm was developed in $10e^{-3}$ g.L^{-1} influent nutrient media. This initial biofilm was then exposed to a constant concentration of $10e^{-3}$ g.L^{-1} resistant soluble DNA in the influent. In the figure above, images of biofilm development over time are displayed for μ^R values 0 - .140 h^{-1}, with each row representing a different μ^R value. Nonresistant cells are blue and resistant cells are red. The total numbers of resistant cells are listed by biofilm height to the right of each respective biofilm image. Total resistant cell data are presented as averages with associated standard deviations. Simulations were run for 30 days and data points are an average of 5 runs; each run had a distinct seed value. However the images above are from a single, representative simulation.
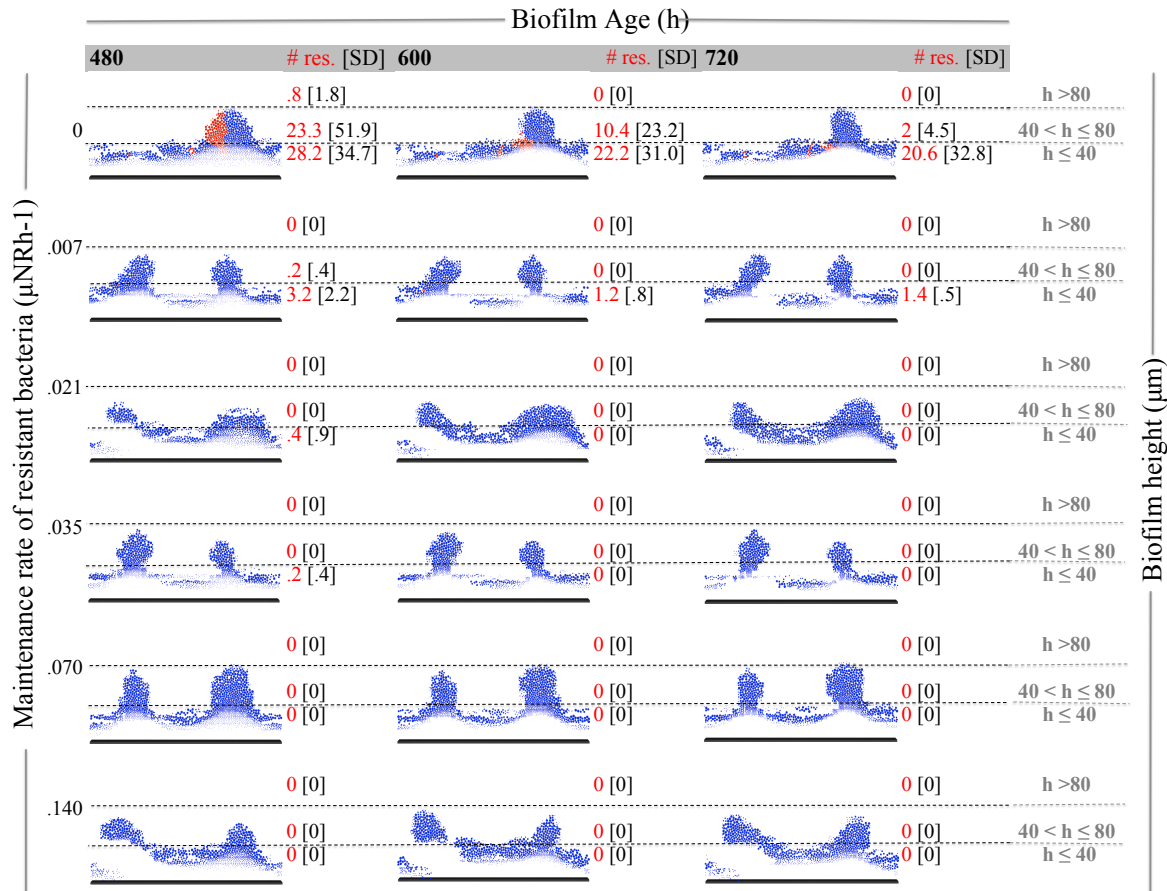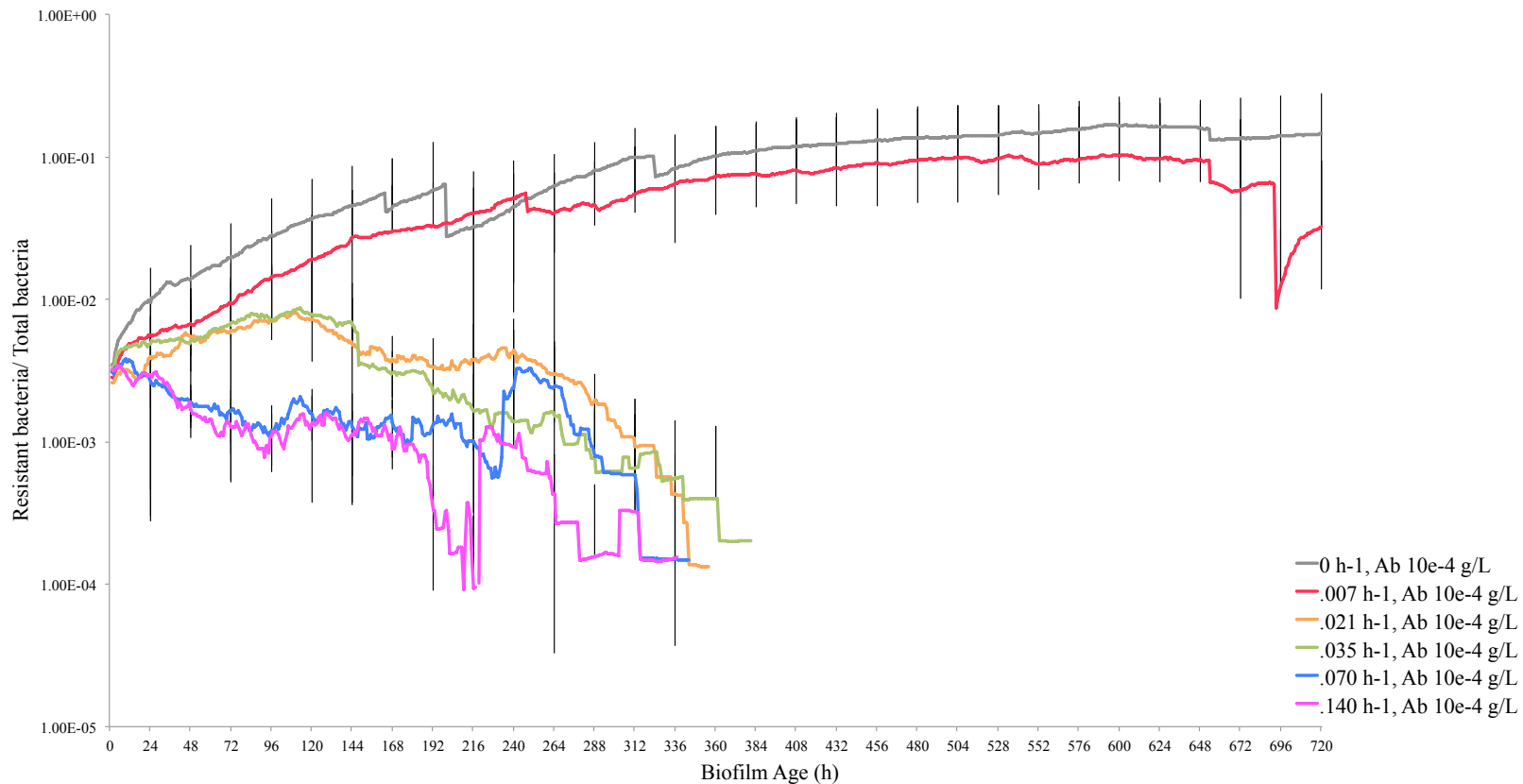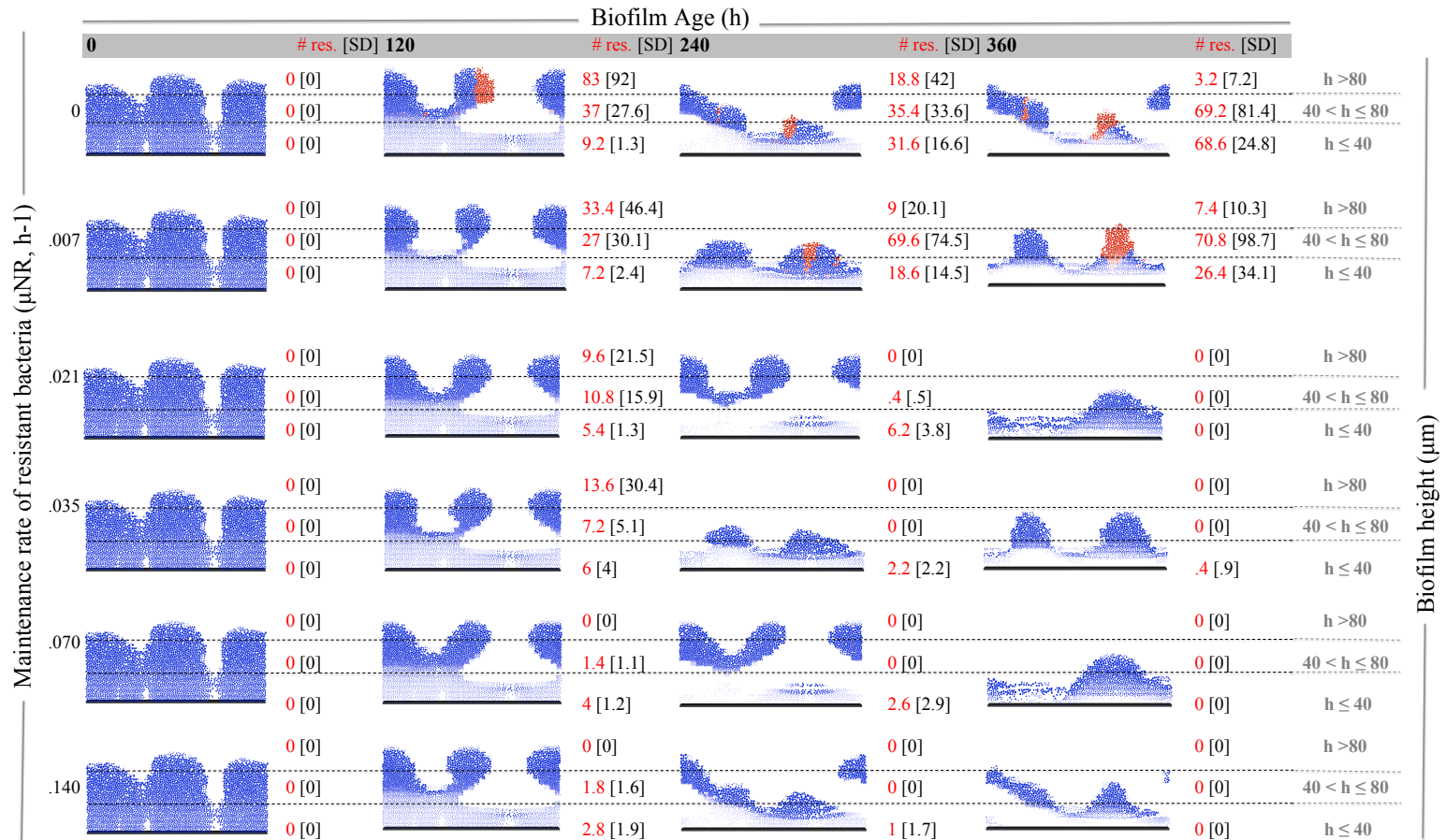
Figure 4.3c: Biofilm images: effect fitness burden value on the proportion of resistant cells in a biofilm exposed to 10e^{-4} g/L antimicrobial (480-720h). A 3-day nonresistant biofilm was developed in 10e^{-3} g.L^{-1} influent nutrient media. This initial biofilm was then exposed to a constant concentration of 10e^{-3} g.L^{-1} resistant soluble DNA in the influent. In the figure above, images of biofilm development over time are displayed for μ^R values 0 - .140 h^{-1}, with each row representing a different μ^R value. Nonresistant cells are blue and resistant cells are red. The total numbers of resistant cells are listed by biofilm height to the right of each respective biofilm image. Total resistant cell data are presented as averages with associated standard deviations. Simulations were run for 30 days and data points are an average of 5 runs; each run had a distinct seed value. However the images above are from a single, representative simulation.
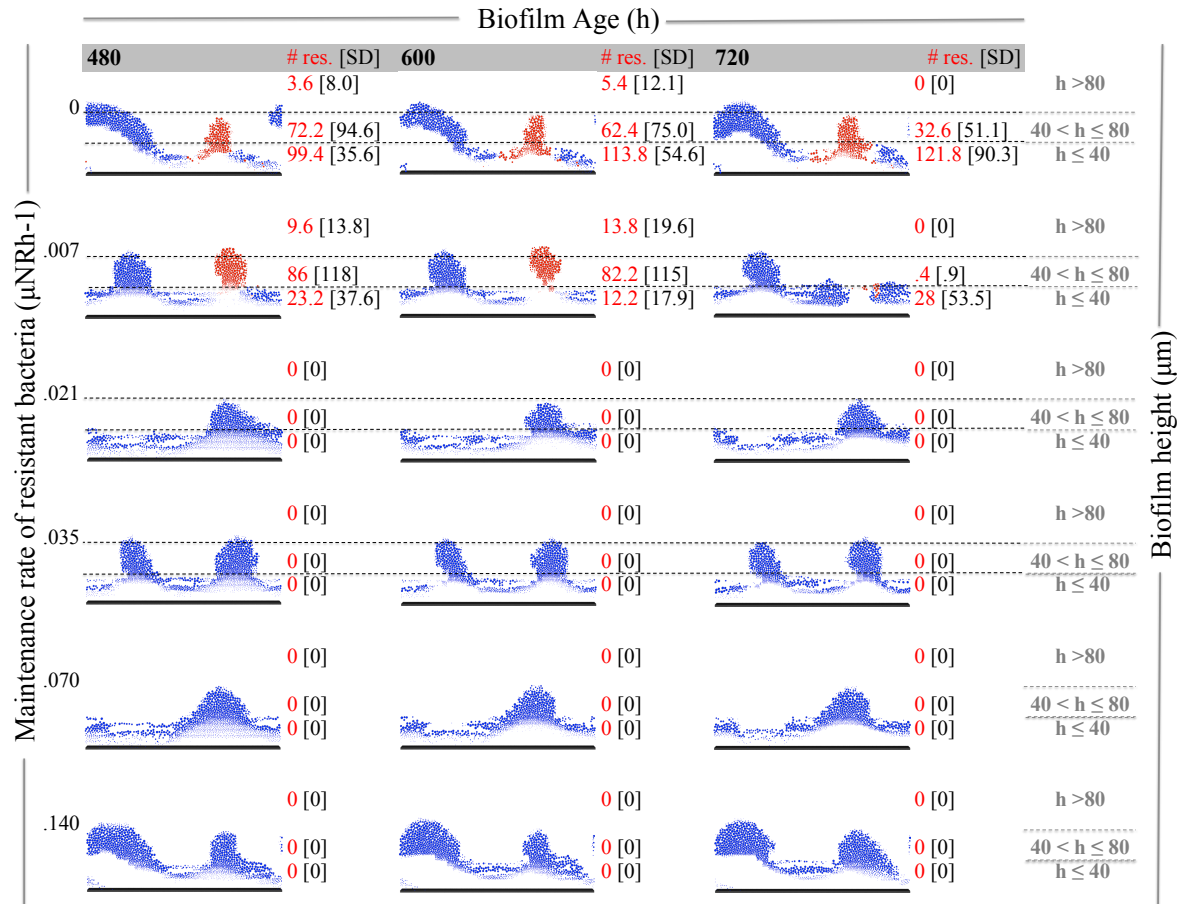
Figure 4.4a: Effect fitness burden value on the proportion of resistant cells in a biofilm exposed to 1.25e^{-3} g/L antimicrobial. A 3-day nonresistant biofilm was developed in 10e^{-3} g.L^{-1} influent nutrient media. This initial biofilm was then exposed to a constant concentration of 10e^{-3} g.L^{-1} resistant soluble DNA & 1.25e^{-3} g/L antimicrobial in the influent. In the current model all bacteria, regardless of resistance make-up, experience a baseline maintenance reaction. However, expressing the resistance gene imposes a metabolic drain on the host bacterium and resistant bacteria undergo an additional maintenance reaction to account for this added cost. The rate of this reaction (μ^R) is a percentage of the bacteria growth rate (μ^G_{max}). In the figure above, resistant bacteria cell/ total bacteria cell curves are charted for μ^R values 0 - .140 h^{-1}. Simulations were run for 30 days and the current graph represents one set of simulation runs.

Biofilm Age (h)

	# res. [SD]	120	# res. [SD]	240	# res. [SD]	360	# res. [SD]	

Maintenance rate of resistant bacteria (μNR, h-1)

Biofilm height (μm)

0

0 [0]   70.6 [157.9]   0 [0]   .4 [.5]   h >80

0 [0]   27.4 [41.8]   16 [19.3]   97.8 [109.1]   40 < h ≤ 80

0 [0]   8.4 [2.3]   37.6 [30.1]   111.6 [81.1]   h ≤ 40

.007

0 [0]   44 [98.3]   0 [0]   0 [0]   h >80

0 [0]   25.4 [45.6]   3.6 [5.9]   18.8 [41]   40 < h ≤ 80

0 [0]   5.8 [3.1]   14.8 [10.7]   18 [17.2]   h ≤ 40

.021

0 [0]   7 [15.6]   0 [0]   0 [0]   h >80

0 [0]   10.6 [7.7]   .4 [.5]   0 [0]   40 < h ≤ 80

0 [0]   6.2 [2.6]   3.4 [3.2]   1.2 [1.8]   h ≤ 40

.035

0 [0]   1.8 [4.0]   1.8 [4.0]   0 [0]   h >80

0 [0]   6.4 [5.5]   .4 [.9]   0 [0]   40 < h ≤ 80

0 [0]   4.6 [1.5]   4.8 [3.6]   .4 [.5]   h ≤ 40

.070

0 [0]   0 [0]   0 [0]   0 [0]   h >80

0 [0]   .8 [.8]   0 [0]   0 [0]   40 < h ≤ 80

0 [0]   2.8 [.8]   2.8 [1.5]   0 [0]   h ≤ 40

.140

0 [0]   0 [0]   0 [0]   0 [0]   h >80

0 [0]   1 [1]   0 [0]   0 [0]   40 < h ≤ 80

0 [0]   2.8 [2.2]   2 [2.3]   0 [0]   h ≤ 40

Figure 4.4b: Biofilm images: effect fitness burden value on the proportion of resistant cells in a biofilm exposed to 1.25e^{-3} g/L antimicrobial (0-360h). A 3-day nonresistant biofilm was developed in 10e^{-3} g.L^{-1} influent nutrient media. This initial biofilm was then exposed to a constant concentration of 10e^{-3} g.L^{-1} resistant soluble DNA in the influent. In the figure above, images of biofilm development over time are displayed for μ^R values 0 - .140 h^{-1}, with each row representing a different μ^R value. Nonresistant cells are blue and resistant cells are red. The total numbers of resistant cells are listed by biofilm height to the right of each respective biofilm image. Total resistant cell data are presented as averages with associated standard deviations. Simulations were run for 30 days and data points are an average of 5 runs; each run had a distinct seed value. However the images above are from a single, representative simulation.
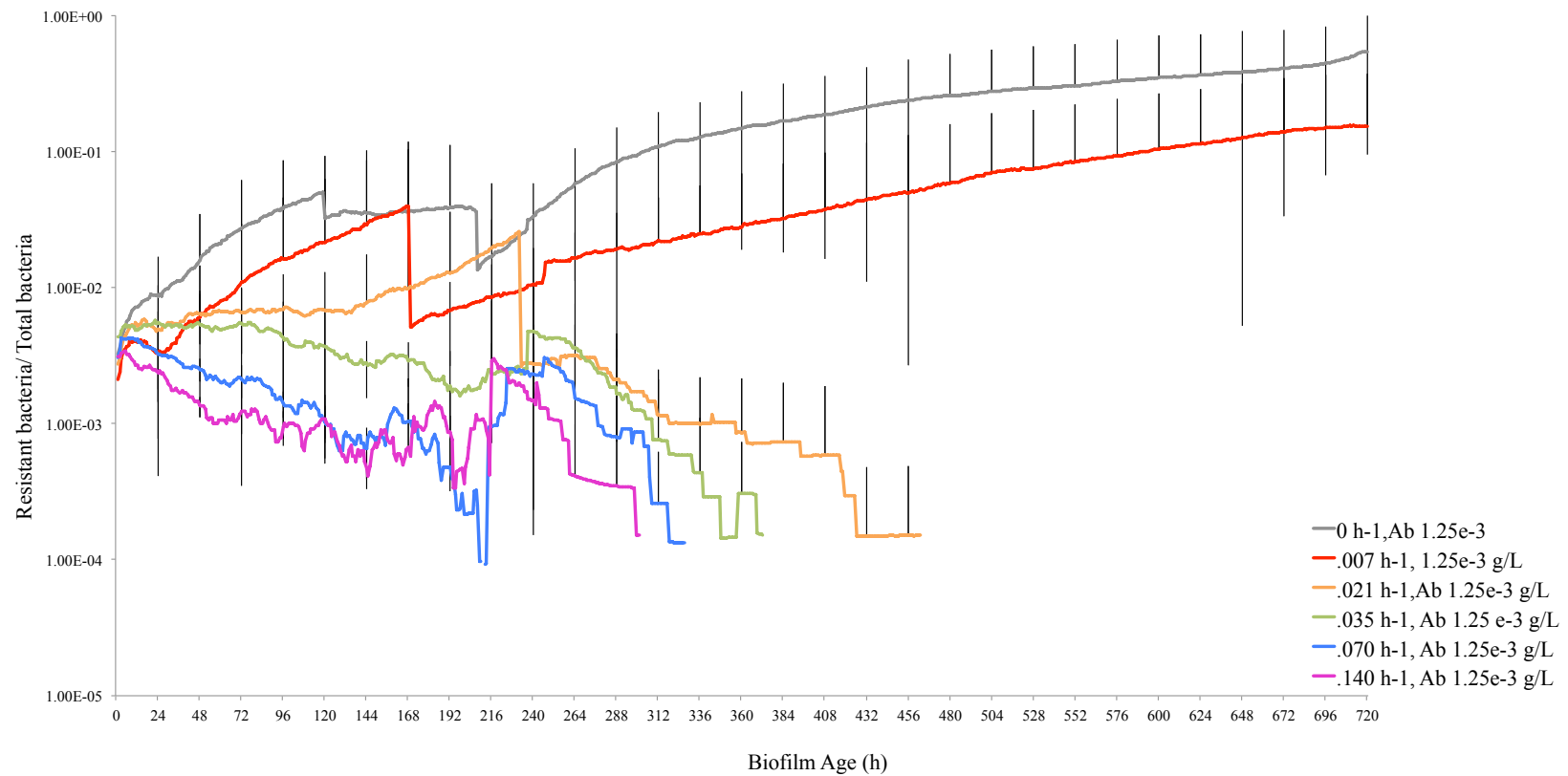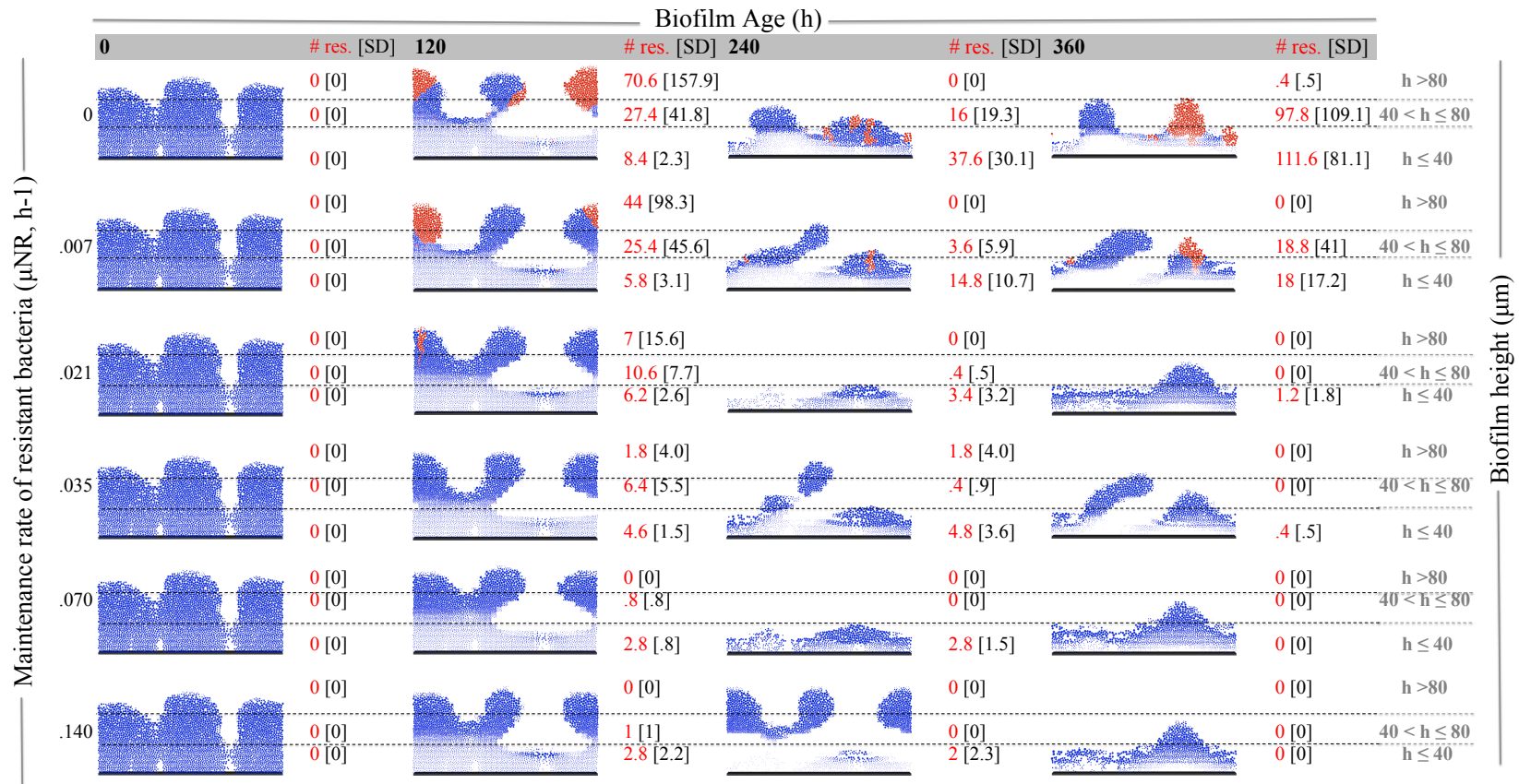
111

Figure 4.4c: Biofilm images: effect fitness burden value on the proportion of resistant cells in a biofilm exposed to 1.25e^{-3} g/L antimicrobial (480-720h). A 3-day nonresistant biofilm was developed in 10e^{-3} g.L^{-1} influent nutrient media. This initial biofilm was then exposed to a constant concentration of 10e^{-3} g.L^{-1} resistant soluble DNA in the influent. In the figure above, images of biofilm development over time are displayed for μ^R values 0 - .140 h^{-1}, with each row representing a different μ^R value. Nonresistant cells are blue and resistant cells are red. The total numbers of resistant cells are listed by biofilm height to the right of each respective biofilm image. Total resistant cell data are presented as averages with associated standard deviations. Simulations were run for 30 days and data points are an average of 5 runs; each run had a distinct seed value. However the images above are from a single, representative simulation.
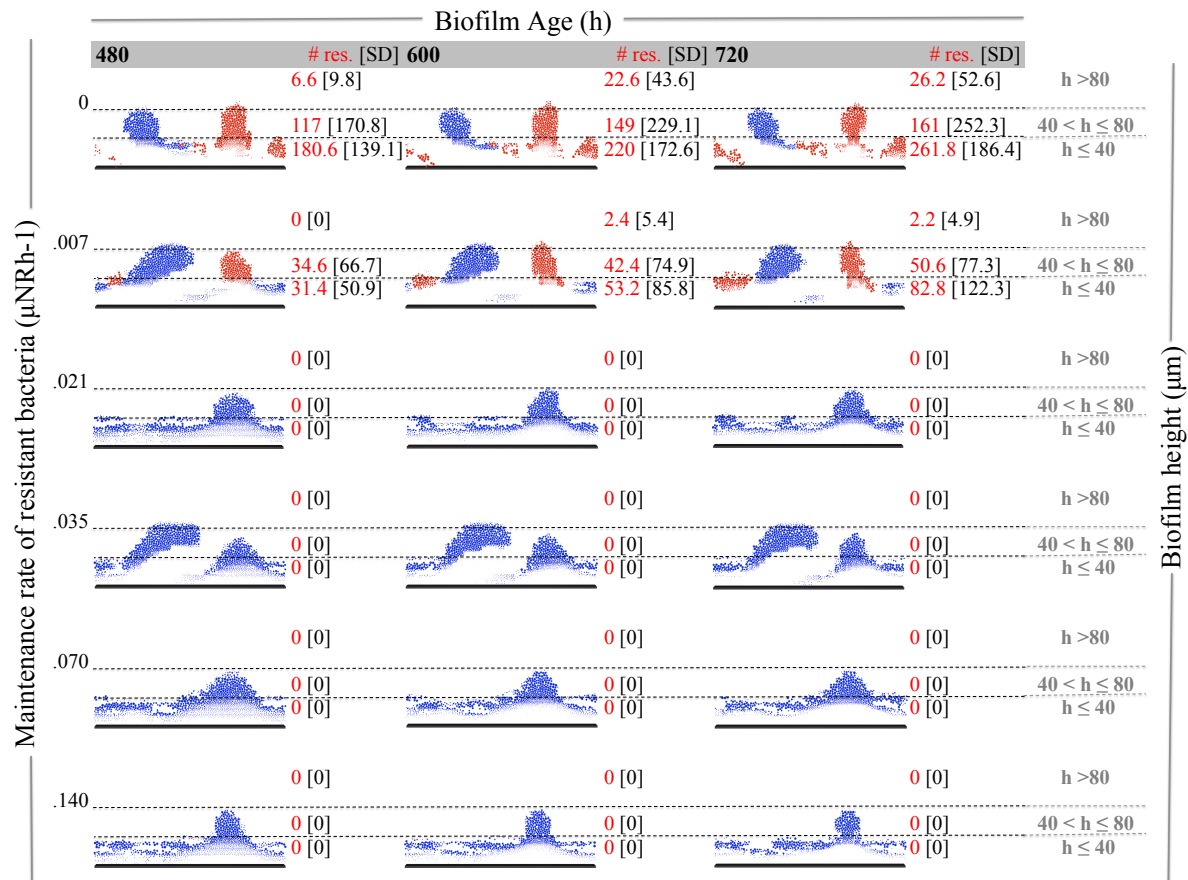
Figure 4.5a: Effect fitness burden value on the proportion of resistant cells in a biofilm exposed to 2.5e^{-3} g/L antimicrobial. A 3-day nonresistant biofilm was developed in 10e^{-3} g.L^{-1} influent nutrient media. This initial biofilm was then exposed to a constant concentration of 10e^{-3} g.L^{-1} resistant soluble DNA & 2.5e^{-3} g/L antimicrobial in the influent. In the current model all bacteria, regardless of resistance make-up, experience a baseline maintenance reaction. However, expressing the resistance gene imposes a metabolic drain on the host bacterium and resistant bacteria undergo an additional maintenance reaction to account for this added cost. The rate of this reaction (μ^R) is a percentage of the bacteria growth rate (μ^G_{max}). In the figure above, resistant bacteria cell/ total bacteria cell curves are charted for μ^R values 0 - .140 h^{-1}. Simulations were run for 30 days and the current graph represents one set of simulation runs.

113

Biofilm Age (h)

$\mu^{NR}h^{-1}$	0	# res. [SD]	120	# res. [SD]	240	# res. [SD]	360	# res. [SD]	Biofilm height (µm)
0		0 [0]		143.4 [156.7]		68.6 [133.4]		13 [19.6]	h >80
		0 [0]		102 [80.1]		278 [162.3]		232.2 [168.2]	40 < h ≤ 80
		0 [0]		39 [71.6]		354.2 [319]		595.6 [341.9]	h ≤ 40
.007		0 [0]		99.6 [140.9]		0 [0]		9.8 [15.3]	h >80
		0 [0]		70.4 [87.7]		96 [139.4]		185.2 [269.7]	40 < h ≤ 80
		0 [0]		5 [2]		185.4 [253.8]		306.2 [409.9]	h ≤ 40
.021		0 [0]		102.2 [169.2]		0 [0]		0 [0]	h >80
		0 [0]		70.2 [109.4]		22.2 [45.9]		89.4 [134.6]	40 < h ≤ 80
		0 [0]		5.8 [2.4]		187.6 [300.6]		286.6 [409.1]	h ≤ 40
.035		0 [0]		49.4 [69.7]		.2 [.4]		0 [0]	h >80
		0 [0]		57.6 [72.7]		7 [10.6]		15.4 [34.4]	40 < h ≤ 80
		0 [0]		3.2 [2.8]		11.4 [18.3]		116.2 [259.3]	h ≤ 40
.070		0 [0]		0 [0]		0 [0]		0 [0]	h >80
		0 [0]		1.2 [1.3]		0 [0]		0 [0]	40 < h ≤ 80
		0 [0]		3 [1.2]		2.3 [1.3]		0 [0]	h ≤ 40
.140		0 [0]		0 [0]		0 [0]		0 [0]	h >80
		0 [0]		.2 [.4]		0 [0]		0 [0]	40 < h ≤ 80
		0 [0]		1.4 [.9]		4 [2.5]		.6 [.5]	h ≤ 40

Maintenance rate of resistant bacteria ($\mu^{NR}h^{-1}$)

Figure 4.5b: Biofilm images: effect fitness burden value on the proportion of resistant cells in a biofilm exposed to 2.5e^{-3} g/L antimicrobial (0-360h). A 3-day nonresistant biofilm was developed in 10e^{-3} g.L^{-1} influent nutrient media. This initial biofilm was then exposed to a constant concentration of 10e^{-3} g.L^{-1} resistant soluble DNA in the influent. In the figure above, images of biofilm development over time are displayed for μ^R values 0 - .140 h^{-1}, with each row representing a different μ^R value. Nonresistant cells are blue and resistant cells are red. The total numbers of resistant cells are listed by biofilm height to the right of each respective biofilm image. Total resistant cell data are presented as averages with associated standard deviations. Simulations were run for 30 days and data points are an average of 5 runs; each run had a distinct seed value. However the images above are from a single, representative simulation.
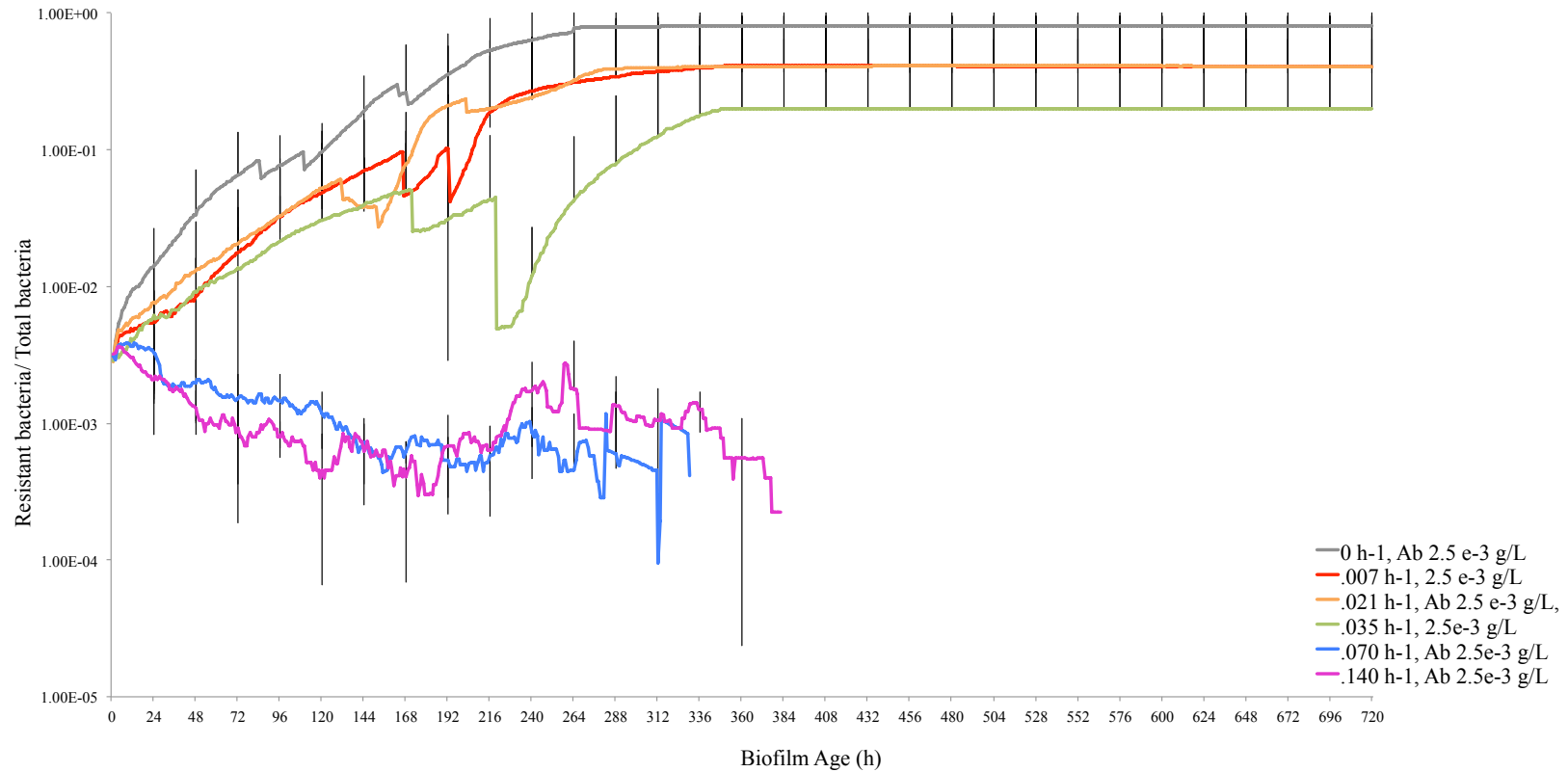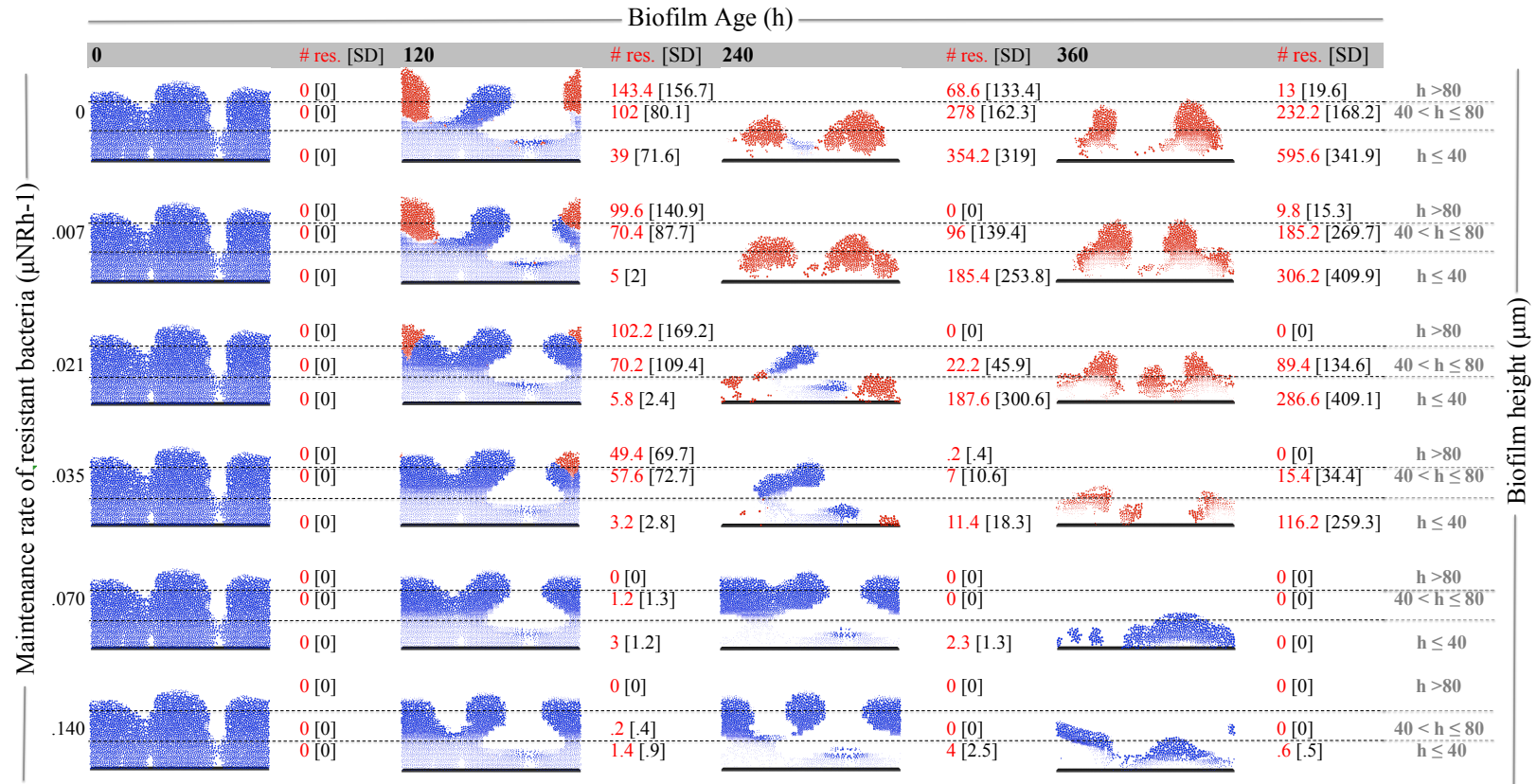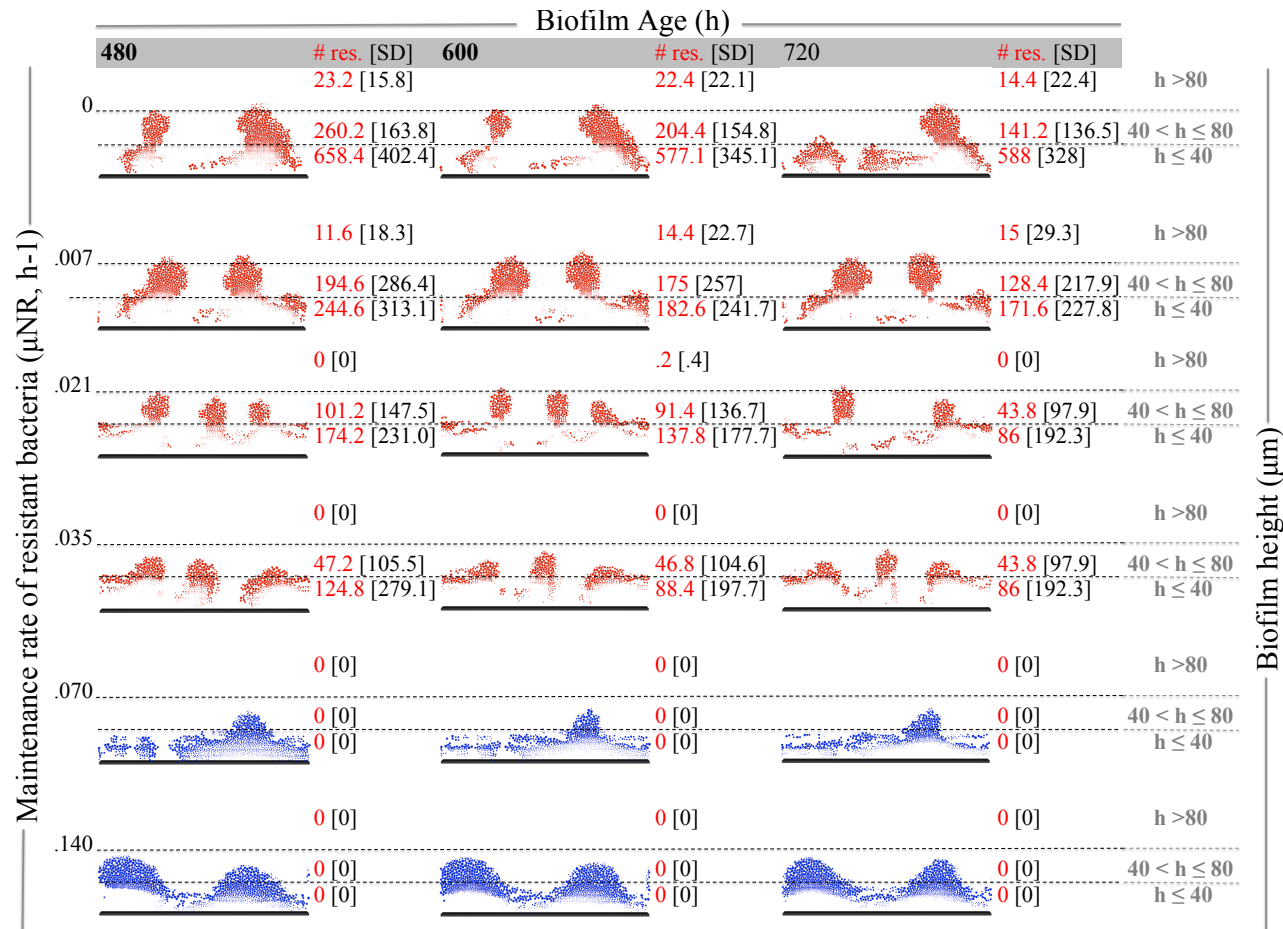
Biofilm Age (h)

Maintenance rate of resistant bacteria (μR, h-1)	480 # res. [SD]	600 # res. [SD]	720 # res. [SD]	Biofilm height band
0	23.2 [15.8]	22.4 [22.1]	14.4 [22.4]	h >80
	260.2 [163.8]	204.4 [154.8]	141.2 [136.5]	40 < h ≤ 80
	658.4 [402.4]	577.1 [345.1]	588 [328]	h ≤ 40
.007	11.6 [18.3]	14.4 [22.7]	15 [29.3]	h >80
	194.6 [286.4]	175 [257]	128.4 [217.9]	40 < h ≤ 80
	244.6 [313.1]	182.6 [241.7]	171.6 [227.8]	h ≤ 40
.021	0 [0]	.2 [.4]	0 [0]	h >80
	101.2 [147.5]	91.4 [136.7]	43.8 [97.9]	40 < h ≤ 80
	174.2 [231.0]	137.8 [177.7]	86 [192.3]	h ≤ 40
.035	0 [0]	0 [0]	0 [0]	h >80
	47.2 [105.5]	46.8 [104.6]	43.8 [97.9]	40 < h ≤ 80
	124.8 [279.1]	88.4 [197.7]	86 [192.3]	h ≤ 40
.070	0 [0]	0 [0]	0 [0]	h >80
	0 [0]	0 [0]	0 [0]	40 < h ≤ 80
	0 [0]	0 [0]	0 [0]	h ≤ 40
.140	0 [0]	0 [0]	0 [0]	h >80
	0 [0]	0 [0]	0 [0]	40 < h ≤ 80
	0 [0]	0 [0]	0 [0]	h ≤ 40

Biofilm height (μm)

Figure 4.5c: Biofilm images: Effect fitness burden value on the proportion of resistant cells in a biofilm exposed to 2.5e^{-3} g/L antimicrobial (480-720h). A 3-day nonresistant biofilm was developed in 10e^{-3} g.L^{-1} influent nutrient media. This initial biofilm was then exposed to a constant concentration of 10e^{-3} g.L^{-1} resistant soluble DNA in the influent. In the figure above, images of biofilm development over time are displayed for μ^R values 0 - .140 h^{-1}, with each row representing a different μ^R value. Nonresistant cells are blue and resistant cells are red. The total numbers of resistant cells are listed by biofilm height to the right of each respective biofilm image. Total resistant cell data are presented as averages with associated standard deviations. Simulations were run for 30 days and data points are an average of 5 runs; each run had a distinct seed value. However the images above are from a single, representative simulation. Results cover the time range 480 –
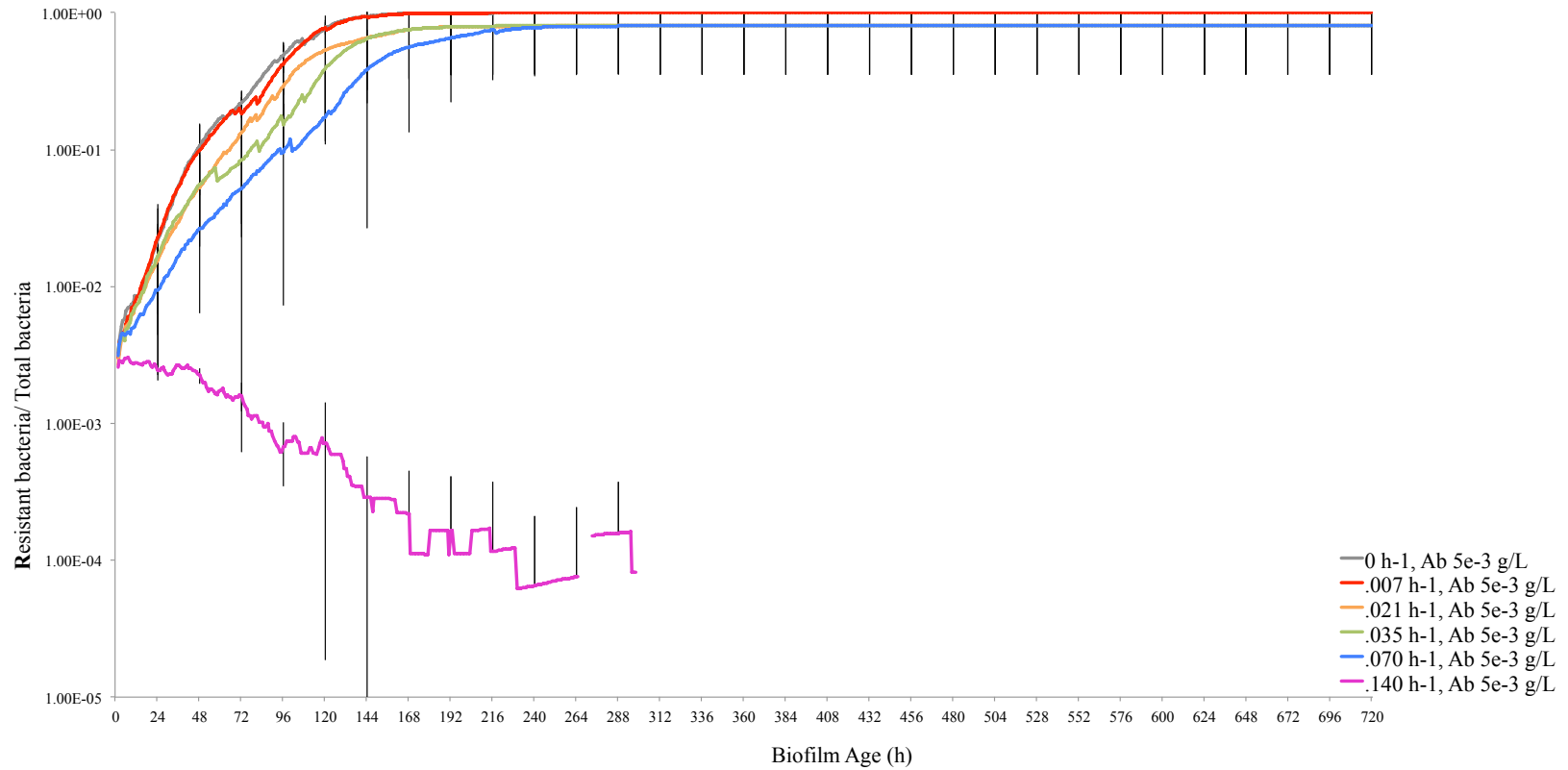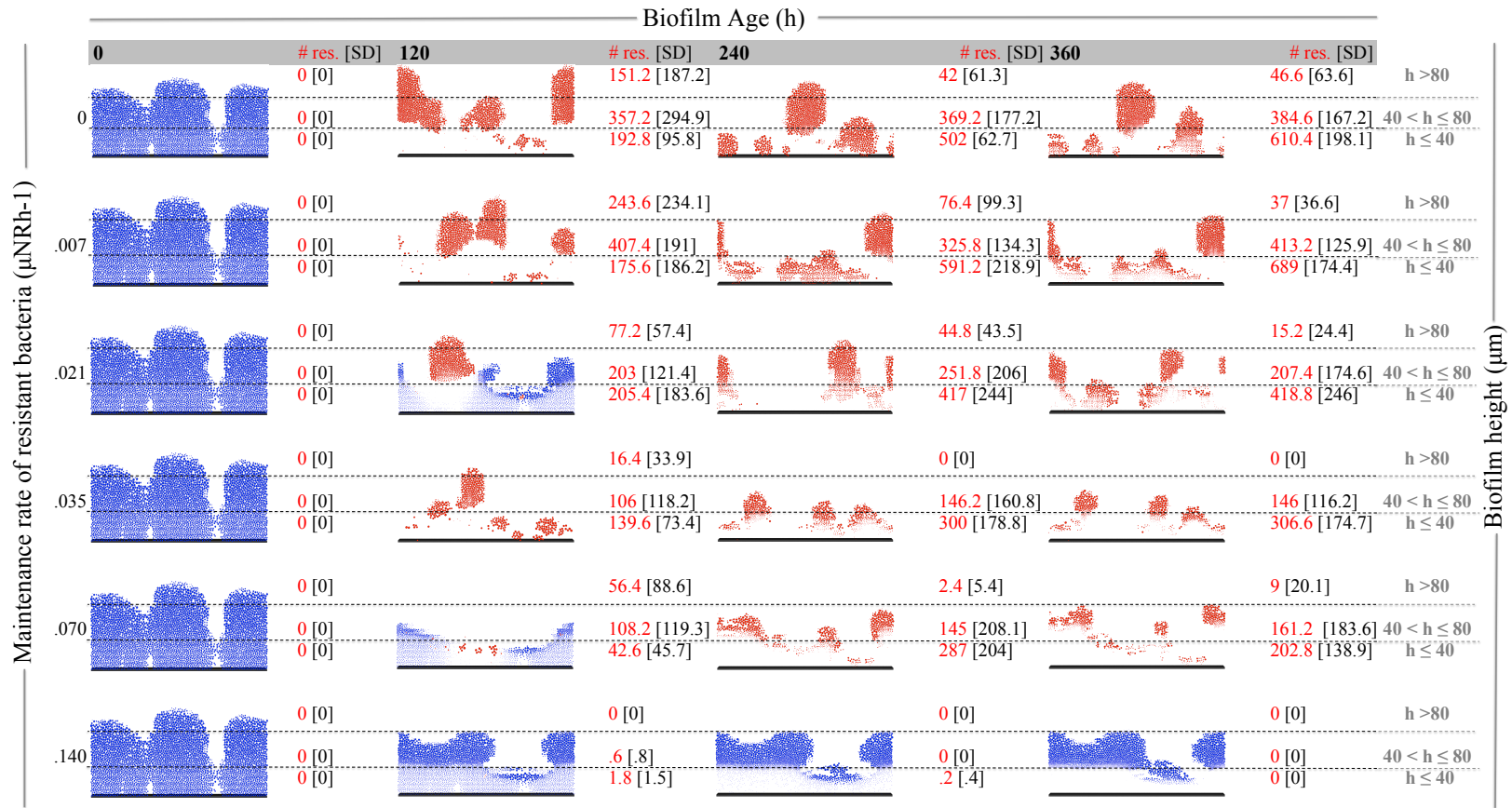
Figure 4.6a: Effect fitness burden value on the proportion of resistant cells in a biofilm exposed to 5.0e^{-3} g/L antimicrobial. A 3-day nonresistant biofilm was developed in 10e^{-3} g.L^{-1} influent nutrient media. This initial biofilm was then exposed to a constant concentration of 10e^{-3} g.L^{-1} resistant soluble DNA & 5.0e^{-3} g/L antimicrobial in the influent. In the current model all bacteria, regardless of resistance make-up, experience a baseline maintenance reaction. However, expressing the resistance gene imposes a metabolic drain on the host bacterium and resistant bacteria undergo an additional maintenance reaction to account for this added cost. The rate of this reaction (μ^R) is a percentage of the bacteria growth rate (μ^G_{max}). In the figure above, resistant bacteria cell/ total bacteria cell curves are charted for μ^R values 0 - .140 h^{-1}. Simulations were run for 30 days and and the current graph represents one set of simulation runs.

Biofilm Age (h)

μNRh-1	0 # res. [SD]	120 # res. [SD]	240 # res. [SD]	360 # res. [SD]	Biofilm height (μm)
0	0 [0]	151.2 [187.2]	42 [61.3]	46.6 [63.6]	h >80
	0 [0]	357.2 [294.9]	369.2 [177.2]	384.6 [167.2]	40 < h ≤ 80
	0 [0]	192.8 [95.8]	502 [62.7]	610.4 [198.1]	h ≤ 40
.007	0 [0]	243.6 [234.1]	76.4 [99.3]	37 [36.6]	h >80
	0 [0]	407.4 [191]	325.8 [134.3]	413.2 [125.9]	40 < h ≤ 80
	0 [0]	175.6 [186.2]	591.2 [218.9]	689 [174.4]	h ≤ 40
.021	0 [0]	77.2 [57.4]	44.8 [43.5]	15.2 [24.4]	h >80
	0 [0]	203 [121.4]	251.8 [206]	207.4 [174.6]	40 < h ≤ 80
	0 [0]	205.4 [183.6]	417 [244]	418.8 [246]	h ≤ 40
.035	0 [0]	16.4 [33.9]	0 [0]	0 [0]	h >80
	0 [0]	106 [118.2]	146.2 [160.8]	146 [116.2]	40 < h ≤ 80
	0 [0]	139.6 [73.4]	300 [178.8]	306.6 [174.7]	h ≤ 40
.070	0 [0]	56.4 [88.6]	2.4 [5.4]	9 [20.1]	h >80
	0 [0]	108.2 [119.3]	145 [208.1]	161.2 [183.6]	40 < h ≤ 80
	0 [0]	42.6 [45.7]	287 [204]	202.8 [138.9]	h ≤ 40
.140	0 [0]	0 [0]	0 [0]	0 [0]	h >80
	0 [0]	.6 [.8]	0 [0]	0 [0]	40 < h ≤ 80
	0 [0]	1.8 [1.5]	.2 [.4]	0 [0]	h ≤ 40

Maintenance rate of resistant bacteria (μNRh-1)

Figure 4.6b: Biofilm images: effect fitness burden value on the proportion of resistant cells in a biofilm exposed to 5.0e^{-3} g/L antimicrobial (0-360h). A 3-day nonresistant biofilm was developed in 10e^{-3} g.L^{-1} influent nutrient media. This initial biofilm was then exposed to a constant concentration of 10e^{-3} g.L^{-1} resistant soluble DNA in the influent. In the figure above, images of biofilm development over time are displayed for μ^R values 0 - .140 h^{-1}, with each row representing a different μ^R value. Nonresistant cells are blue and resistant cells are red. The total numbers of resistant cells are listed by biofilm height to the right of each respective biofilm image. Total resistant cell data are presented as averages with associated standard deviations. Simulations were run for 30 days and data points are an average of 5 runs; each run had a distinct seed value. However the images above are from a single, representative simulation.
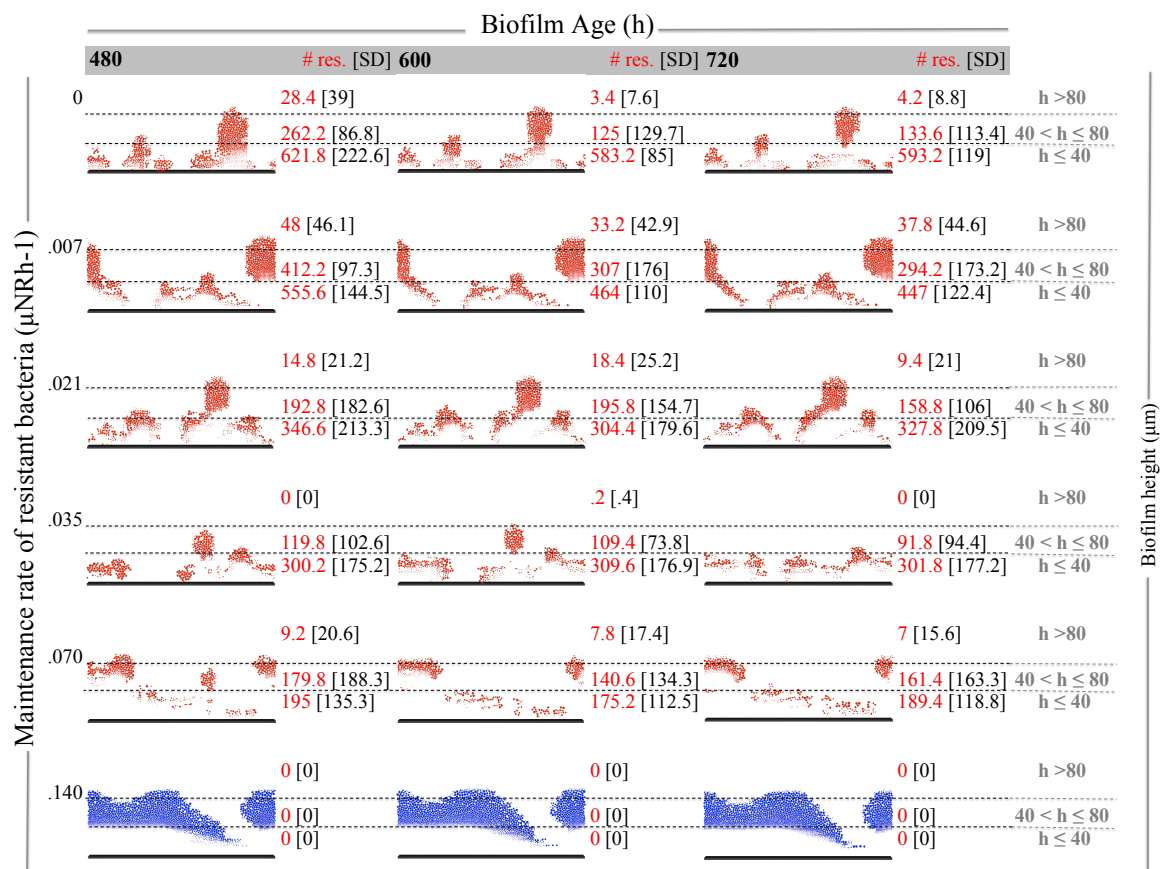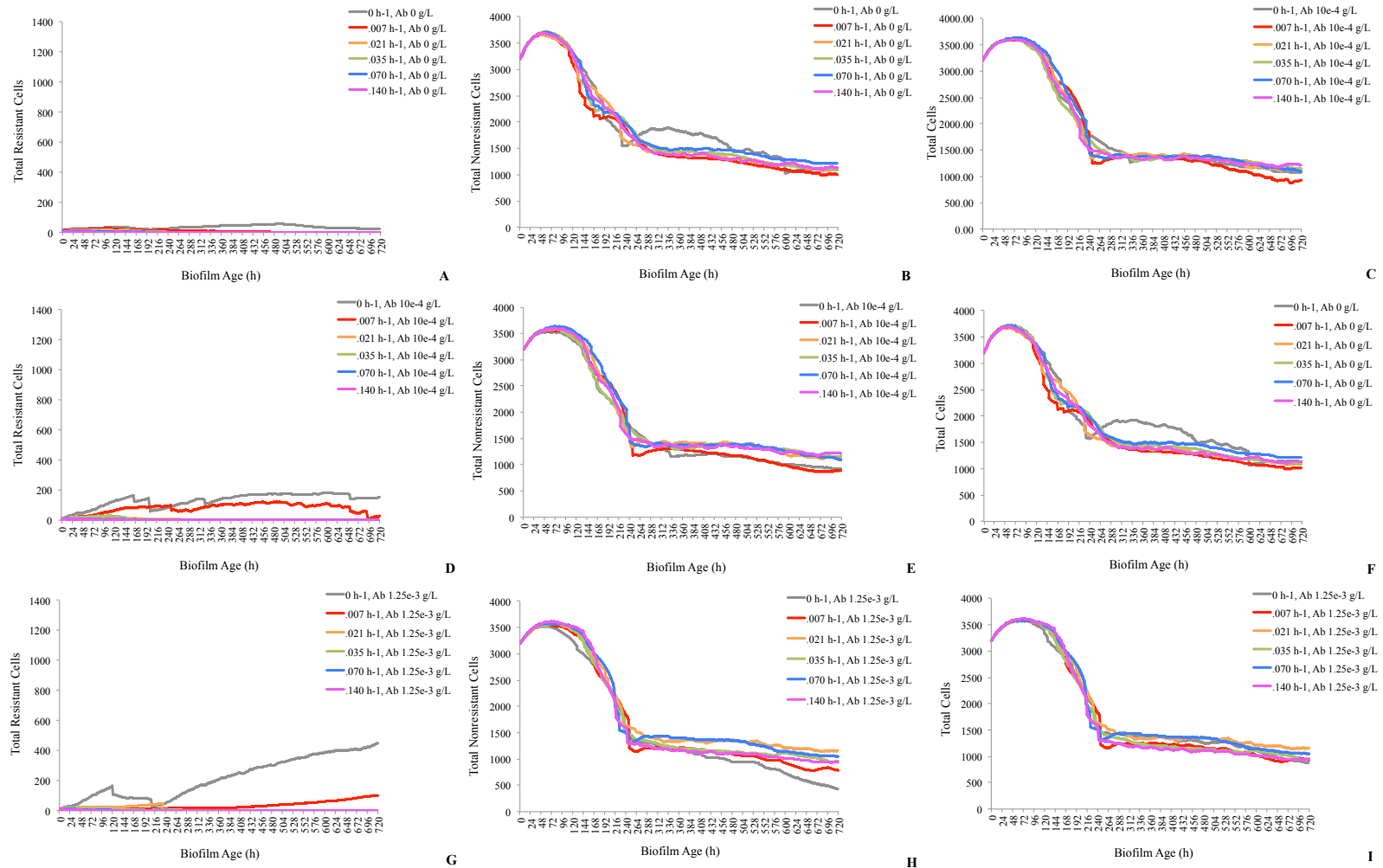
117

Biofilm Age (h)

	480	# res. [SD]	600	# res. [SD]	720	# res. [SD]	

Maintenance rate of resistant bacteria (μNRh-1)

Biofilm height (μm)

μR = 0
- 28.4 [39] / 3.4 [7.6] / 4.2 [8.8] — h >80
- 262.2 [86.8] / 125 [129.7] / 133.6 [113.4] — 40 < h ≤ 80
- 621.8 [222.6] / 583.2 [85] / 593.2 [119] — h ≤ 40

μR = .007
- 48 [46.1] / 33.2 [42.9] / 37.8 [44.6] — h >80
- 412.2 [97.3] / 307 [176] / 294.2 [173.2] — 40 < h ≤ 80
- 555.6 [144.5] / 464 [110] / 447 [122.4] — h ≤ 40

μR = .021
- 14.8 [21.2] / 18.4 [25.2] / 9.4 [21] — h >80
- 192.8 [182.6] / 195.8 [154.7] / 158.8 [106] — 40 < h ≤ 80
- 346.6 [213.3] / 304.4 [179.6] / 327.8 [209.5] — h ≤ 40

μR = .035
- 0 [0] / .2 [.4] / 0 [0] — h >80
- 119.8 [102.6] / 109.4 [73.8] / 91.8 [94.4] — 40 < h ≤ 80
- 300.2 [175.2] / 309.6 [176.9] / 301.8 [177.2] — h ≤ 40

μR = .070
- 9.2 [20.6] / 7.8 [17.4] / 7 [15.6] — h >80
- 179.8 [188.3] / 140.6 [134.3] / 161.4 [163.3] — 40 < h ≤ 80
- 195 [135.3] / 175.2 [112.5] / 189.4 [118.8] — h ≤ 40

μR = .140
- 0 [0] / 0 [0] / 0 [0] — h >80
- 0 [0] / 0 [0] / 0 [0] — 40 < h ≤ 80
- 0 [0] / 0 [0] / 0 [0] — h ≤ 40

Figure 4.6c: Biofilm images: Effect fitness burden value on the proportion of resistant cells in a biofilm exposed to 5.0e^{-3} g/L antimicrobial (480-720h). A 3-day nonresistant biofilm was developed in 10e^{-3} g.L^{-1} influent nutrient media. This initial biofilm was then exposed to a constant concentration of 10e^{-3} g.L^{-1} resistant soluble DNA in the influent. In the figure above, images of biofilm development over time are displayed for μ^R values 0 - .140 h^{-1}, with each row representing a different μ^R value. Nonresistant cells are blue and resistant cells are red. The total numbers of resistant cells are listed by biofilm height to the right of each respective biofilm image. Total resistant cell data are presented as averages with associated standard deviations. Simulations were run for 30 days and data points are an average of 5 runs; each run had a distinct seed value. However the images above are from a single, representative simulation.

118

Figures 4.7.1 a-o: The number of total resistant cells, total nonresistant cells and total cells in a biofilm over time, part1. Description on subsequent page.

119
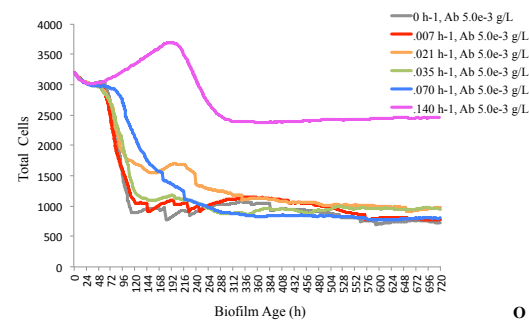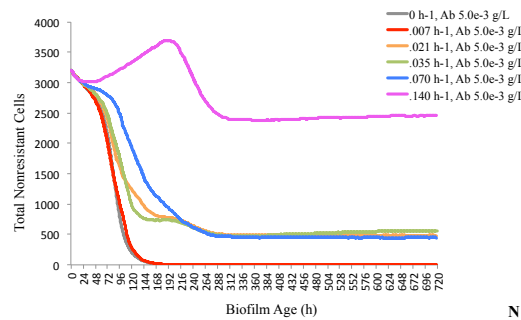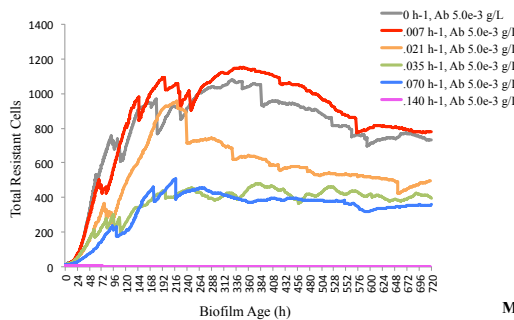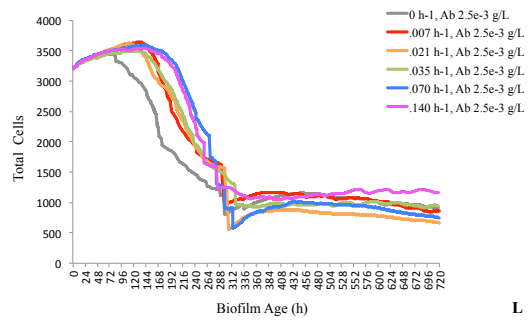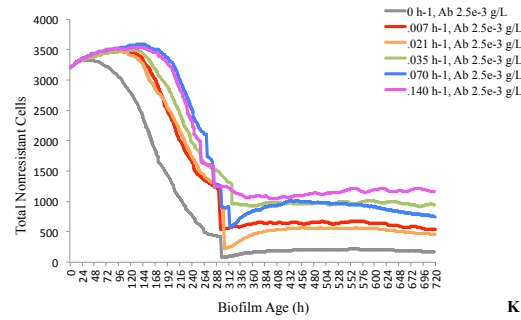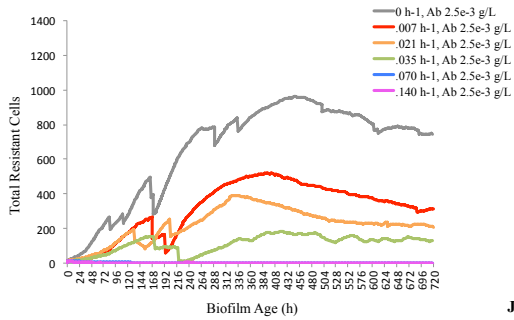
Figures 4.7.2 a-o: The number of total resistant cells, total nonresistant cells and total cells in a biofilm over time, part2. A 3-day nonresistant biofilm was developed in 10e^{-3} g.L^{-1} influent nutrient media. This initial biofilm was then exposed to a constant concentration of 10e^{-3} g.L^{-1} resistant soluble DNA and varying antibiotic concentration. Figures a, d, g, j & m display the total resistant cells over time in a biofilm exposed to 10e^{-3} g.L^{-1} resistant soluble DNA and increasing antibiotic concentration. Figures b, e, h, k & n display the total nonresistant cells over time in a biofilm exposed to 10e^{-3} g.L^{-1} resistant soluble DNA and increasing antibiotic concentration. Figures c, f, i, l & o display the total (resistant + nonresistant) cells over time in a biofilm exposed to 10e^{-3} g.L^{-1} resistant soluble DNA and increasing antibiotic concentration. Within each figure, a-o, cell curves are charted for μ^R values 0 - .140 h^{-1}. All data points are an average of 5 runs, each with a distinct seed value. Standard deviation values were calculated but are not included in the above graphs.

120
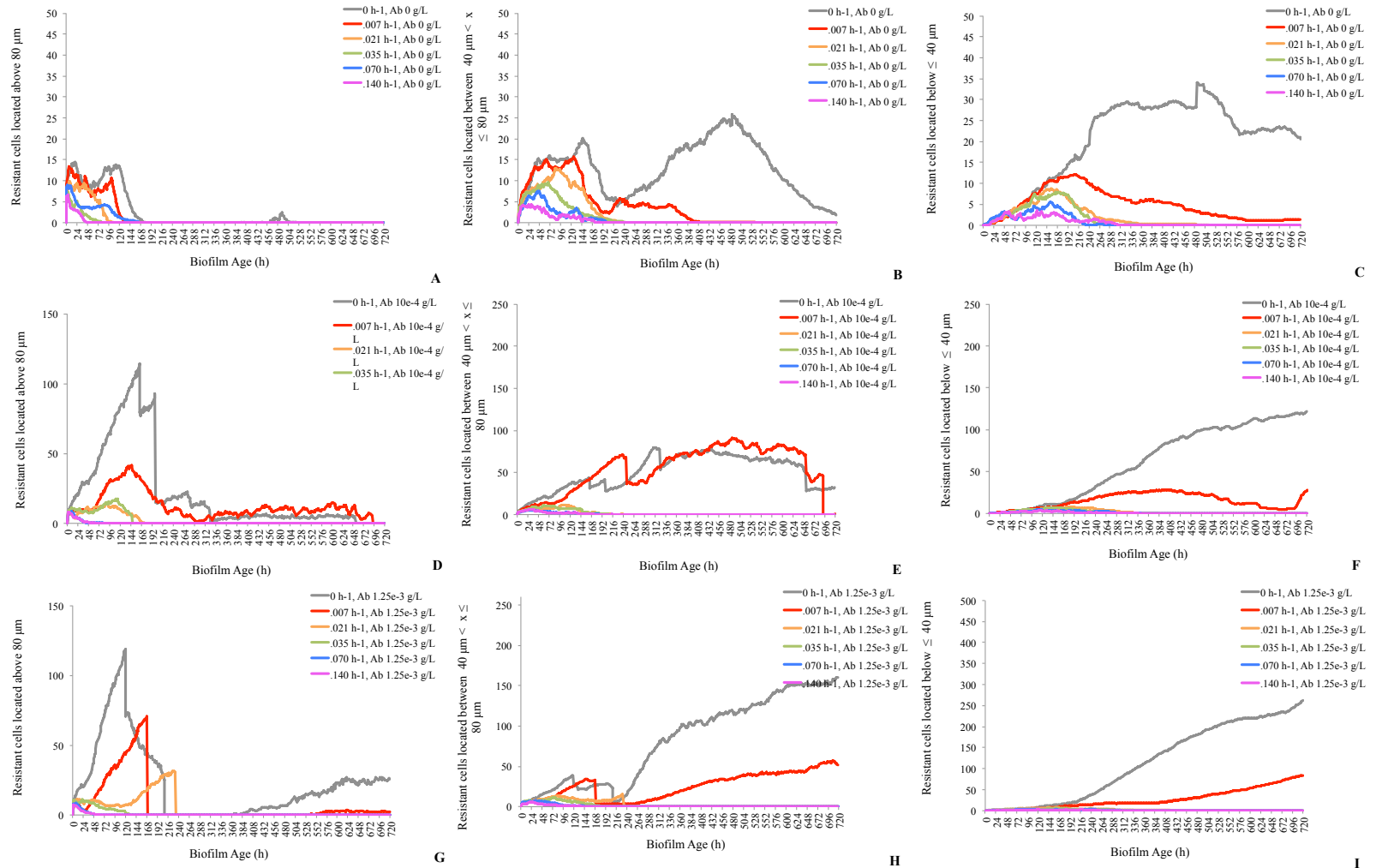
Figures 4.8.1 a-o: The number of resistant cells by location in a biofilm over time, part 1. Description on the next page.
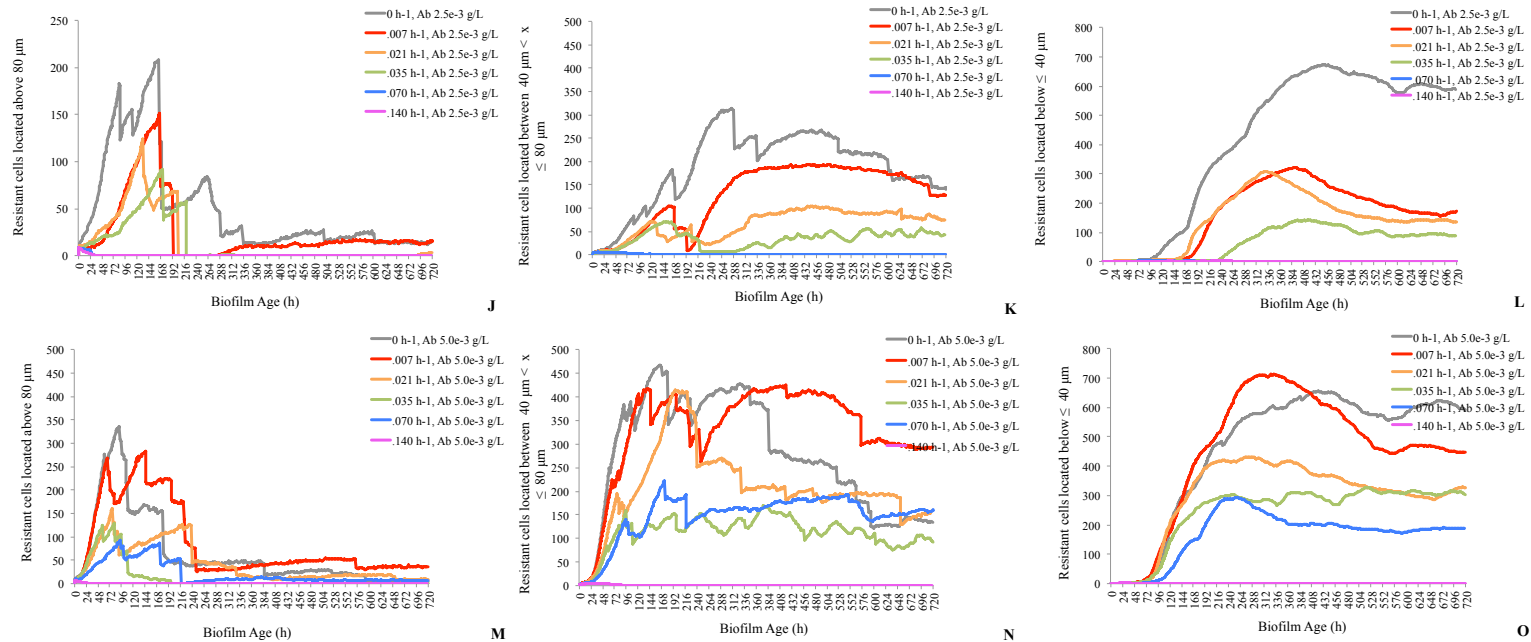
Figures 4.8.2 a-o: The number of resistant cells by location in a biofilm over time, part 2. A 3-day nonresistant biofilm was developed in $10e^{-3}$ $g.L^{-1}$ influent nutrient media. This initial biofilm was then exposed to a constant concentration of $10e^{-3}$ $g.L^{-1}$ resistant soluble DNA and varying antibiotic concentration. Figures a, d, g, j & m display the total resistant cells located above 80 μm in a biofilm exposed to $10e^{-3}$ $g.L^{-1}$ resistant soluble DNA and increasing antibiotic concentration. Figures b, e, h, k & n display the total nonresistant cells located between 40 - 80 μm (40 μm < x ≤ 80 μm) in a biofilm exposed to $10e^{-3}$ $g.L^{-1}$ resistant soluble DNA and increasing antibiotic concentration. Figures c, f, i, l & o display the total cells locates below 40 μm (x ≤ 40 μm) over time in a biofilm exposed to $10e^{-3}$ $g.L^{-1}$ resistant soluble DNA and increasing antibiotic concentration. Within each figure, a-o, cell curves are charted for μ^R values 0 - .140 h^{-1}. All data points are an average of 5 runs, each with a distinct seed value. Standard deviation values were calculated but are not included in the above graphs.

4.6 References

1. Costerton, J. and Z. Lewandowski, *Microbial biofilms*, in *Annual Reviews in ….* 1995.
2. Hall-Stoodley, L., J.W. Costerton, and P. Stoodley, *Bacterial biofilms: from the Natural environment to infectious diseases*, in *Nat Rev Micro*. 2004. p. 95-108.
3. Barkay, T. and B.F. Smets, *Horizontal gene flow in microbial communities*, in *ASM NEWS-AMERICAN SOCIETY FOR MICROBIOLOGY*. 2005, AMERICAN SOCIETY FOR MICROBIOLOGY. p. 412.
4. Thomas, C.M. and K.M. Nielsen, *Mechanisms of, and Barriers to, Horizontal Gene Transfer between Bacteria*, in *Nat Rev Micro*. 2005. p. 711-721.
5. Andersson, D.I. and D. Hughes, *Antibiotic resistance and its cost: is it possible to reverse resistance?*, in *Nat Rev Micro*. 2010, Nature Publishing Group. p. 260-271.
6. Martinez, J.L., *The role of natural environments in the evolution of resistance traits in pathogenic bacteria*, in *Proceedings of the Royal Society B: Biological Sciences*. 2009. p. 2521-2530.
7. Aminov, R.I., *The role of antibiotics and antibiotic resistance in nature*, in *Environ Microbiol*. 2009. p. 2970-2988.
8. Kummerer, K., *Significance of antibiotics in the environment*, in *Journal of Antimicrobial Chemotherapy*. 2003. p. 5-7.
9. Ding, C. and J. He, *Effect of antibiotics in the environment on microbial populations*, in *Appl Microbiol Biotechnol*. 2010. p. 925-941.
10. Andersson, D.I. and D. Hughes, *Persistence of antibiotic resistance in bacterial populations*, in *FEMS Microbiology Reviews*. 2011. p. 901-911.
11. Kang, Y.-S. and W. Park, *Trade-off between antibiotic resistance and biological fitness in Acinetobacter sp. strain DR1*, in *Environ Microbiol*. 2010. p. 1304-1318.
12. Barbosa, T.M. and S.B. Levy, *The impact of antibiotic use on resistance development and persistence.*, in *Drug Resist. Updat.* 2000. p. 303-311.
13. Aminov, R.I. and R.I. Mackie, *Evolution and ecology of antibiotic resistance genes*, in *FEMS Microbiology Letters*. 2007. p. 147-161.
14. Salyers, A.A. and C.F. Amábile-Cuevas, *Why are antibiotic resistance genes so resistant to elimination?*, in *Antimicrobial Agents and Chemotherapy*. 1997. p. 2321-2325.
15. Ferreira da Silva, M., et al., *Antimicrobial resistance patterns in Enterobacteriaceae isolated from an urban wastewater treatment plant*, in *FEMS Microbiology Ecology*. p. 166-176.
16. Jury, K.L., et al., *Antibiotic resistance dissemination and sewage treatment plants*, in *Current Research, Technology and Education Topics in Applied Microbiology and Microbial Biotechnology*. 2010. p. 509-519.
17. Pei, R., et al., *Effect of River Landscape on the sediment concentrations of antibiotics and corresponding antibiotic resistance genes (ARG)*, in *Water Research*. 2006. p. 2427-2435.

18. Heuer, H., H. Schmitt, and K. Smalla, *Antibiotic resistance gene spread due to manure application on agricultural fields.*, in *Current Opinion in Microbiology*. 2011. p. 236-243.

19. D'Costa, V.M., E. Griffiths, and G.D. Wright, *Expanding the soil antibiotic resistome: exploring environmental diversity*, in *Current Opinion in Microbiology*. 2007. p. 481-489.

20. Heuer, H. and K. Smalla, *Manure and sulfadiazine synergistically increased bacterial antibiotic resistance in soil over at least two months.*, in *Environ Microbiol*. 2007. p. 657-666.

21. Guardabassi, L., et al., *Antibiotic resistance in Acinetobacter spp. isolated from sewers receiving waste effluent from a hospital and a pharmaceutical plant.*, in *Applied and Environmental Microbiology*. 1998. p. 3499-3502.

22. Iwane, T., T. Urase, and K. Yamamoto, *Possible impact of treated wastewater discharge on incidence of antibiotic resistant bacteria in river water.*, in *Water Sci. Technol.* 2001. p. 91-99.

23. Park, J.C., et al., *Antibiotic selective pressure for the maintenance of antibiotic resistant genes in coliform bacteria isolated from the aquatic environment.*, in *Water Sci. Technol.* 2003. p. 249-253.

24. Knapp, C.W., et al., *Indirect evidence of transposon-mediated selection of antibiotic resistance genes in aquatic systems at low-level oxytetracycline exposures*, in *Environ. Sci. Technol.* 2008, ACS Publications. p. 5348-5353.

25. van Hoek, A.H.A.M., et al., *Acquired antibiotic resistance genes: an overview.*, in *Front Microbiol*. 2011. p. 203.

26. al., N.e., *Horizontal Gene Transfer: Uptake of Extracellular DNA by Bacteria*, in *Encyclopedia of microbiology*, M. Schaechter, Editor. 2009, Elsevier/Academic Press: Oxford, UK. p. 6 v.

27. Wright, G.D., *The antibiotic resistome: the nexus of chemical and genetic diversity*, in *Nat Rev Micro*. 2007. p. 175-186.

28. Andersson, D.I. and B.R. Levin, *The biological cost of antibiotic resistance.*, in *Current Opinion in Microbiology*. 1999. p. 489-493.

29. Andersson, D.I., *The biological cost of mutational antibiotic resistance: any practical conclusions?*, in *Current Opinion in Microbiology*. 2006. p. 461-465.

30. Björkman, J. and D.I. Andersson, *The cost of antibiotic resistance from a bacterial perspective*, in *Drug Resistance Updates*. 2000. p. 237-245.

31. Guo, B., et al., *Predicting bacterial fitness cost associated with drug resistance*, in *Journal of Antimicrobial Chemotherapy*. 2012. p. 928-932.

32. Martínez, J.L. and F. Rojo, *Metabolic regulation of antibiotic resistance*, in *FEMS Microbiology Reviews*. 2011. p. 768-789.

33. Starikova, I., et al., *Fitness costs of various mobile genetic elements in Enterococcus faecium and Enterococcus faecalis*, in *Journal of Antimicrobial Chemotherapy*. 2013. p. 2755-2765.

34. Angst, D.C. and A.R. Hall, *The cost of antibiotic resistance depends on evolutionary history in Escherichia coli*, in *BMC Evolutionary Biology*. 2013, BMC Evolutionary Biology. p. 1-1.

35. Starikova, I., et al., *A Trade-off between the Fitness Cost of Functional Integrases and Long-term Stability of Integrons*, in *PLoS Pathog*. 2012. p. e1003043.

36. Lee, S.W. and G. Edlin, *Expression of tetracycline resistance in pBR322 derivatives reduces the reproductive fitness of plasmid-containing Escherichia coli.*, in *Gene*. 1985. p. 173-180.

37. Sander, P., et al., *Fitness Cost of Chromosomal Drug Resistance-Conferring Mutations*, in *Antimicrobial Agents and Chemotherapy*. 2002. p. 1204-1211.

38. Bannister, B.A., S.H. Gillespie, and J. Jones, *Infection: microbiology and management*. Order title:Infection : microbiology and management. 2006, Malden, Mass. ; Oxford: Blackwell Pub. vii, 544 p.

39. Williams, H.G., et al., *Natural transformation in river epilithon.*, in *Applied and Environmental Microbiology*. 1996. p. 2994-2998.

40. Merkey, B.V., et al., *Growth dependence of conjugation explains limited plasmid invasion in biofilms: an individual-based modelling study*, in *Environ Microbiol*. 2011. p. 2435-2452.

41. Stewart, F.M. and B.R. Levin, *The Population Biology of Bacterial Plasmids: A PRIORI Conditions for the Existence of Conjugationally Transmitted Factors.*, in *Genetics*. 1977. p. 209-228.

42. Levin, B.R., F.M. Stewart, and V.A. Rice, *The kinetics of conjugative plasmid transmission: fit of a simple mass action model*, in *Plasmid*. 1979, Elsevier. p. 247-260.

43. Knudsen, G.R., et al., *Predictive model of conjugative plasmid transfer in the rhizosphere and phyllosphere.*, in *Applied and Environmental Microbiology*. 1988. p. 343-347.

44. Clewlow, L.J., N. Cresswell, and E.M. Wellington, *Mathematical Model of Plasmid Transfer between Strains of Streptomycetes in Soil Microcosms.*, in *Applied and Environmental Microbiology*. 1990. p. 3139-3145.

45. Simonsen, L., et al., *Estimating the rate of plasmid transfer: an end-point method.*, in *J. Gen. Microbiol.* 1990. p. 2319-2325.

46. Andrup, L. and K. Andersen, *A comparison of the kinetics of plasmid transfer in the conjugation systems encoded by the F plasmid from Escherichia coli and plasmid pCF10 from Enterococcus faecalis*, in *Microbiology (Reading, Engl.)*. 1999, Soc General Microbiol. p. 2001-2009.

47. Andrup, L., et al., *Kinetics of conjugative transfer: a study of the plasmid pXO16 from Bacillus thuringiensis subsp. israelensis.*, in *Plasmid*. 1998. p. 30-43.

48. Lardon, L.A., et al., *iDynoMiCS: next-generation individual-based modelling of biofilms*, in *Environ Microbiol*. 2011. p. no-no.

49. Juni, E., *Genetics and physiology of Acinetobacter*, in *Annual Reviews in Microbiology*. 1978.

50. Juni, E., *Interspecies transformation of Acinetobacter: genetic evidence for a ubiquitous genus.*, in *J. Bacteriol.* 1972. p. 917-931.

51. Hendrickx, L., M. Hausner, and S. Wuertz, *Natural genetic transformation in monoculture Acinetobacter sp. strain BD413 biofilms.*, in *Applied and Environmental Microbiology*. 2003. p. 1721-1727.

52. Momba, M., et al., *An overview of biofilm formation in distribution systems and its impact on the deterioration of water quality*. 2000, Water Reseach Council.

53. Palmen, R., et al., *Physiological characterization of natural transformation in Acinetobacter calcoaceticus.*, in *J. Gen. Microbiol.* 1993. p. 295-305.

54. Palmen, R. and K.J. Hellingwerf, *Acinetobacter calcoaceticus liberates chromosomal DNA during induction of competence by cell lysis.*, in *Curr. Microbiol.* 1995. p. 7-10.

55. Zhang, Y., et al., *Wastewater treatment contributes to selective increase of antibiotic resistance among Acinetobacter spp.*, in *Science of the Total Environment, The.* 2009, Elsevier B.V. p. 3702-3706.

56. Grimm, V., et al., *A standard protocol for describing individual-based and agent-based models*, in *Ecological Modelling.* 2006. p. 115-126.

57. Picioreanu, C., M.v. Loosdrecht, and J.J. Heijnen, *Discrete-differential modelling of biofilm structure*, in *Water Sci. Technol.* 1999, Elsevier. p. 115-122.

58. Barbe, V., et al., *Unique features revealed by the genome sequence of Acinetobacter sp. ADP1, a versatile and naturally transformation competent bacterium.*, in *Nucleic Acids Res.* 2004. p. 5766-5779.

59. Allesen-Holm, M., et al., *A characterization of DNA release in Pseudomonas aeruginosa cultures and biofilms.*, in *Molecular Microbiology.* 2006. p. 1114-1128.

60. Noguera, D.R. and C. Picioreanu, *Results from the multi-species benchmark problem 3 (BM3) using two-dimensional models.*, in *Water Sci. Technol.* 2004. p. 169-176.

61. Rittmann, B.E., et al., *Results from the multi-species benchmark problem (BM3) using one-dimensional models.*, in *Water Sci. Technol.* 2004. p. 163-168.

62. Dockery, J. and I. Klapper, *Finger formation in biofilm layers*, in *SIAM Journal on Applied Mathematics.* 2001, SIAM. p. 853-869.

63. Stewart, P.S. and M.J. Franklin, *Physiological heterogeneity in biofilms*, in *Nat Rev Micro.* 2008. p. 199-210.

64. Bayles, K.W., *The biological role of death and lysis in biofilm development.*, in *Nat Rev Micro.* 2007. p. 721-726.

65. Kim, J., et al., *Tolerance of dormant and active cells in Pseudomonas aeruginosa PA01 biofilm to antimicrobial agents.*, in *Journal of Antimicrobial Chemotherapy.* 2009. p. 129-135.

66. Wu, J. and C. Xi, *Evaluation of Different Methods for Extracting Extracellular DNA from the Biofilm Matrix*, in *Applied and Environmental Microbiology.* 2009. p. 5390-5395.

67. Lorenz, M.G. and W. Wackernagel, *Bacterial gene transfer by natural genetic transformation in the environment.*, in *Microbiol. Rev.* 1994. p. 563-602.

68. Elliott, K.T. and E.L. Neidle, *Acinetobacter baylyi ADP1: Transforming the choice of model organism*, in *IUBMB Life.* 2011. p. 1075-1080.

69. Hülter, N. and W. Wackernagel, *Double illegitimate recombination events integrate DNA segments through two different mechanisms during natural transformation of Acinetobacter baylyi.*, in *Molecular Microbiology.* 2008. p. 984-995.

70. de Vries, J. and W. Wackernagel, *Integration of foreign DNA during natural transformation of Acinetobacter sp. by homology-facilitated illegitimate recombination.*, in *Proc. Natl. Acad. Sci. U.S.A.* 2002. p. 2094-2099.

71. Young, D.M. and L.N. Ornston, *Functions of the mismatch repair gene mutS from Acinetobacter sp. strain ADP1.*, in *J. Bacteriol.* 2001. p. 6822-6831.

72. Nielsen, K.M., K. Smalla, and J.D. van Elsas, *Natural transformation of Acinetobacter sp. strain BD413 with cell lysates of Acinetobacter sp., Pseudomonas fluorescens, and Burkholderia cepacia in soil microcosms.*, in *Applied and Environmental Microbiology*. 2000. p. 206-212.

73. Juni, E. and A. Janik, *Transformation of Acinetobacter calco-aceticus (Bacterium anitratum).* in *J. Bacteriol.* 1969. p. 281-288.

74. Watson, S.K. and P.E. Carter, *Environmental influences on Acinetobacter sp. strain BD413 transformation in soil*, in *Biology and Fertility of Soils*. 2008, Springer. p. 83-92.

75. Chamier, B., M.G. Lorenz, and W. Wackernagel, *Natural Transformation of Acinetobacter calcoaceticus by Plasmid DNA Adsorbed on Sand and Groundwater Aquifer Material.*, in *Applied and Environmental Microbiology*. 1993. p. 1662-1667.

76. Molin, S. and T. Tolker-Nielsen, *Gene transfer occurs with enhanced efficiency in biofilms and induces enhanced stabilisation of the biofilm structure*, in *Current Opinion in Biotechnology*. 2003. p. 255-261.

77. Glick, B.R., *Metabolic load and heterologous gene expression*, in *Biotechnology advances*. 1995, Elsevier. p. 247-261.

78. Sun, Z., et al., *Antibiotic Resistance in Pseudomonas Aeruginosais Associated with Decreased Fitness*, in *Cell Physiol Biochem*. 2013. p. 347-354.

79. Seoane, J., et al., *A new extant respirometric assay to estimate intrinsic growth parameters applied to study plasmid metabolic burden*, in *Biotechnol. Bioeng.* 2010. p. 141-149.

80. Martinez, J.L. and F. Baquero, *Minireview: Mutation Frequencies and Antibiotic Resistance*, in *Antimicrobial Agents and Chemotherapy*. 2000. p. 1771-1777.

81. Kohanski, M.A., D.J. Dwyer, and J.J. Collins, *How antibiotics kill bacteria: from targets to networks*, in *Nat Rev Micro*. 2010, Nature Publishing Group. p. 423-435.

82. Szomolay, B., et al., *Adaptive responses to antimicrobial agents in biofilms*, in *Environ Microbiol*. 2005. p. 1186-1191.

83. Chambless, J.D., S.M. Hunt, and P.S. Stewart, *A three-dimensional computer model of four hypothetical mechanisms protecting biofilms from antimicrobials.*, in *Applied and Environmental Microbiology*. 2006. p. 2005-2013.

84. Hunt, S.M., M.A. Hamilton, and P.S. Stewart, *A 3D model of antimicrobial action on biofilms*, in *Water Science & Technology*. 2005. p. 143-148.

85. COGAN, N., R. CORTEZ, and L. FAUCI, *Modeling physiological resistance in bacterial biofilms*, in *Bulletin of Mathematical Biology*. 2005. p. 831-853.

86. Roberts, M.E. and P.S. Stewart, *Modeling antibiotic tolerance in biofilms by accounting for nutrient limitation.*, in *Antimicrobial Agents and Chemotherapy*. 2004. p. 48-52.

87. Walters, M.C., et al., *Contributions of Antibiotic Penetration, Oxygen Limitation, and Low Metabolic Activity to Tolerance of Pseudomonas aeruginosa Biofilms to Ciprofloxacin and Tobramycin*, in *Antimicrobial Agents and Chemotherapy*. 2003. p. 317-323.

88. Stewart, P.S., *Theoretical aspects of antibiotic diffusion into microbial biofilms.*, in *Antimicrobial Agents and Chemotherapy*. 1996. p. 2517-2522.

89. Stewart, P.S., *Biofilm accumulation model that predicts antibiotic resistance of Pseudomonas aeruginosa biofilms.*, in *Antimicrobial Agents and Chemotherapy*. 1994. p. 1052-1058.

90. Roberts, M.E., *Modelling protection from antimicrobial agents in biofilms through the formation of persister cells*, in *Microbiology*. 2005. p. 75-80.

91. Dodds, M.G., K.J. Grobe, and P.S. Stewart, *Modeling biofilm antimicrobial resistance.*, in *Biotechnol. Bioeng.* 2000. p. 456-465.

92. Brooun, A., S. Liu, and K. Lewis, *A dose-response study of antibiotic resistance inPseudomonas aeruginosa biofilms*, in *Antimicrobial Agents and Chemotherapy*. 2000, Am Soc Microbiol. p. 640-646.

93. Palmen, R., P. Buijsman, and K.J. Hellingwerf, *Physiological regulation of competence induction for natural transformation in Acinetobacter calcoaceticus*, in *Archives of Microbiology*. 1994, Springer. p. 344-351.

94. Martínez, J.L. and F. Baquero, *Interactions among strategies associated with bacterial infection: pathogenicity, epidemicity, and antibiotic resistance*, in *Clin. Microbiol. Rev.* 2002, Am Soc Microbiol. p. 647-679.

95. Wright, G.D., *Antibiotic resistance in the environment: a link to the clinic?*, in *Current Opinion in Microbiology*. 2010, Elsevier Ltd. p. 589-594.

96. Cantón, R., *Antibiotic resistance genes from the environment: a perspective through newly identified antibiotic resistance mechanisms in the clinical setting*, in *Clin Microbiol Infect*. 2009. p. 20-25.

97. Josephson, J., *The Microbial "Resistome"*, in *Environ. Sci. Technol.* 2006. p. 6531-6534.

98. Martínez, J.L., F. Baquero, and D.I. Andersson, *Predicting antibiotic resistance*, in *Nat Rev Micro*. 2007, Nature Publishing Group. p. 958-965.

99. Finland, M., *Emergence of antibiotic resistance in hospitals, 1935-1975.*, in *Rev. Infect. Dis.* 1979. p. 4-22.

100. Davies, J. and D. Davies, *Origins and evolution of antibiotic resistance.*, in *Microbiol. Mol. Biol. Rev.* 2010. p. 417-433.

101. Cookson, B., *Clinical significance of emergence of bacterial antimicrobial resistance in the hospital environment.*, in *J. Appl. Microbiol.* 2005. p. 989-996.

102. Hawkey, P.M., *The growing burden of antimicrobial resistance*, in *Journal of Antimicrobial Chemotherapy*. 2008. p. i1-i9.

103. Graffunder, E.M., et al., *Risk factors associated with extended-spectrum beta-lactamase-producing organisms at a tertiary care hospital.*, in *J. Antimicrob. Chemother.* 2005. p. 139-145.

104. Lautenbach, E., et al., *Imipenem resistance among pseudomonas aeruginosa isolates: risk factors for infection and impact of resistance on clinical and economic outcomes.*, in *Infect Control Hosp Epidemiol*. 2006. p. 893-900.

105. Martínez, J.A., et al., *Prior use of carbapenems may be a significant risk factor for extended-spectrum beta-lactamase-producing Escherichia coli or Klebsiella spp. in patients with bacteraemia.*, in *J. Antimicrob. Chemother*. 2006. p. 1082-1085.

106. Kolar, M., K. Urbaneck, and T. Latal, *Antibiotic selective pressure and development of bacterial resistance.*, in *International Journal of Antimicrobial Agents*. 2001. p. 357-363.

107. Levin, B.R., *Models for the spread of resistant pathogens.*, in *Neth J Med*. 2002. p. 58-64; discussion 64-6.

108. Austin, D.J., K.G. Kristinsson, and R.M. Anderson, *The relationship between the volume of antimicrobial consumption in human communities and the frequency of resistance.*, in *Proc. Natl. Acad. Sci. U.S.A.* 1999. p. 1152-1156.

109. Hellweger, F., X. Ruan, and S. Sanchez, *A Simple Model of Tetracycline Antibiotic Resistance in the Aquatic Environment (with Application to the Poudre River)*, in *IJERPH*. 2011. p. 480-497.

110. Chen, I. and D. Dubnau, *DNA uptake during bacterial transformation.*, in *Nat Rev Micro*. 2004. p. 241-249.

111. Porstendörfer, D., U. Drotschmann, and B. Averhoff, *A novel competence gene, comP, is essential for natural transformation of Acinetobacter sp. strain BD413.*, in *Applied and Environmental Microbiology*. 1997. p. 4150-4157.

Supplemental Table 1: Computational grid size & corresponding total cell count post 72 h biofilm growth

Grid Domain Size (height, width)[1]	# bacteria agents at 0hr.[2]	# bacteria agents at 72hr.[3]	Computation time (min.)
33, 33	10	3206	6.8
33, 65	10	5342	12.1
33, 129	10	10812	29.7
33, 257	10	19004	58.1
33, 513	10	37089	134.7
33, 1025	10	53519	248.8
33, 2049	10	error*	N/A
33, 4097	10	error*	N/A
33, 8193	10	error*	N/A
33, 16385	10	error*	N/A
33, 33	100	3523	7.2
33, 65	100	6743	15.2
33, 129	100	12830	31.8
33, 257	100	24702	73.9
33, 513	100	45901	165.7
33, 1025	100	85827	392.9
33, 1025	500	98095	357.04
33, 1025	600	99798	349.9
33, 2049	100	error*	N/A
33, 4097	100	error*	N/A
33, 8193	100	error*	N/A
33, 16385	100	error*	N/A

The computational grid is a 2D grid defined by height and width. The algorithm used to solve for solute concentration fields requires that the height and width measurements be a power of two plus one. (Lardon et al. 2011)[1]

The number of bacteria agents present at initialization is set in the XML document.[2]

Nonresistant biofilms were grown for 72 hr.[3]

Simulation Run ID	COD_{in} (g.L^{-1}) Influent nutrient media concentration	Constant bulk concentration	μ_{NR} (h^{-1}) Maintenance rate of bacteria	μ^G_{max} (h-1) Maximal bacteria growth rate	κ_{Det} (µm.h)$^{-1}$ Erosion rate	max_{Th} (µm) Biofilm max thickness
A1	0.01	TRUE	0.133	0.7	5.00E-06	100
A2	0.01	FALSE	0.133	0.7	5.00E-06	100
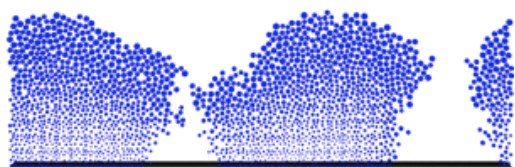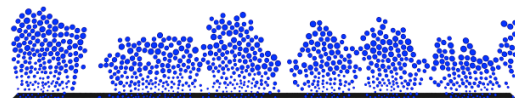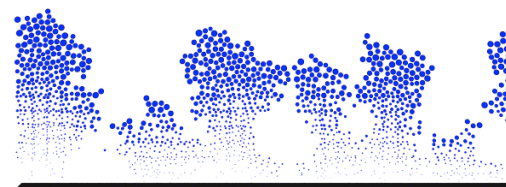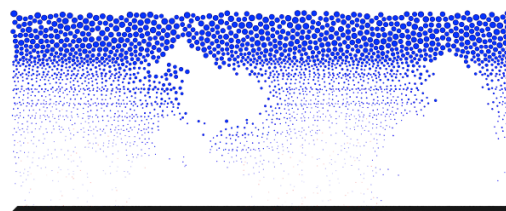
24 hr. Biofilm   48 hr. Biofilm   72 hr. Biofilm
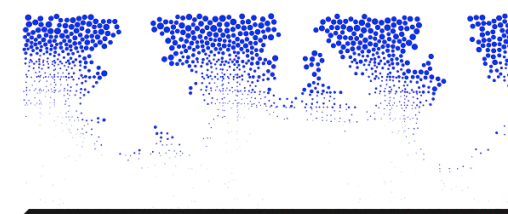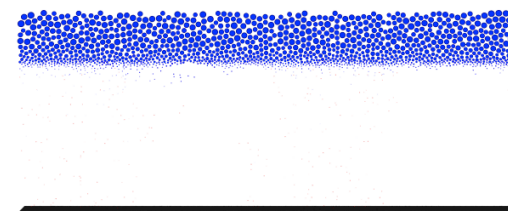
Supplemental **Figure 1a: Effect of changing constant bulk concentration settings.** The constant bulk concentration settings can be modified to set whether the concentration of the bulk fluid is assumed to be constant (TRUE) or is affected by the mass balance between the reactions occurring in the biofilm and the influent media feed (FALSE). The settings for simulation A1 are listed in the text box and simulation images for the 24, 48 & 72 hr. biofilms are listed below. This layout is repeated for simulation A2. The one difference between the two simulations is the constant bulk concentration setting and the difference is highlighted accordingly.

Simulation Run ID	CODin (g.L⁻¹) Influent nutrient media concentration	Constant bulk concentration	μNR (h⁻¹) Maintenance rate of bacteria	μGmax (h-1) Maximal bacteria growth rate	κDet (μm.h)⁻¹ Erosion rate	maxTh (μm) Biofilm max thickness
A2	0.01	FALSE	0.133	0.7	5.00E-06	100
A3	0.01	FALSE	0.0133	0.7	5.00E-06	100

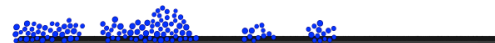24 hr. Biofilm   48 hr. Biofilm   72 hr. Biofilm

A2

A3
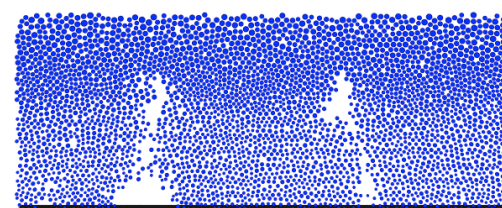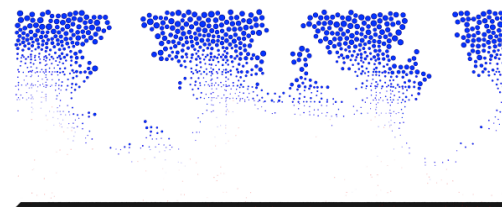
Supplemental **Figure 1b: Effect of changing the maintenance rate of bacteria (μNR).** Every reaction in idynomics is described by a μmax, which is the maximum rate of a reaction (in units of hr⁻¹). The settings for simulation A2 are listed in the text box and simulation images for the 24, 48 & 72 hr. biofilms are listed below. This layout is repeated for simulation A3. The one difference between the two simulations is the maintenance reaction μmax and the difference is highlighted accordingly. In simulation A3, μNR has been decreased by 10-fold compared to the same parameter setting in simulation A2.

Simulation Run ID	COD$_{in}$ (g.L^{-1}) Influent nutrient media concentration	Constant bulk concentration	μ_{NR} (h^{-1}) Maintenance rate of bacteria	μ^{G}_{max} (h-1) Maximal bacterial growth rate	κ_{Det} (µm.h)$^{-1}$ Erosion rate	max$_{Th}$ (µm) Biofilm max thickness
A3	0.01	FALSE	0.0133	0.7	5.00E-06	100
A4	0.01	FALSE	0.0133	0.07	5.00E-06	100

24 hr. Biofilm   48 hr. Biofilm   72 hr. Biofilm

A3

A4
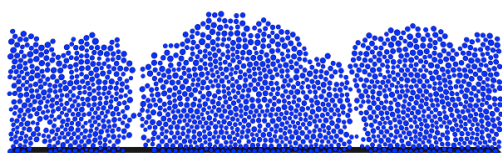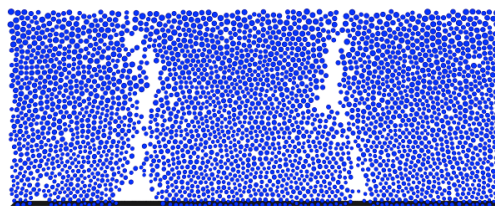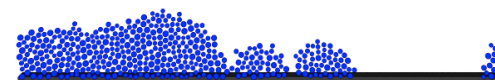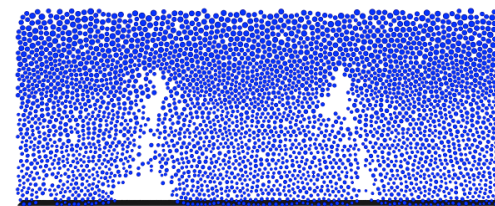
***Supplemental* Figure 1c: Effect of changing the maximal bacterial growth rate (μ^{G}_{max}).** Every reaction in idynomics is described by a μ_{max}, which is the maximum rate of a reaction (in units of hr^{-1}). The settings for simulation A3 are listed in the text box and simulation images for the 24, 48 & 72 hr. biofilms are listed below. This layout is repeated for simulation A4. The one difference between the two simulations is the growth reaction μ_{max} and the difference is highlighted accordingly. In simulation A4, the growth reaction μ^{G}_{max} has been decreased by 10-fold compared to the same parameter setting in simulation A3.
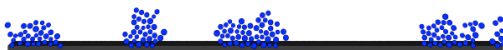
Simulation Run ID	COD_{in} (g.L^{-1}) Influent nutrient media concentration	Constant bulk concentration	μ_{NR} (h^{-1}) Maintenance rate of bacteria	μ^{G}_{max} (h-1) Maximal bacteria growth rate	κ_{Det} (μm.h)$^{-1}$ Erosion rate	max_{Th} (μm) Biofilm max thickness
A3	0.01	FALSE	0.0133	0.7	5.00E-06	100
A5	0.001	FALSE	0.0133	0.7	5.00E-06	100

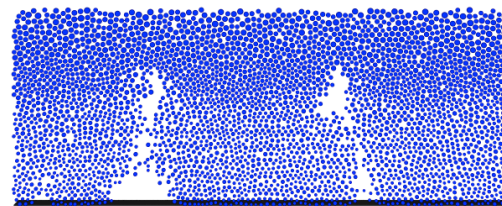24 hr. Biofilm   48 hr. Biofilm   72 hr. Biofilm

A3

A5
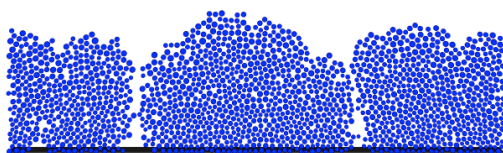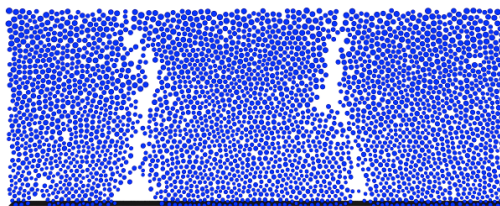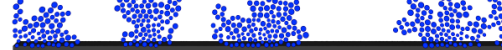
Supplemental **Figure 1d: Effect of changing the influent nutrient media concentration (COD$_{in}$)**. Influent media concentration can affect biofilm growth. The settings for simulation A3 are listed in the text box and simulation images for the 24, 48 & 72 hr. biofilms are listed below. This layout is repeated for simulation A5. The one difference between the two simulations is the media concentration and the difference is highlighted accordingly. In simulation A5, the COD$_{in}$ has been decreased by 10-fold compared to the same parameter setting in simulation A3.
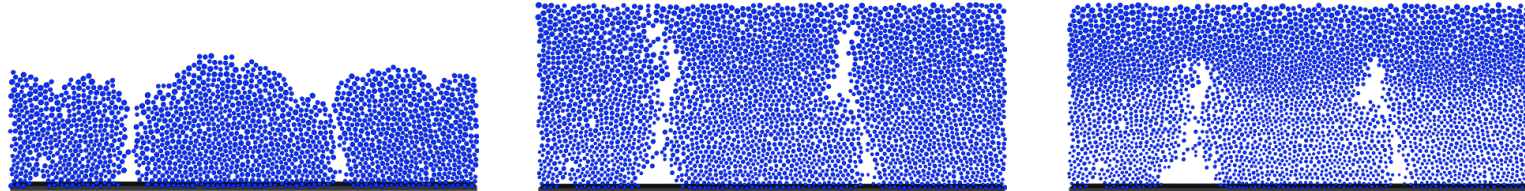
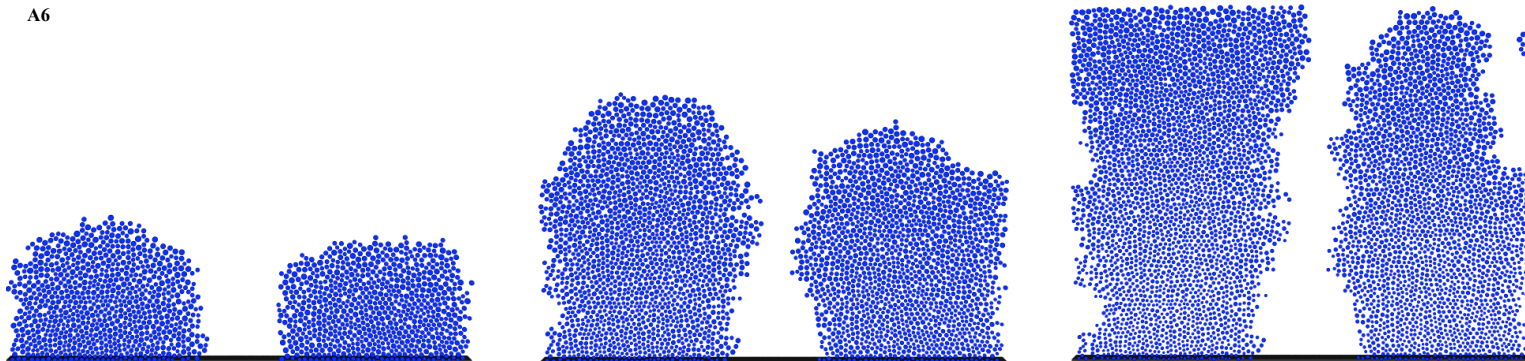| Simulation Run ID	COD_{in} (g.L^{-1}) Influent nutrient media concentration	Constant bulk concentration	μ_{NR} (h^{-1}) Maintenance rate of bacteria	μ^G_{max} (h-1) Maximal bacteria growth rate	κ_{Det} (μm.h)$^{-1}$ Erosion rate	max_{Th} (μm) Biofilm max thickness
A3	0.01	FALSE	0.0133	0.7	5.00E-06	100
A6	0.01	FALSE	0.0133	0.7	5.00E-06	200

24 hr. Biofilm 48 hr. Biofilm 72 hr. Biofilm

A3

A6

***Supplemental* Figure 1e: Effect of changing the biofilm max thickness (max$_{TH}$).** The maximum thickness of the biofilm can be set to ensure that the full biofilm region remains in the computational domain rather than being artificially cut-off. The settings for simulation A3 are listed in the text box and simulation images for the 24, 48 & 72 hr. biofilms are listed below. This layout is repeated for simulation A6. The one difference between the two simulations is the maximum thickness of the biofilm and the difference is highlighted accordingly. The max$_{th}$ of biofilm in simulation A6 is 100 μm more than that of the biofilm in simulation A3.

Simulation Run ID	COD_{in} (g.L^{-1}) Influent nutrient media concentration	Constant bulk concentration	μ_{NR} (h^{-1}) Maintenance rate of bacteria	μ^G_{max} (h-1) Maximal bacteria growth rate	κ_{Det} (μm.h)$^{-1}$ Erosion rate	max_{Th} (μm) Biofilm max thickness
A6	0.01	FALSE	0.0133	0.7	5.00E-06	200
A7	0.01	FALSE	0.0133	0.7	5.00E-05	200
A8	0.01	FALSE	0.0133	0.7	5.00E-04	200

24 hr. Biofilm   48 hr. Biofilm   72 hr. Biofilm

A6

A7

A8
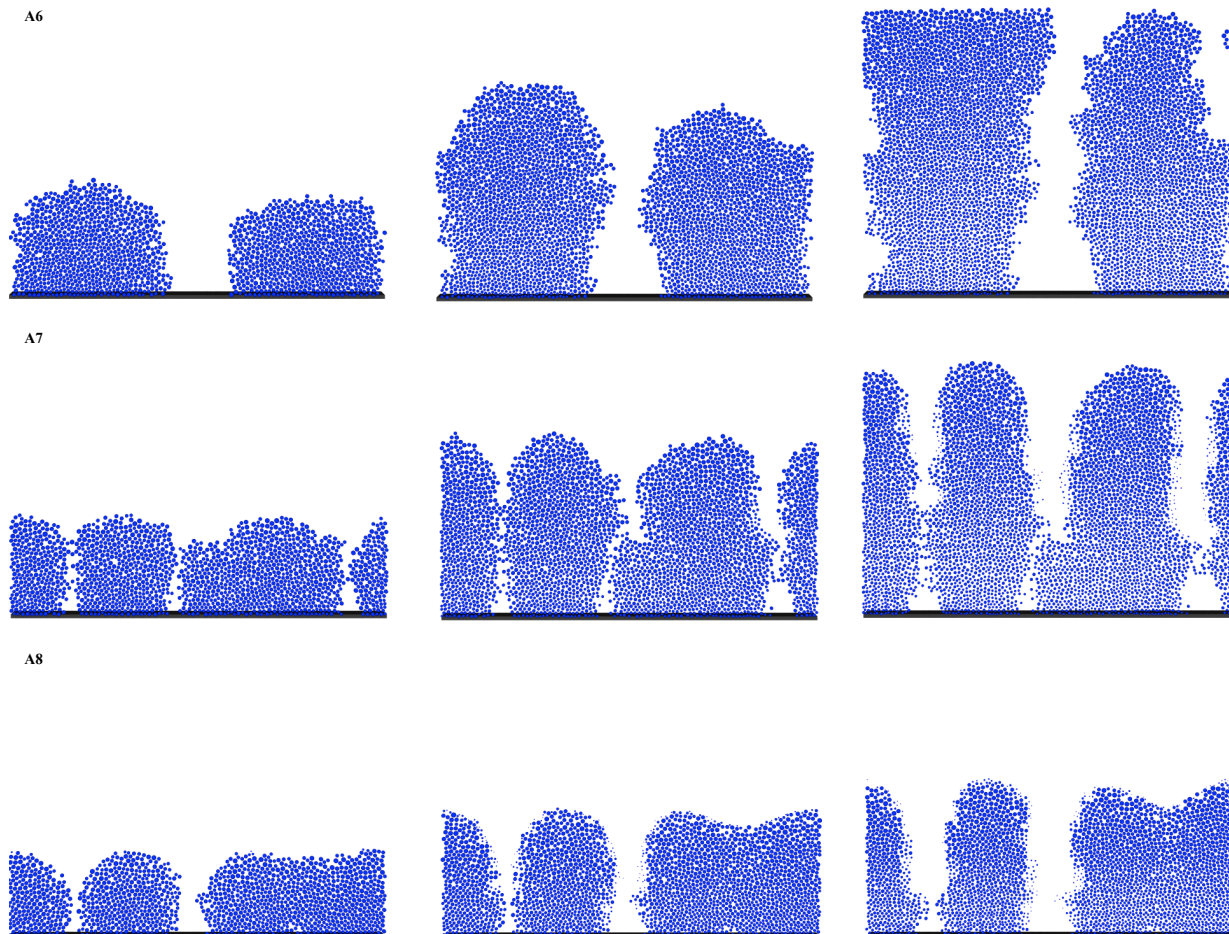
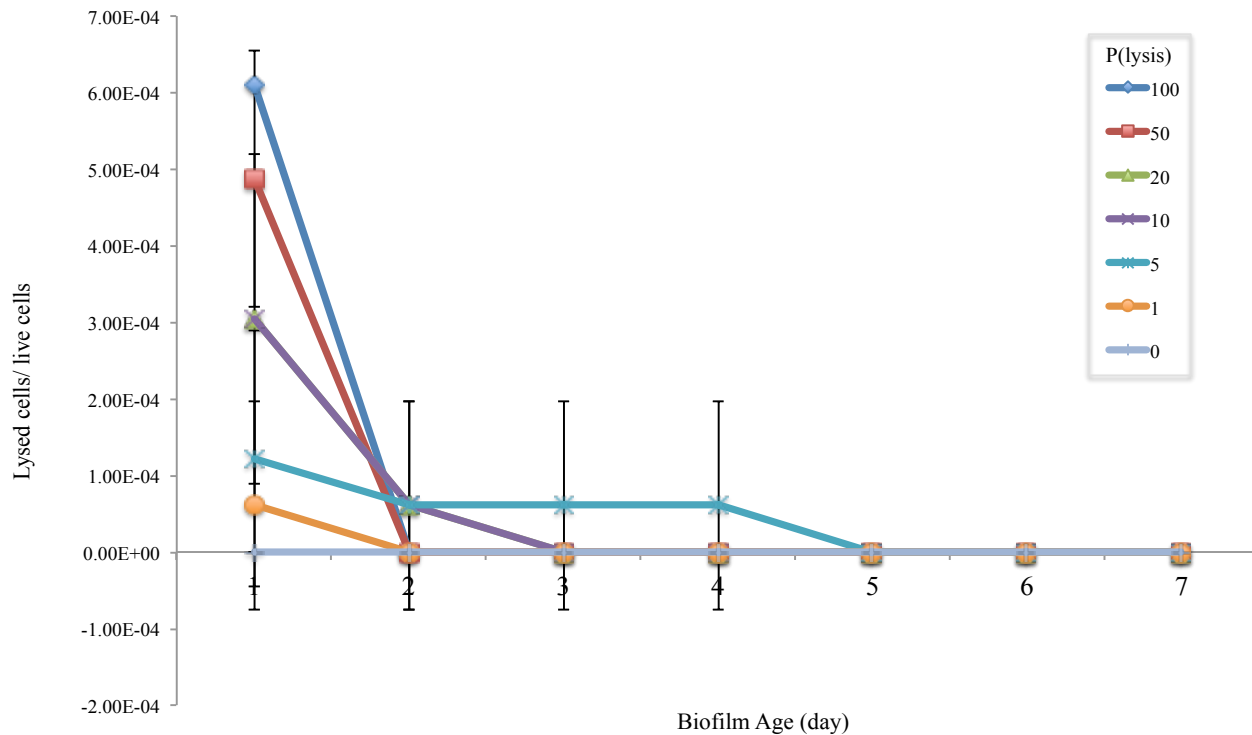*Supplemental* **Figure 1f.**: **Effect of changing erosion rate (κ_{Det}).** Varying the erosion rate can affect the overall biofilm structure. The erosion strength is the erosion rate times the square of the local biofilm height. For the purposes of our simulations, once cells detach from the biofilm they are no longer accounted for/disappear from the simulation 'world.' The settings for simulation A6 are listed in the text box and simulation images for the 24, 48 & 72 hr. biofilms are listed below. This layout is repeated for simulations A7 & A8. The one difference between the three simulations is the erosion rate and this difference is highlighted accordingly. The κ_{Det} value progressively increases by 10-fold from simulation A6 to simulation A8.
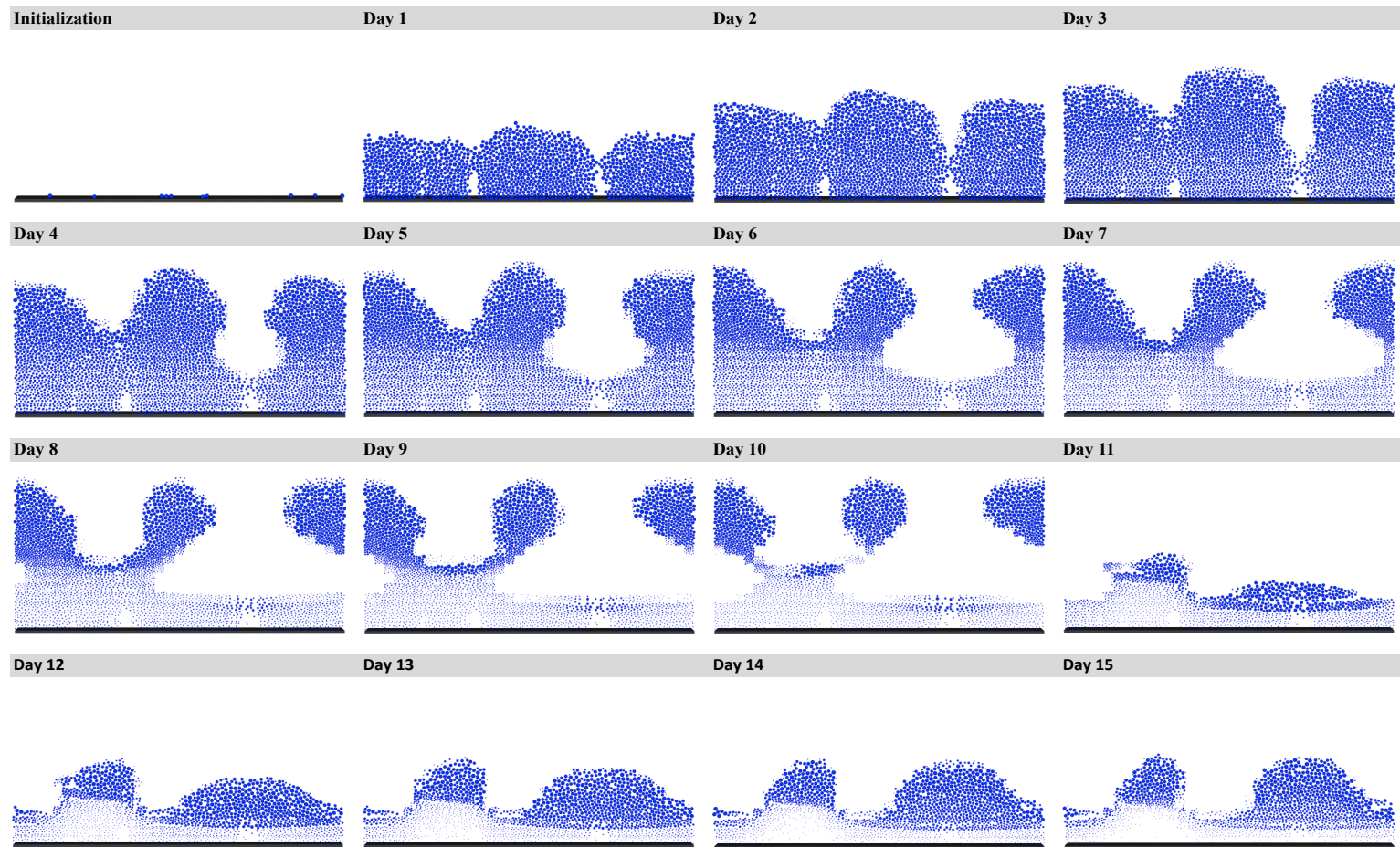
***Supplemental* Figure 2: Long-term growth of a single species biofilm.** Long-term growth of a single species biofilm under going growth and maintenance is displayed above. The model world was initialized with 10 non-resistant bacteria agents and with the following environmental parameter settings: influent nutrient media concentration (COD_{in}) $10e^{-3}$ g.L^{-1}, erosion rate (κ_{Det}) $5e^{-4}$ (um.hr)$^{-1}$, maximal bacteria growth rate (μ^G_{max}) .7 hr^{-1}, maintenance rate of bacteria (μ_{NR}) .0133 hr^{-1} and probability of lysis (P(lysis)) 1%.
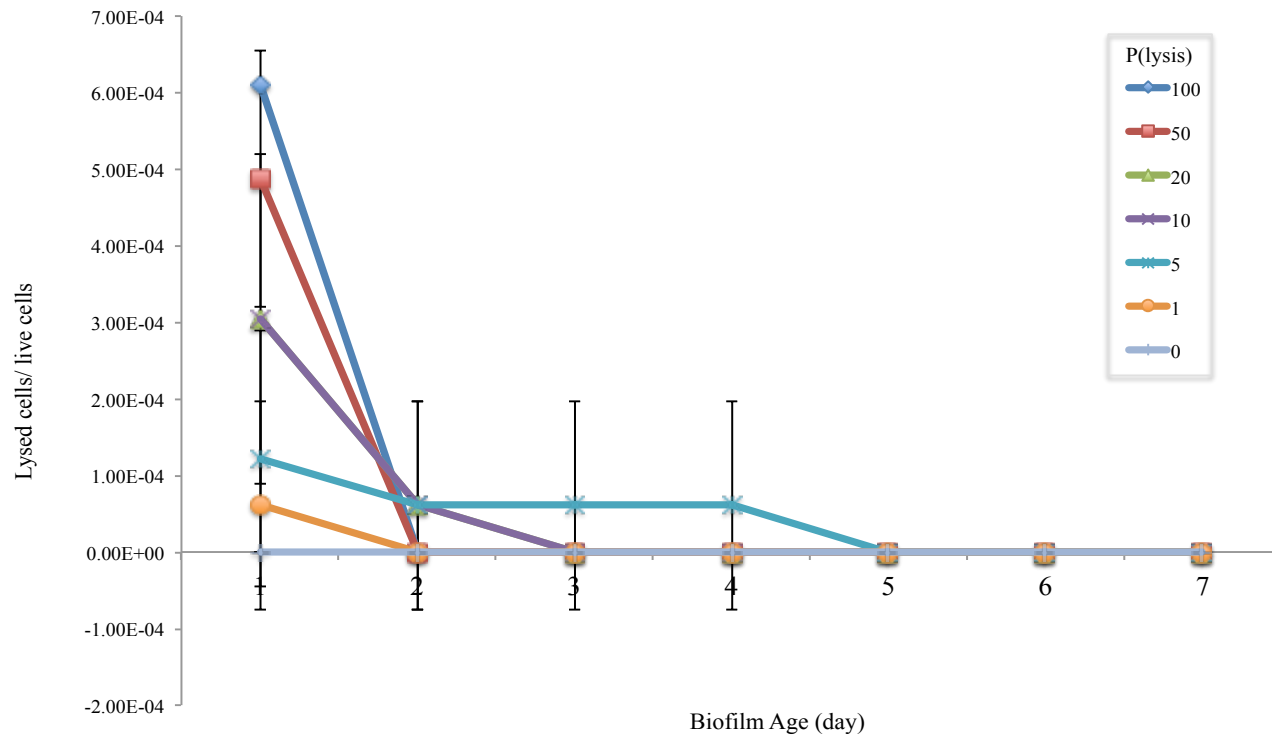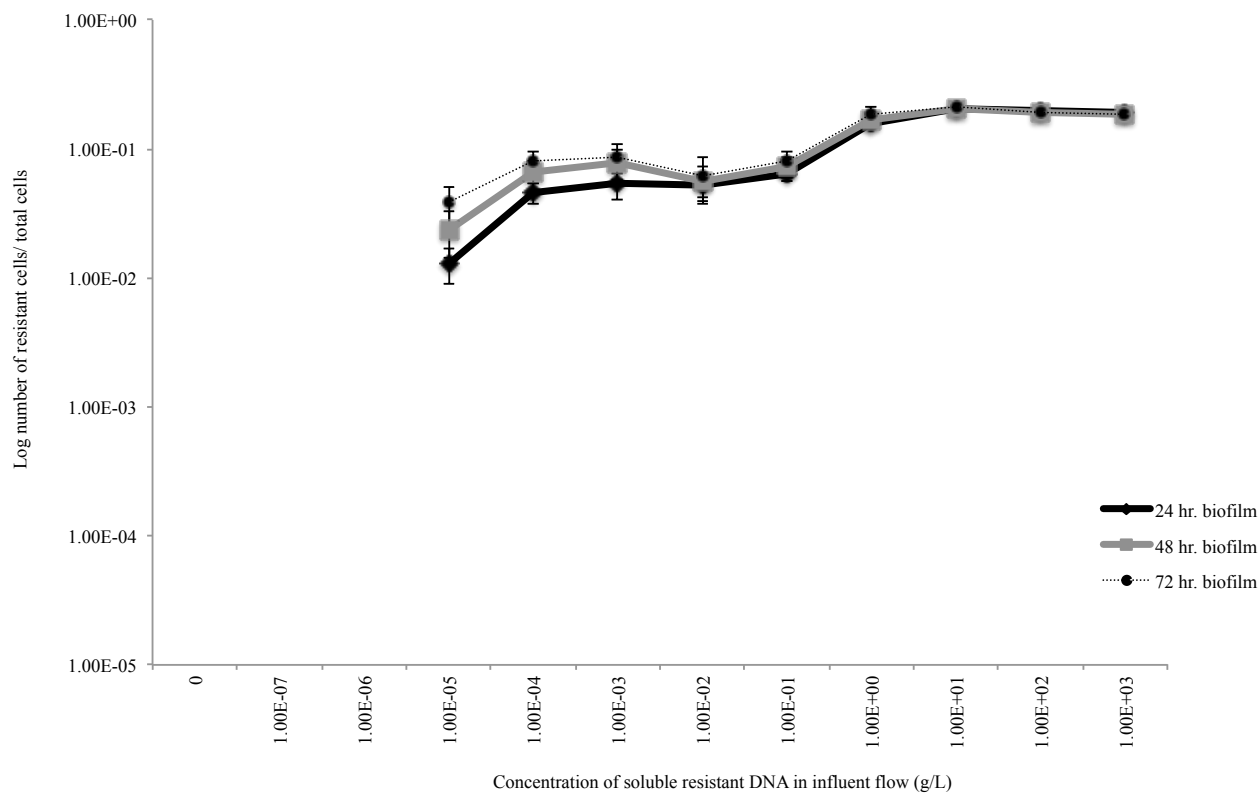
***Supplemental* Figure 3a: Effect of changing the probability of lysis [P(lysis)] in a biofilm not undergoing growth and maintenance functions.** Cells that approach the death radius due to starvation have a certain probability of lysis [P(lysis)]. Those cells that lyse produce DNA that is solubilized to become soluble DNA and those cells that do not lyse, stay as dormant cells. The graph above looks at the effect of changing the P(lysis) on the ratio of lysed cells/ live cells in a static biofilm. An initial single species, non-resistant biofilm was grown for 3 days. This initial biofilm structure was then used as the starting point for the experimental simulation data graphed above. For all experimental simulations, growth and maintenance functions were turned off to produce a static biofilm structure. In addition detachment rate (κ_{Det}) was set to 0 um^{-1}hr^{-1}. A set of 5 simulations were run for each P(lysis) value graphed above with varying seed values. The ratio of lysed cells/ live cells was averaged across these 5 simulations. Standard deviations were calculated and are included on the graph above as well.

***Supplemental* Figure 3b: Effect of changing the probability of lysis [P(lysis)] on the lysed cells to live cells ratio in a biofilm undergoing growth and maintenance functions.** Cells that approach the death radius due to starvation have a certain probability of lysis [P(lysis)]. Those cells that lyse produce DNA that is solubilized to become soluble DNA and those cells that do not lyse, stay as dormant cells. The graph above looks at the effect of changing the P(lysis) on the ratio of lysed cells/ live cells in a biofilm undergoing growth and maintenance functions. An initial single species, non-resistant biofilm was grown for 3 days. This initial biofilm structure was then used as the starting point for the experimental simulation data graphed above. All subsequent experimental simulations were run on a biofilm that was undergoing growth and maintenance functions with an influent media concentration (COD_{in}) of $10e^{-3}$ $g.L^{-1}$ in the influent flow. In addition, the detachment rate (κ_{Det}) was set to $5e^{-4}$ $um^{-1}hr^{-1}$. A set of 5 simulations were run for each probability of lysis value graphed above with varying seed values. The ratio of lysed cells/ live cells was averaged across these 5 simulations. Standard deviations were calculated and are included on the graph above as well.
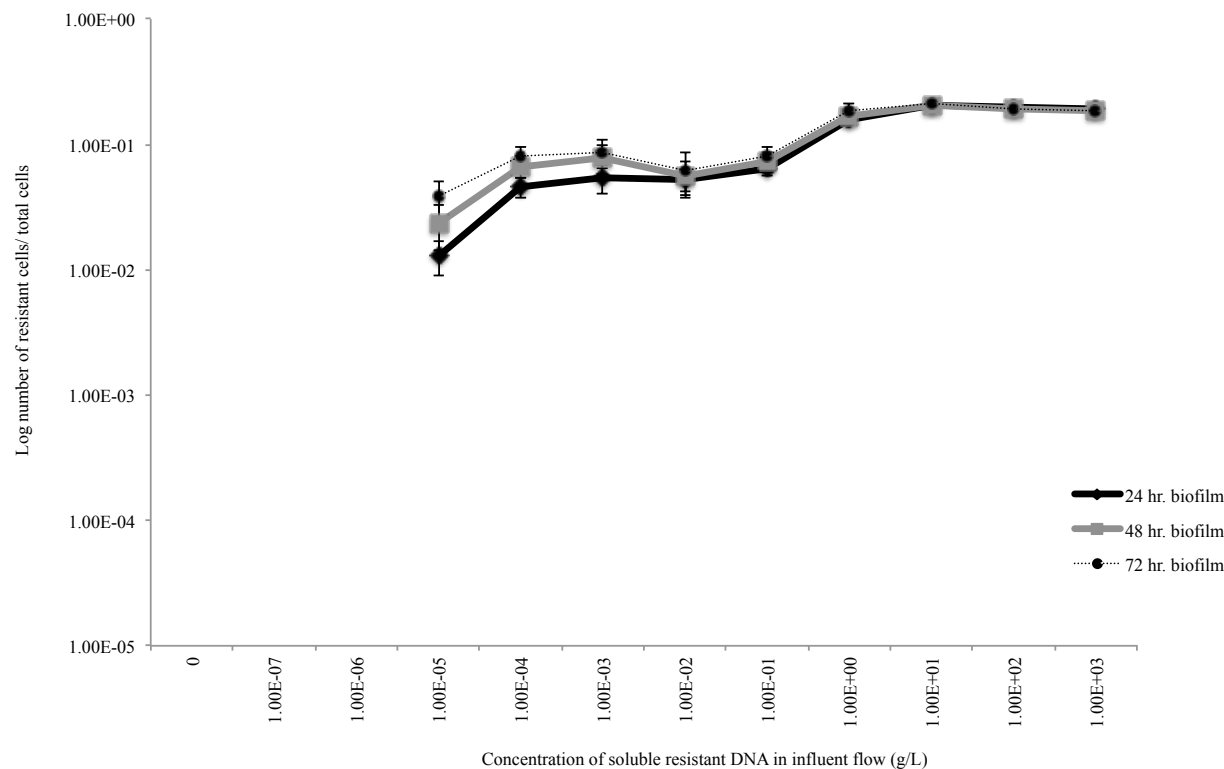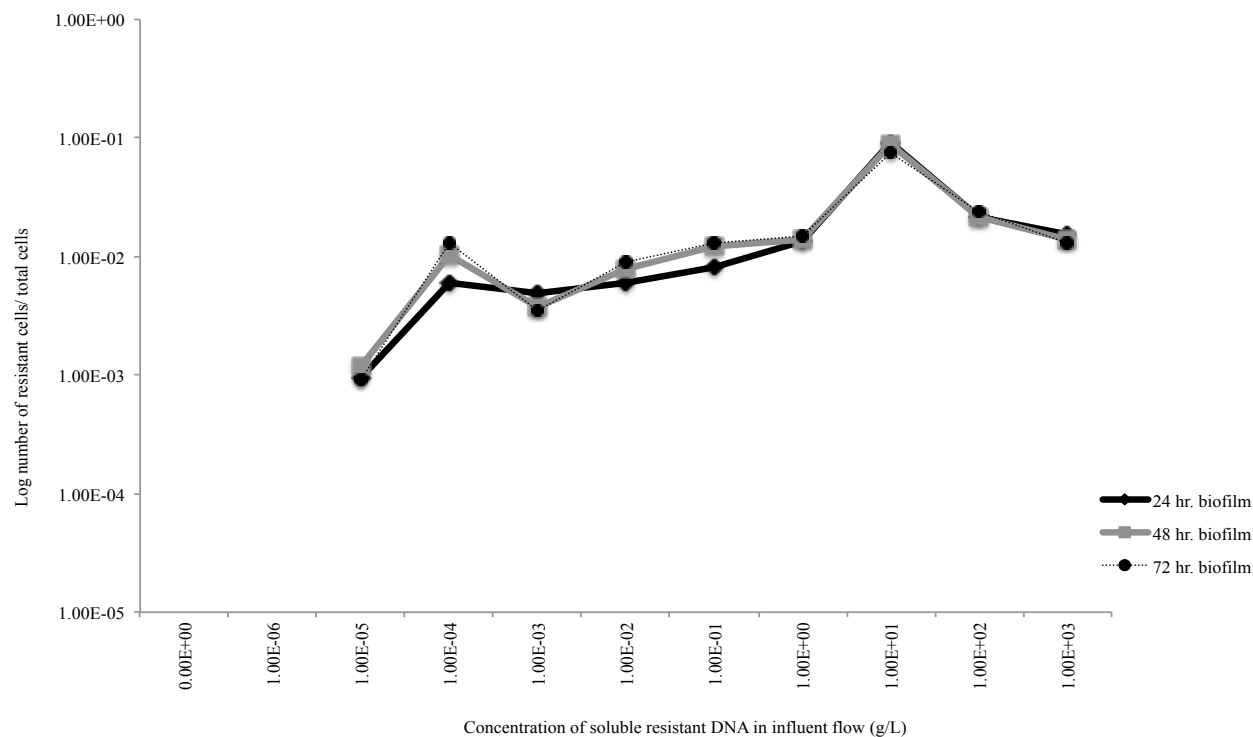
Supplemental **Figure 4a: Effect of increasing the resistant DNA concentration in the influent flow on the total transformants in a biofilm undergoing growth and maintenance functions with a resistance probability value of 20%.** The graph above looks at the effect of changing the resistant DNA concentration in the influent flow of a biofilm undergoing growth and maintenance. An initial single species, non-resistant biofilm was grown for 3 days. This initial biofilm structure was then used as the starting point for the experimental simulation data graphed above. All subsequent experimental simulations were run on a biofilm that was undergoing growth and maintenance functions with an influent media concentration (COD_{in}) of $10e^{-3}$ g.L^{-1}. In addition the erosion rate (κ_{Det}) was set to $5e^{-4}$ um^{-1}hr^{-1} and the probability of lysis of cells P(lysis) was set to 1%. All simulations were run with a resistance probability value of 20%. A set of 5 simulations were run for each resistant soluble DNA concentration value graphed above, with varying seed values. Standard deviations were calculated and are included on the graph above as well. Note that in these simulations, metabolic burden associated with the resistance gene is not considered.

Supplemental* Figure 4b: Effect of increasing the resistant DNA concentration in the influent flow on the total transformants in a biofilm undergoing growth and maintenance functions with a resistance probability value of 10%. The graph above looks at the effect of changing the resistant DNA concentration in the influent flow of a biofilm undergoing growth and maintenance. An initial single species, non-resistant biofilm was grown for 3 days. This initial biofilm structure was then used as the starting point for the experimental simulation data graphed above. All subsequent experimental simulations were run on a biofilm that was undergoing growth and maintenance functions with a media concentration of $10e^{-3}$ g/L in the influent flow. In addition the detachment or erosion rate was set to $5e^{-4}$ $um^{-1}hr^{-1}$ and the probability of lysis of cells that have approached the death threshold was set to 1%. All simulations were run with a resistance probability value of .10. A set of 5 simulations were run for each resistant DNA concentration value graphed above with varying seed values. Standard deviations were calculated and are included on the graph above as well. Note that in these simulations, metabolic burden associated with the resistance gene is not considered.
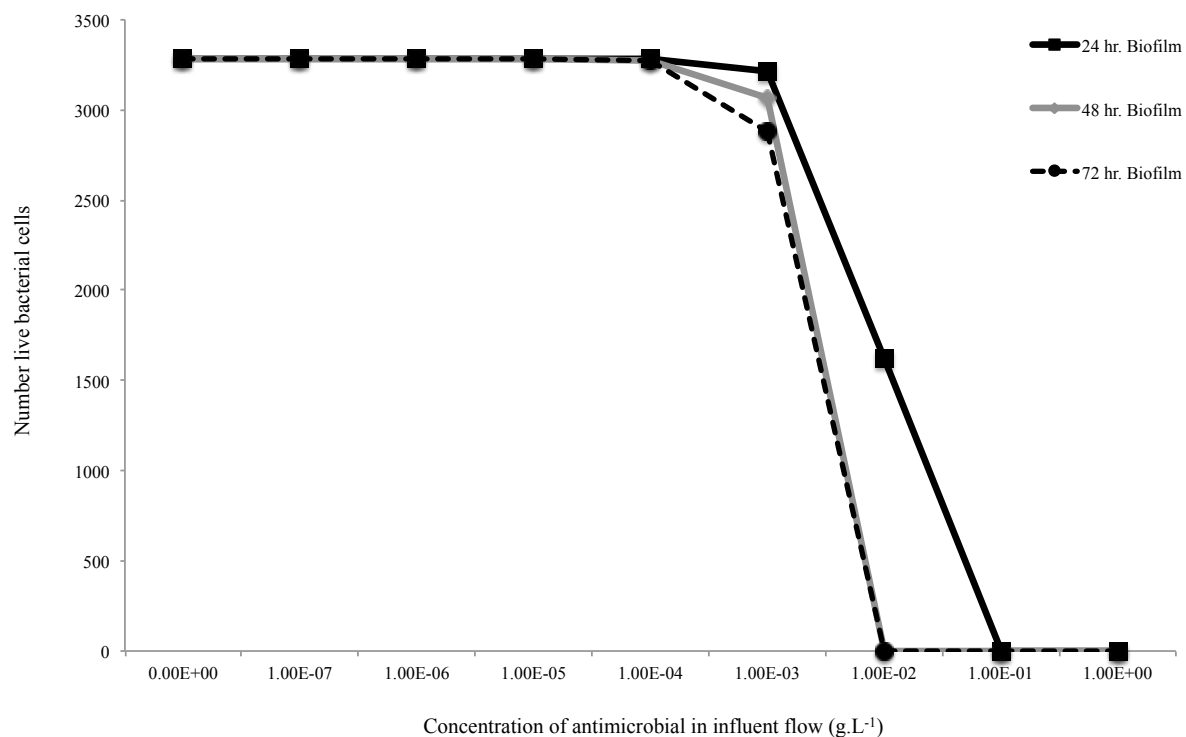
Supplemental **Figure 4c: Effect of increasing the resistant DNA concentration in the influent flow on the total transformants in a biofilm undergoing growth and maintenance functions with a resistance probability value of 2%.** The graph above looks at the effect of changing the resistant DNA concentration in the influent flow of a biofilm undergoing growth and maintenance. An initial single species, non-resistant biofilm was grown for 3 days. This initial biofilm structure was then used as the starting point for the experimental simulation data graphed above. All subsequent experimental simulations were run on a biofilm that was undergoing growth and maintenance functions with a media concentration of $10e^{-3}$ g/L in the influent flow. In addition the detachment or erosion rate was set to $5e^{-4}$ $um^{-1}hr^{-1}$ and the probability of lysis of cells that have approached the death threshold was set to 1%. All simulations were run with a resistance probability value of .02. A set of 5 simulations were run for each resistant DNA concentration value graphed above with varying seed values. Standard deviations were calculated and are included on the graph above as well. Note that in these simulations, metabolic burden associated with the resistance gene is not considered.
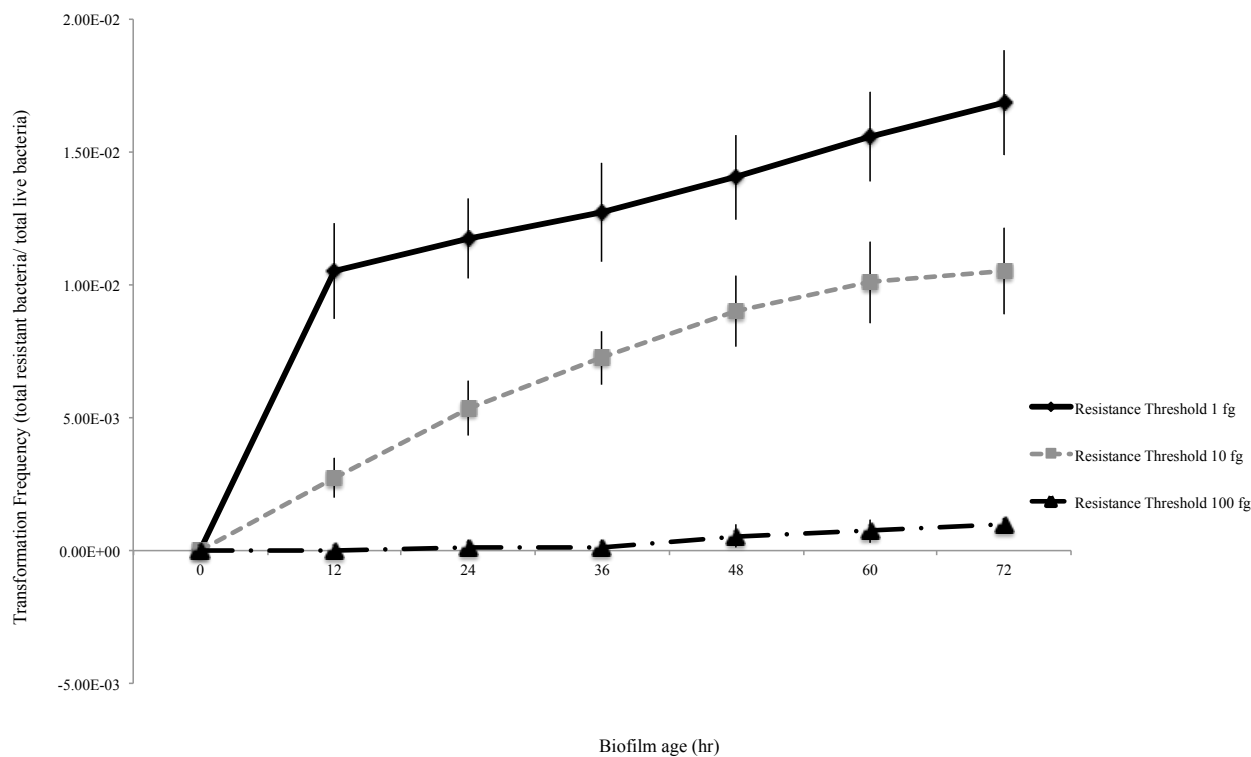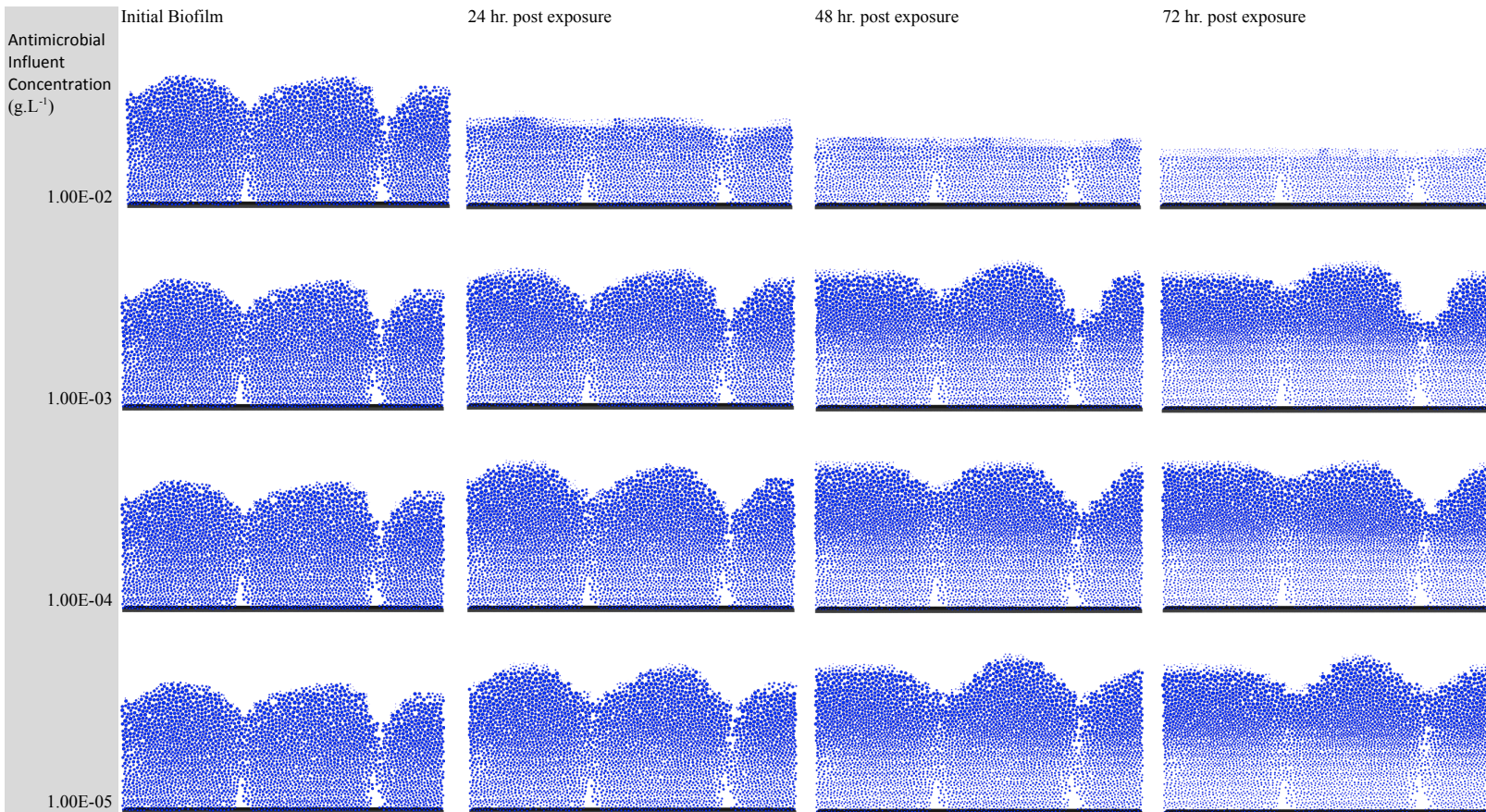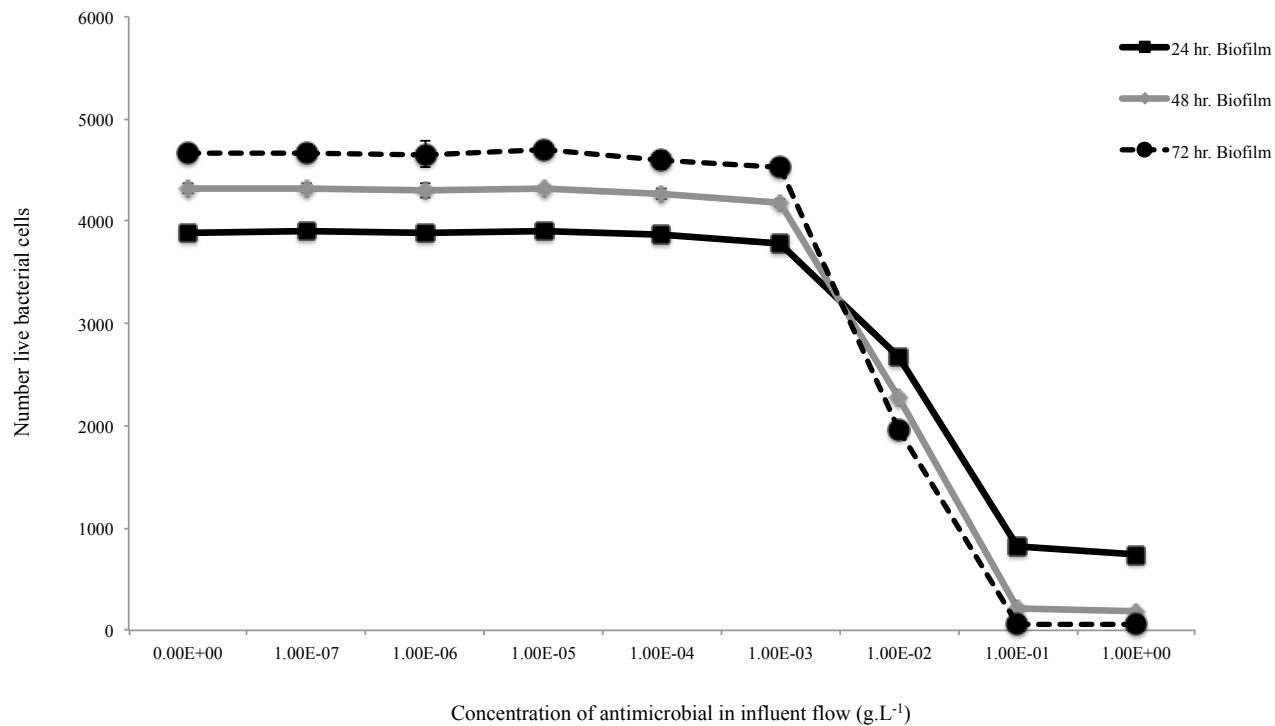
Supplemental **Figure 5: Effect of changing the resistance switch threshold (Th$_{res}$) for resistance gene expression on the transformation frequency in a biofilm not undergoing growth and maintenance functions.** In this model, bacterial cells have a probability of transformation [P(resistant)] upon approaching a resistance switch threshold (Th$_{res}$) of resistant soluble DNA that has been taken up by the cell. The graph above looks at the effect of changing Th$_{res}$ on the transformation curve. An initial single species, non-resistant biofilm was grown for 3 days. This initial biofilm structure was then used as the starting point for the experimental simulation data graphed above. For all experimental simulations, growth and maintenance functions were turned off to produce a static biofilm structure. In addition, soluble resistant DNA was added to the system at an influx concentration of $10e^{-6}$ g.L^{-1} and transformation frequencies were calculated for the first 72 hours post addition of resistant DNA. Each transformation frequency point is an average of 5 simulations run with 5 different seed values. Standard deviations were calculated and are included on the graph above as well.

***Supplemental* Figure 6a: Effect of increasing the antimicrobial concentration in the influent flow of a biofilm not undergoing growth and maintenance functions.** The graph above looks at the effect of changing the antimicrobial concentration in the influent flow of a biofilm not undergoing growth and maintenance functions. An initial single species, non-resistant biofilm was grown for 3 days. This initial biofilm structure was then used as the starting point for the experimental simulation data graphed above. For all experimental simulations, growth and maintenance functions were turned off to produce a static biofilm structure. In addition, erosion rate (κ_{Det}) was set to 0 um^{-1}hr^{-1} and the probability of lysis [P(lysis)] was set to 0%. A set of 5 simulations were run for each antimicrobial concentration value graphed above with varying seed values. The number of live heterotrophs were averaged across these 5 simulations. Standard deviations were calculated and are included on the graph above as well.

Column headers: Initial Biofilm | 24 hr. post exposure | 48 hr. post exposure | 72 hr. post exposure

Row labels (Antimicrobial Influent Concentration (g.L^{-1})): 1.00E-02, 1.00E-03, 1.00E-04, 1.00E-05
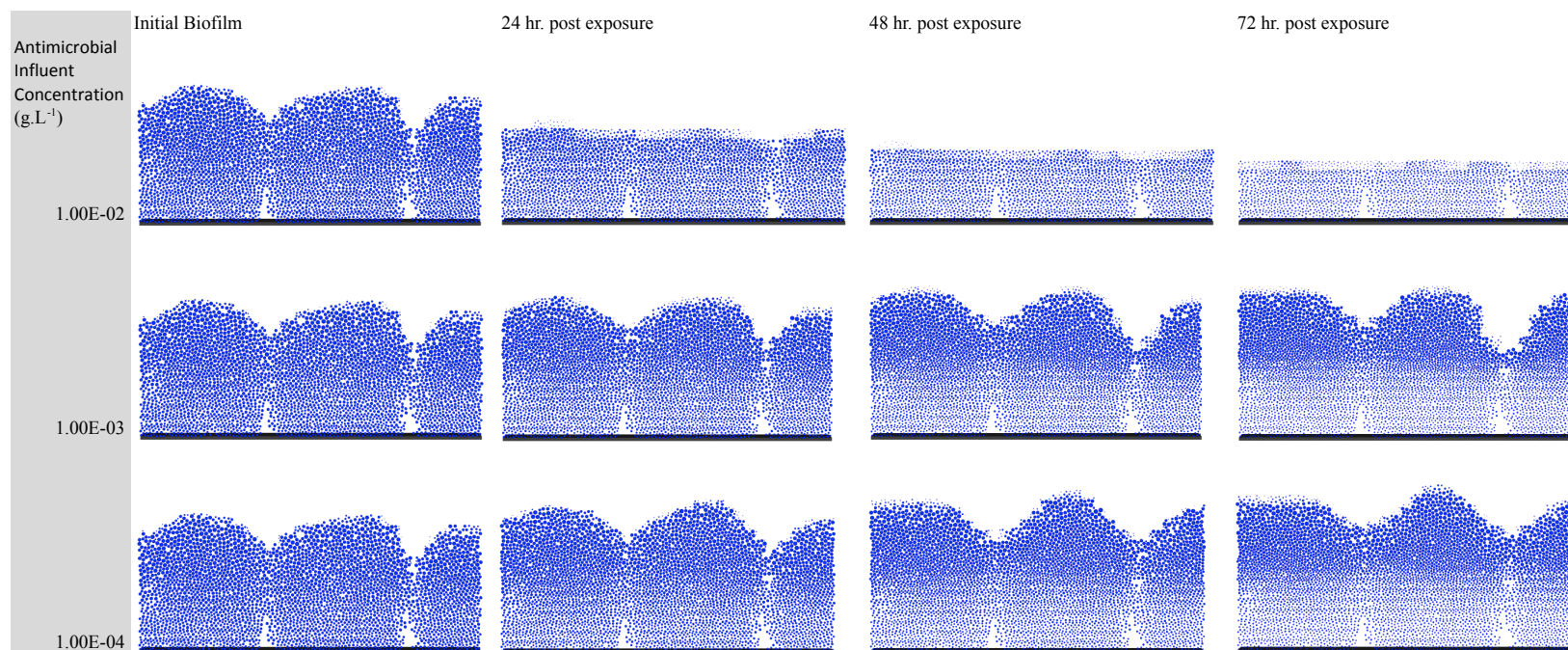
Supplemental Figure 6b: Effect of increasing the antimicrobial concentration in the influent flow of a biofilm not undergoing growth and maintenance functions – simulation images. The figure above is a compilation of simulation images that are most representative of the biofilm structure trends seen in response to changing the antimicrobial concentration in the influent flow of a biofilm not undergoing growth and maintenance functions. An initial single species, non-resistant biofilm was grown for 3 days. This initial biofilm structure was then used as the starting point for subsequent experimental simulations. For all experimental simulations, growth and maintenance functions were turned off to produce a static biofilm structure. In addition the erosion rate (κ_{Det}) was set to 0 um^{-1}hr^{-1} and the probability of lysis [P(lysis)] was set to 0%. Any visible trend was most evident between antimicrobial concentrations of 1.00^{-5} g.L^{-1} to 1.00^{-2} g.L^{-1}, thus displayed images were limited to this range.

***Supplemental* Figure 6c: Effect of increasing the antimicrobial concentration in the influent flow of a biofilm undergoing growth and maintenance functions.** The graph above looks at the effect of changing the antimicrobial concentration in the influent flow of a biofilm undergoing growth and maintenance. An initial single species, non-resistant biofilm was grown for 3 days. This initial biofilm structure was then used as the starting point for the experimental simulation data graphed above. All subsequent experimental simulations were run on a biofilm that was undergoing growth and maintenance functions with an influent media concentration (COD_{in}) of $10e^{-3}$ g.L^{-1}. In addition, the erosion rate (κ_{Det}) was set to $5e^{-4}$ um^{-1}hr^{-1} and the probability of lysis [P(lysis)] was set to 1%. A set of 5 simulations were run for each antimicrobial concentration value graphed above with varying seed values. The number of live heterotrophs were averaged across these 5 simulations. Standard deviations were calculated and are included on the graph above as well.

| | Initial Biofilm | 24 hr. post exposure | 48 hr. post exposure | 72 hr. post exposure |

Antimicrobial Influent Concentration $(g.L^{-1})$

1.00E-02

1.00E-03

1.00E-04

Supplemental **Figure 6d: Effect of increasing the antimicrobial concentration in the influent flow of a biofilm undergoing growth and maintenance functions - simulation images.** The figure above is a compilation of simulation images that are most representative of the biofilm structure trends seen in response to changing the antimicrobial concentration in the influent flow of a biofilm undergoing growth and maintenance. An initial single species, non-resistant biofilm was grown for 3 days. This initial biofilm structure was then used as the starting point for subsequent experimental simulations. All experimental simulations were run on a biofilm that was undergoing growth and maintenance functions with an influent media concentration (COD_{in}) of $10e^{-3}$ $g.L^{-1}$ in the influent flow. In addition the erosion rate (κ_{Det}) was set to $5e^{-4}$ $um^{-1}hr^{-1}$ and the probability of lysis [P(lysis)] was set to 1%. Any visible trend was most evident between antimicrobial concentrations of 1.00^{-4} $g.L^{-1}$ to 1.00^{-2} $g.L^{-1}$, thus displayed images were limited to this range.

Chapter 5

Conclusions & Future Directions

This dissertation research focuses on natural transformation in bacterial biofilms and the formation and spread of antibiotic resistant bacteria in water networks. Both laboratory and agent-based models examined factors, physiologic and external, that influence transformation frequency in monoculture *Acinetobacter baylyi* strain BD413 biofilms. Study findings contribute to a better understanding of differential competence gene expression between biofilm cells and their planktonic counterparts and the effect of external antibiotic pressure on resistance gene spread within a biofilm. In general, this work adds to the growing body of literature focused on the potential repercussions of prolific antibiotic use and prevalence of resistance determinants in the environment. Conclusions and observations are based on experiments conducted under optimized lab conditions and theoretical model output. Therefore, these studies are precursors to downstream research that may directly influence policy regarding prophylactic antibiotic use in the agricultural industry, water treatment procedures and reclaimed water practices. Summarized below are the major study conclusions as well as suggestions for future work.

5.1 Conclusions

The first set of laboratory experiments assessed transformation frequencies in AC811 biofilms cultured in dynamic flow cells. Exposure of biofilms to streptomycin resistant (strep[r]), tetracycline resistant (tet[r]), and kanamycin resistant (kan[r]) donor DNA resulted in detectable transformation frequencies in both the detached cells in effluent from the once-through flow system and in biofilm cells scraped from the flow cell. Transformation frequencies calculated from effluent and from biofilm samples were at least 10-fold higher in biofilms exposed to kan[r] amplified PCR product than in biofilms exposed to tet[r] pWH1266 plasmid DNA. Biofilms are common in flowing systems and can come in contact with resistant determinants within these same compartments.[1, 2] We cannot generalize to gene transfer phenomena in environmental compartments, most likely colonized with multispecies biofilms, based on monoculture biofilm experiments conducted under optimized laboratory conditions. However, these results suggest that natural transformation can occur in mature biofilms developed under nutrient poor conditions in dynamic flow systems. Furthermore, presence of transformed detached cells implies that these conditions promote dissemination of resistant cells.

The next set of laboratory experiments compared transformation frequencies of biofilm cells with their planktonic counterparts in static and dynamic flow laboratory models. Transformation frequencies of biofilm cells grown in microtiter plates were compared with overlying suspended cells and with planktonic batch culture cells recovered at the exponential phase. Gene transfer frequencies were also compared between biofilm cells

grown in a once-through flow system for 12, 24, 48 & 72 h with planktonic cells grown in batch culture and recovered at the exponential, early-stationary and late-stationary phases. The microtiter data show that the transformation frequencies of suspended cells and planktonic cells were at least 10-fold higher than that of the biofilm cells. Similarly, the flow system experiment data indicate that transformation frequencies of the planktonic samples at various growth stages were approximately 10-fold higher than frequencies of corresponding biofilm samples. These results were surprising considering the prevailing hypothesis of increased competence of cells in the biofilm growth mode.[3]

Comparison of *comP* gene expression trends in biofilm and planktonic cells suggests that the observed frequency differences are due to a variation in competence state between biofilm and free-floating cells. The number of *comP* gene transcripts per AC811 biofilm cell decreased over time. Whereas, similar to previous results, the number of *comP* gene transcripts per planktonic cell decreased over the course of the exponential phase and then increased to maximal levels in the stationary phase.[4] Previous work indicates that DNA uptake apparatus, including ComP, is already synthesized prior to maximal competence induction.[4] The number of *comP* gene transcripts in early and late stage exponential planktonic batch cultures is significantly higher than in mature BD413 biofilms. This suggests that the DNA uptake machinery is not synthesized to the same extent in BD413 planktonic and biofilm cells, possibly accounting for observed transformation frequency differences. Our results contradict the prevailing hypothesis of increased competence of biofilm cells as compared to planktonic cells and suggest that observations of gene transfer

in a specific biofilm system may not be generalizable to all biofilms such as mixed species biofilms. Transformation in biofilms is influenced by structural factors in addition to competence and acquisition of resistance genes by cells in the biofilm growth mode is not limited to transformation. Therefore, studies focusing on structural advantages provided by the biofilm and detailed studies of each gene transfer mechanism in different biofilm systems are warranted in order to provide a comprehensive understanding of the role of biofilms in the development of antibiotic resistance.

The final section of this dissertation work focuses on the development of an agent-based model to test hypotheses that may be difficult to conduct in the laboratory setting. The model presented in this work is an extension of the individual-based Dynamics of Microbial Communities Simulator (iDynoMiCS) software that provides an ibM simulation of biofilm growth.[5] This modified model additionally simulates DNA uptake, transformation and antimicrobial inhibition of bacterial growth in single-species biofilms. The larger scope of the work was to develop a transformation model that can be used to identify factors that may influence transformation and drive future laboratory research. Model output includes the number of resistant cells in a biofilm over time and by location within the biofilm structure as well as a time series of biofilm images. An application of the model is presented in this dissertation. We assessed the effect of resistance gene burden value on the persistence of resistant bacteria in a biofilm exposed to donor DNA and varying antimicrobial concentration. Data trends in simulation output were consistent with prevalent assumptions about antibiotic exposure and resistance expansion. One particular

151

hypothesis is that a decrease in selective pressure will benefit the susceptible bacteria and allow them to displace resistant strains.[6] The exception to this generalization is bacteria harboring low cost or no cost resistance mechanisms. These bacterial will persist even in the absence of antibiotic, and this is reflected in the model results.[7, 8] In general, increased antimicrobial concentration exposure resulted in more pervasive resistance expansion. For the higher burden values, this increase was mostly apparent at higher antimicrobial concentration values. The results also indicated that for certain simulation conditions, data patterns did not emerge in younger biofilms. Finally, image analyses implied that increasing influent antimicrobial concentration seems to promote dispersal of resistant cells from the biofilm structure. This study is an example of model utility in situations where laboratory experiments may be difficult to conduct. The ephemeral nature of high cost resistance genes decreases the likelihood that such resistance determinants can be detected in the environment or isolated and studied in a laboratory setting. However, this extended iDynoMiCS model allows us to demonstrate trends in the absence of appropriate bacterial strains for *in vitro* experiments.

Identifying factors that influence transformation in biofilms in water systems and promote the formation and spread of antibiotic resistant bacteria has implications beyond the environmental setting. There is evidence that antibiotic resistant mechanisms in nosocomial pathogens have their origins in the environmental resistome.[6, 9-11] *Acinetobacter* spp. are found in multiple environmental compartments, making the naturally competent *Acinetobacter baylyi* an appropriate model organism to monitor

resistance trends. Laboratory and modeling studies such as those presented in this work hopefully signal the need for more research aimed at better understanding gene transfer in biofilms and linking the environment to the clinic. In addition, the utility of models as a tool to supplement ongoing studies should not be underestimated. The use of both laboratory and agent-based models provided an in-depth study of the various factors that influence natural transformation and resistance gene expansion in *Acinetobacter baylyi* strain BD413 biofilms such as exposure to donor DNA, competence gene expression, resistance gene metabolic burden and antimicrobial inhibition.

5.2 Future Work

Natural transformation in water network biofilms is a complex issue. Simplified laboratory and agent-based models presented in this dissertation work provide a foundation for this research topic. While is not possible to make assumptions about gene transfer in the environment based on dissertation results alone, modifying current models may make them more generalizable. Models that can closely approximate biofilm characteristics and environmental conditions in water treatment and distribution systems will be helpful in identifying factors that promote gene transfer in the environment. Environmental trends can be portentous of resistance expansion in the clinical setting with gene flow occurring between the two compartments.[12, 13] So, such data would also be instrumental in intervention plan development.

There are several avenues for additional research. Future laboratory experiments may include: development of multi-species biofilms in once-through flow systems, exposure of biofilms to influent antibiotic compounds and to donor DNA isolated from environmental water samples, and varying environmental conditions that may impact transformation frequency such as ambient temperature and flow-rate. In addition, methods that can assess transformation while keeping the biofilm structure intact should be utilized.[14] Current agent-based model simulations include a constant antimicrobial exposure. However, input of antibiotics in the real world may occur in a single pulse or multiple pulses.[15] It would be interesting to examine the effect of antimicrobial cessation, post prolonged exposure, on the resistance make-up of the biofilm. The antibiotic can also be applied in predefined intervals. Additional source code modifications would expand the utility of the model. These include: a compensatory mechanism, the ability to use antimicrobial as a growth substrate and growth phase dependent competence. Environmental measures of different variables could also strengthen models. Examples include antibiotic half-lives, antibiotic concentrations and antibiotic resistance gene concentrations in various aquatic systems.

5.3 References

1. Huq, A., et al., *Biofilms in water, its role and impact in human disease transmission.*, in *Current Opinion in Biotechnology*. 2008. p. 244-247.
2. Xi, C., et al., *Prevalence of antibiotic resistance in drinking water treatment and distribution systems.*, in *Applied and Environmental Microbiology*. 2009. p. 5714-5718.
3. Roberts, A.P., P. Mullany, and M. Wilson, *Gene transfer in bacterial biofilms.*, in *Meth. Enzymol.* 2001. p. 60-65.
4. Porstendörfer, D., et al., *ComP, a pilin-like protein essential for natural competence in Acinetobacter sp. Strain BD413: regulation, modification, and cellular localization.*, in *J. Bacteriol.* 2000. p. 3673-3680.
5. Lardon, L.A., et al., *iDynoMiCS: next-generation individual-based modelling of biofilms*, in *Environ Microbiol*. 2011. p. no-no.
6. Wright, G.D., *The antibiotic resistome: the nexus of chemical and genetic diversity*, in *Nat Rev Micro*. 2007. p. 175-186.
7. Andersson, D.I. and D. Hughes, *Persistence of antibiotic resistance in bacterial populations*, in *FEMS Microbiology Reviews*. 2011. p. 901-911.
8. Salyers, A.A. and C.F. Amábile-Cuevas, *Why are antibiotic resistance genes so resistant to elimination?*, in *Antimicrobial Agents and Chemotherapy*. 1997. p. 2321-2325.
9. Josephson, J., *The Microbial "Resistome"*, in *Environ. Sci. Technol.* 2006. p. 6531-6534.
10. Martínez, J.L., F. Baquero, and D.I. Andersson, *Predicting antibiotic resistance*, in *Nat Rev Micro*. 2007, Nature Publishing Group. p. 958-965.
11. Aminov, R.I. and R.I. Mackie, *Evolution and ecology of antibiotic resistance genes*, in *FEMS Microbiology Letters*. 2007. p. 147-161.
12. Allen, H.K., et al., *Call of the wild: antibiotic resistance genes in natural environments*. 2010, Nature Publishing Group. p. 1-9.
13. Zhang, X.-X., T. Zhang, and H.H. Fang, *Antibiotic resistance genes in water environment*, in *Appl Microbiol Biotechnol*. 2009, Springer. p. 397-414.
14. Hendrickx, L. and S. Wuertz, *Investigating in situ natural genetic transformation of Acinetobacter sp. BD413 in biofilms with confocal laser scanning microscopy*, in *Genetic Engineering: Principles and Methods*. 2004, Springer. p. 159-173.
15. Ding, C. and J. He, *Effect of antibiotics in the environment on microbial populations*, in *Appl Microbiol Biotechnol*. 2010. p. 925-941.